

IPPJ-AM-42

STOPPING POWER THEORIES
FOR CHARGED PARTICLES
IN INERTIAL CONFINEMENT FUSION PLASMAS
(EMPHASIS ON HOT AND DENSE MATTERS)

S. KARASHIMA, T. WATANABE
T. KATO AND H. TAWARA

INSTITUTE OF PLASMA PHYSICS
NAGOYA UNIVERSITY

NAGOYA, JAPAN



**STOPPING POWER THEORIES FOR CHARGED PARTICLES
IN INERTIAL CONFINEMENT FUSION PLASMAS
(EMPHASIS ON HOT AND DENSE MATTERS)**

Shosuke KARASHIMA,* Tsutomu WATANABE,**
Takako KATO and Hiroyuki TAWARA

Institute of Plasma Physics, Nagoya University
Chikusa-ku, Nagoya 464, Japan

September 1985

Permanent address:

- * Science University of Tokyo, Tokyo 162, Japan
- ** Institute of Physical and Chemical Research,
Wako-shi 351-01, Saitama, Japan

This document is prepared as a preprint of compilation of atomic data for fusion research sponsored fully or partly by the IPP/Nagoya University. This is intended for future publication in a journal or will be included in a data book after some evaluations or rearrangements of its contents. This document should not be referred without the agreement of the authors. Enquiries about copyright and reproduction should be addressed to Research Information Center, IPP/Nagoya University, Nagoya, Japan.

Abstact

This review surveys the theoretical approaches on the stopping power of the charged particles penetrating through matters. In view of our interest, the particular attention is paid to the problems of the energy losses of projectile ions in hot and dense plasmas in the study of inertial confinement fusion (ICF). General physical and mathematical treatments are also outlined.

§ 1. Introduction

The problems of energy deposition profiles by ion beams and their effect on target materials are of decisive importance in practice of the inertial confinement fusion (ICF). Especially the stopping power of ICF target materials plays an important role in the achievement of nuclear fusion reactions. The theoretical treatments of the stopping power and the straggling phenomena in hot and dense plasmas, however, are quite difficult, compared with those in the cold plasmas, and very few theoretical bases have been established yet. The projectile charge states are also difficult to determine from the viewpoint of experiments.

In this article, our main interest lies in the stopping power of the charged particles in a high density and high temperature matter. In addition, we describe the theoretical methods of stopping power calculations in the dilute plasma and cold matter in order to extend the theories to hot and dense plasmas.

Several experimental results will be also shown in this article for the comparison with the theories of stopping power as references.

In order to represent the methods of approaches which are applicable to different plasma conditions, we display the conditions based on the ideas of Arista and Brandt (27) in Fig.1. The parameter $\chi^2 \equiv e^2 / \hbar v_F$ measures the ratio between potential and kinetic energies of the electrons in a degenerate electron gas. Nondegeneracy can be included in this

parameter through the expression $\chi^2 = \frac{3}{10\pi} \left(\frac{9\pi}{4}\right)^{1/3} \frac{v}{K}$,
 where $v = e^2/r_s a_0$, the mean kinetic energy $k = \frac{1}{2} m v_{th}^2 = \frac{3}{5} E_F + \frac{3}{2} kT$; $\frac{3}{5} E_F =$
 mean kinetic energy of a fully degenerate electron gas, $\frac{3}{2} kT =$
 mean kinetic energy of a nondegenerate plasma; $E_F = 1.84/r_s^2$ the
 Fermi energy of the electrons in atomic units. In Fig.1 the
 plasma conditions are shown in metal(M), the sun, and artificial
 plasmas of interest for nuclear fusion in the context of inertial
 confinement plasma (ICP) and magnetic confinement of plasma(MCP).
 The line denoted $\chi^2 = 1$ separates the conditions in strong
 interacting plasmas from those in weakly interacting plasmas.
 For the description of the energy loss, the lines $v_e = v_0$ and
 $v_e = v_0/3$ indicate the transition region between the plasmas where
 the classical theories are used (the lower right-hand quadrant)
 and all other plasmas where quantum-mechanical descriptions are
 appropriate. Below the line $\theta = k_B T/E_F = 1$, the plasmas are
 degenerate or cold, meanwhile above the line they are
 nondegenerate or hot.

§ 2. Basic Concept of Stopping Power Theories and The Key Theories of Charged Particles through the Media

Stopping power is the property of target substances that decelerate charged particles traversing them. Physical processes of deceleration of charged particles are mainly due to the excitation and ionization of electrons in the materials. When projectiles are slow, the nuclear collision takes a part in the deceleration processes. Stopping power processes have been considered and formulated in two ways. (1) The one is based on the concept of charged particle collision on atoms or molecules. (2) The second is based on the concept of interaction of incident charged particles with dielectric substances.

The stopping power is defined as the amount of energy loss of incident charged particles per unit length along their track, usually denoted by $(-dE/dx)$.

Let us consider the case where a charged particle of a charge $Z_1 e$ with a velocity v is injected into target materials with Z_2 electrons (in an atom or a molecule) with density n per unit volume and collides with them. If the velocity of the particle exceeds the electron thermal velocity $v_{th} = (2k_B T/m)^{1/2}$ in the target plasma, ($v \gg v_{th}$), the stopping power is given by (56)

$$-\frac{dE}{dx} = \frac{4\pi Z_1^2 e^4}{mv^2} nv Z_2 \ln \Lambda (v_{th}, Z_1) \quad (2.1)$$

Conversely, for low velocities ($v \ll v_{th}$)

$$-\frac{dE}{dx} = \frac{16}{3} \frac{\pi^{1/2} Z_1^2 e^4}{(2k_B T_e)^{3/2}} nv Z_2 m^{1/2} \ln \Lambda (v_{th}, Z_1) \quad (2.2)$$

Here the expressions for low or high temperature limit are given by eqs.(89) and (90) in Ref.(56).

The collision logarithm $\ln \Lambda$ can be expressed in each case by using either classical or quantum-mechanical approximations. In the impact parameter description the result becomes of the form

$$\ln \Lambda = (b_{\max} / b_{\min}), \quad (2.3)$$

where b_{\max} and b_{\min} are the values of the maximum and minimum impact parameters, respectively.

These approximation values are represented in Table I following the Ferrariis and Arista analysis.⁽⁵⁶⁾ The classical and the quantum-mechanical results are separated by using the Bloch parameter⁽⁷¹⁾ $\xi = b_{\text{CL}} / b_{\text{QM}} = Z_1 e^2 / h v_r$; b_{CL} denotes the impact parameter given by the classical approximation and b_{QM} given by the quantum-mechanical approximation. The transitions between these two expressions are described by the collision logarithm in classical or the quantum-mechanical approximation.

In Fig.2, using the Ferrariis and Arista analysis of $\ln \Lambda$ for the energy loss of ions, we illustrate the method of description of the stopping power evaluated for $Z_1=1$ in generally applicable conditions. The classical approximation for the energy loss is applicable to the cases of intermediate projectile velocities, $v_{\text{th}} < v < Z_1 v_0$ (CL2), as well as low velocities, $v < v_{\text{th}} < Z_1 v_0$ (CL1), at low temperatures. On the other hand, the quantum-mechanical approximation is applied to high velocities, $v > v_{\text{th}} > Z_1 v_0$ (QM2), at all temperatures as well as low velocities, $v < Z_1 v_0 < v_{\text{th}}$ at high plasma temperatures. Here v_0 denotes the Bohr

velocity and $v_{th} = (2k_B T_e / m)^{1/2}$ the electron thermal velocity. The transitions between these corresponding cases are described as "transition region". All these approximations are contained in the collision logarithm in the stopping power formula. The arrows in Fig.2 represent the directions of increasing (\uparrow, \rightarrow) (or decreasing (\downarrow, \leftarrow)) ion velocity or increasing (or decreasing) plasma temperatures. For instance, by increasing the temperature, with a fixed ion velocity $v \ll v_{th}$, we go from the classical low-temperature case, CL1, to the quantum-mechanical high-temperature limit, QM1. Thus we can evaluate the stopping power through $\ln \Lambda$ by means of application of the results of Table I and Fig.2.

The stopping power can also be considered as the energy loss of an incident charged particle due to dielectric response when it transverses with high velocities v .

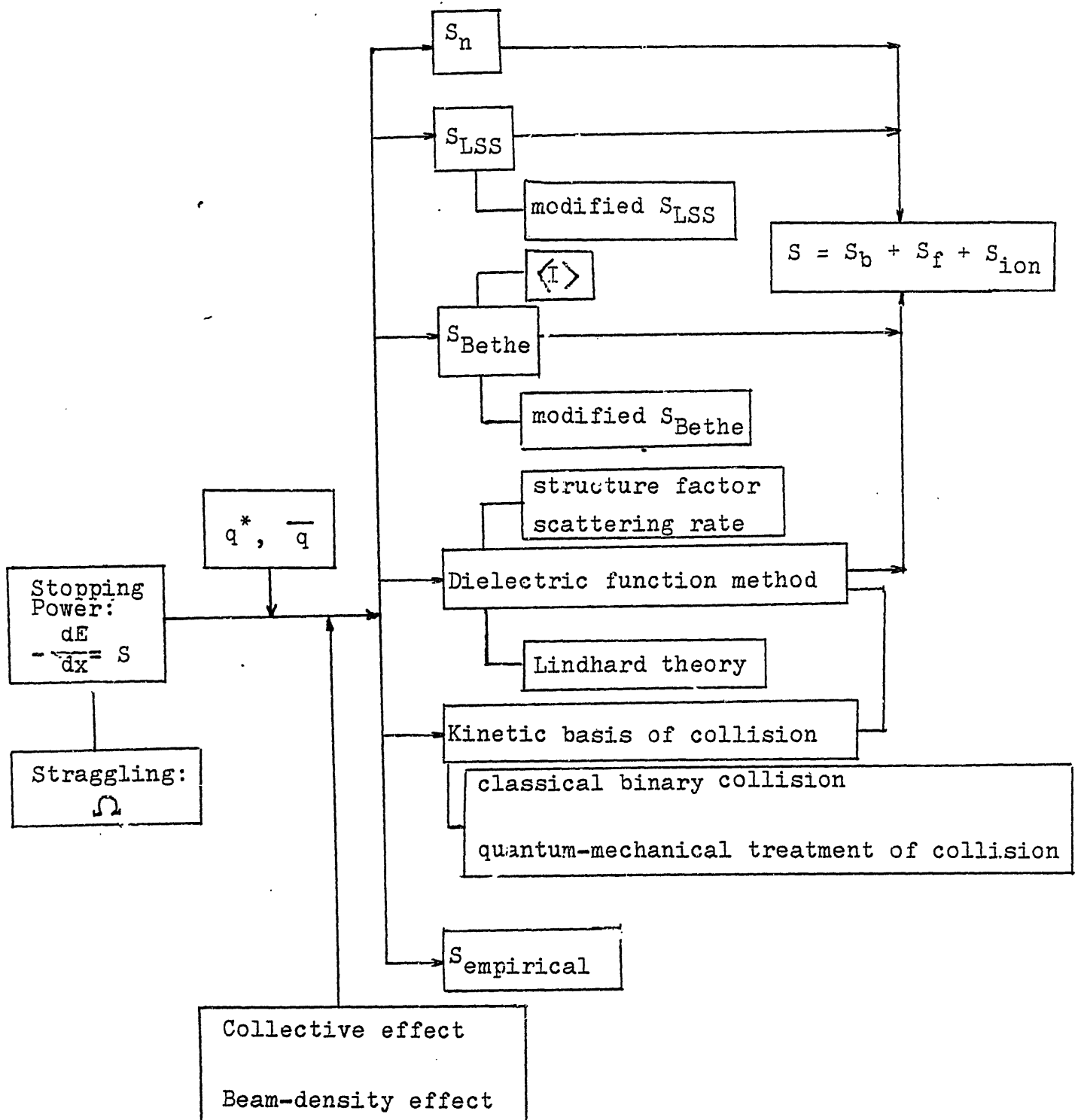
The slowing down process in a partially ionized matter generally is due to the contributions of bound and free electrons in plasmas. We will take into account these contributions as the bound and the free electron effect for the stopping processes. Furthermore, in the energy deposition problems, the collective beam-target interactions and beam density effects also should be taken into account.

On the other hand, the effective charge of projectile ions plays an important role in the stopping power calculations. Effective stopping power charge will be determined by a balance of charge-changing processes in a stopping medium.

We give a summary of these treatments of the stopping power over a wide range of energies, densities, and temperatures in Table II. Literature sources cited correspond to the reference

numbers. The classification of the stopping power theories here can be made in the following way: (A) the approach based on the contribution of bound and free electrons in plasmas to stopping process, (B) the energy loss of an incident charged particle due to dielectric response in the polarized target medium, (C) the method based on the kinematically described collective equations, (D) the description of collective, vicinage and beam-density effects on the treatment of the stopping power, (E) the analysis of experiments and model calculations of the stopping power and the effective charge comprised in the stopping power theory, and (F) semiempirical formulas of the stopping power and others. These approaches from A to F are related one another.

The following illustration represents our summary of the stopping power theories and the relations between the way of theories. Thus, the key theories of the stopping power are tabulated in Table II.



- S_n = nuclear stopping power
- S_{LSS} = stopping power based on the Lindhard, Scharff, and Schiott
- S_{Bethe} = stopping power based on the Bethe theory.
- S_f = stopping power due to free electrons.
- S_b = stopping power due to bound electrons.
- S_{ion} = ion component of stopping power.
- $\langle I \rangle$ = average ionization potential.
- q^* = effective charge of projectile ion.
- \bar{q} = average equilibrium charge of projectile ion.

§ 3. Contribution of Bound and Free Electrons
in a Plasma to Ion Stopping Power

The energy loss of projectile ions in matter is primarily due to the processes of ionization and excitation of the bound electrons surrounding the nucleus. These processes depend strongly on the electron density, temperature, and the ionization state of the matter. For very low incident energies, high- Z_1 ions and high- Z_2 targets, it is necessary in the slowing down of the ion to include the stopping due to the elastic Coulomb collisions between the ion and the target nuclei. The nuclear Coulomb stopping power is given by the empirical form⁽¹⁾:

$$\left(\frac{dE}{dX}\right)_n = c \varepsilon^{1/2} \exp[-45.2 (c' \varepsilon)^{0.2777}], \text{ [MeV/(g/cm}^2\text{)]} \quad (3.1)$$

where $R = \rho x$, $\varepsilon = E/A$ [MeV/amu],

$$c' = \frac{A_1 A_2}{(A_1 + A_2)} \frac{(Z_1^{2/3} + Z_2^{2/3})^{-1/2}}{Z_1 Z_2},$$

$c = 4.14 \times 10^6 \left(\frac{Z_1}{A_1 + A_2}\right)^{3/2} \left(\frac{Z_1 \cdot Z_2}{A_2}\right)^{1/2} (Z_1^{2/3} + Z_2^{2/3})^{-3/4}$
 $A_1 (Z_1)$ and $A_2 (Z_2)$ represent the atomic weights (atomic numbers) of projectile ion and stopping medium, respectively.

The theories of the electronic energy loss are usually based on the Bethe equation to describe the stopping power due to bound electrons for high energy ions. On the other hand, for very low energy ions, the LSS model (Lindhard, Scharff and Schiott)⁽⁶⁶⁾ is appropriate. The electronic portion of this theory, assuming the Thomas-Fermi description of the electron clouds of the ion and the stopping atom, is given by the form:

$$\left(\frac{dE}{dX}\right)_{LSS} = C_{LSS} \sqrt{E}, \quad (3.2)$$

where $C_{LSS} = K(E_L / 1.602 \times 10^{-9})^{1/2} / (R_L \times 10^4) [\text{KeV}^{1/2} / \mu\text{m}]$

$$E_L = (1+A) Z_1 Z_2 e^2 / (Aa) \text{ [erg]}$$

$$a = 0.4683 (Z_1^{2/3} + Z_2^{2/3})^{-1/2} \times 10^{-8} \text{ [cm]}$$

$$R_L = (1+A)^2 / 4\pi A n a^2 \text{ [cm]}$$

$A = A_2 / A_1$, and

$$K = \frac{0.0793 Z_1^{1/2} Z_2^{1/2} (1+A)^{3/2}}{(Z_1^{2/3} + Z_2^{2/3})^{3/4} A_2^{1/2}}$$

The validity of this model is restricted by $Z_1^{1/3} > 137 \times \beta$

($\beta = v/c$).

The basic slowing down processes based on the Bethe theory involve the excitation and ionization of the atomic bound electrons. The Bethe equation⁽⁶³⁾ is usually written by

$$\left(\frac{dE}{dX}\right)_{\text{Bethe}} = \frac{4 \pi N_0 (q^*)^2 \rho e^4 Z_2}{mc^2 \beta^2 A_2} \left[\ln \frac{2mc^2 \beta^2 \gamma^2}{\langle I \rangle} - \beta^2 - \sum_i \frac{C_i}{Z_2} - \frac{\delta}{2} \right], \quad (3.3)$$

where N_0 is the Avogadro number, m the electron mass, q^* the effective charge of ions, δ the polarization-effect correction term, $\langle I \rangle$ the average ionization potential and $\sum_i \frac{C_i}{Z_2}$ denotes the sum of the shell correction terms, and $\gamma = (1 - \beta^2)^{-1/2}$

The ionization potential in ICF plasmas has been discussed⁽¹⁾ using a scaling formula⁽²⁾, the local oscillator model of Lindhard et al.^(3,4,6,67) (LOM model), the generalized oscillator strength (GOS) for (Al ions)^(5,6) and the augmented-LOM (A-LOM).

Figures 3 and 4 show the results⁽¹⁾ of the stopping power in Al

and Au obtained by these models.

Then stopping power due to the bound electrons in cold materials is expressed as:

$$\left(\frac{dE}{dX}\right)_b = \min\left[\left(\frac{dE}{dX}\right)_{\text{Bethe}}, \left(\frac{dE}{dX}\right)_{\text{LSS}}\right] + \left(\frac{dE}{dX}\right)_n, \quad (3.4)$$

where the minimum value in dE/dx is chosen.

An important quantity here is the effective charge q^* of the incident ion beam passing through the stopping medium. Since the direct measurement of q^* is impossible, it has been found usually from the measured stopping powers on the basis of eq.(3.3).

Mehlhorn⁽¹⁾ used the expression of q^* given by Brown and Moak:⁽⁵⁹⁾

$$q^* = Z_1 \left[1 - 1.034 \exp\left[-(v/v_0)/Z^{0.69}\right] \right], \quad (3.5),$$

where the Bohr velocity $v_0 = 2.188 \times 10^8$ cm/sec.

Meyer-ter-Vehn and Metzler^(7,8) used the semi-empirical formula found by Nikolaev and Dmitriev:⁽⁶⁸⁾

$$q^* = Z_1 \left[1 + \left(Z_1^\alpha v_0/u \right)^{1/k} \right]^{-k} \quad (3.6)$$

with the parameter $\alpha = 0.45$, $k = 0.6$, and $v_0 = 3.6 \times 10^8$ cm/s and $u = [v^2 + (v_{th})^2]^{1/2}$, where $v_{th} = (2k_B T/m)^{1/2}$ is the thermal electron velocity and $k_B T$ the temperature of the target material.

Some other least-squares fits to the effective charge have been published by Betz⁽⁷³⁾ and Ziegler⁽⁷⁰⁾. The experimental effective charge of an ion in the stopping material is usually inferred by comparing the stopping power S of high-Z ions to that of protons S_p at the same velocities by

$$S = [q^*(v)]^2 S_p(v). \quad (3.7)$$

As an ion beam heats a target, such as the ablator of ICF target, the target material begins to be ionized. This ionization results in the production of plasma free electrons in the target. The slowing down process of projectiles in partially ionized matter (plasma) is due to both the bound electrons and free electrons.

The plasma free electrons contribute to the stopping power by the effects of the binary collision ($r < r_d$) and plasma oscillation excitation ($r > r_d$), where $r_d = (k_B T_e / 4 n e^2)^{1/2}$ and n is the free electron density. Following Jackson's theory⁽⁷¹⁾, Mehlhorn expressed the free electron stopping power in the form:

$$\left(\frac{dE}{dX}\right)_f = \frac{\omega_p^2 (q^*)^2 e^2}{c^2 \beta^2} G(y_e) \ln \Lambda_f, \quad (3.8)$$

where

$$G(\xi) = \operatorname{erf}(\sqrt{\xi}) - 2 \sqrt{(\xi/\pi)} \exp(-\xi),$$

$$y_e = \beta^2 / \beta_e^2 = (mc^2 \beta^2 / 2k_B T_e), \quad \beta_e = \frac{v_e}{c}, \quad \omega_p^2 = \frac{4\pi n e^2 \bar{q}_2}{m}$$

$$\Lambda_f = \frac{0.764 \beta c}{b_{\min} \omega_p},$$

$$b_{\min} = \max\left(\frac{e^2 Z_1}{A_{12} \bar{u}^2}; \frac{\hbar}{2 A_{12} \bar{u}}\right),$$

\bar{u} means the average relative velocity between the ion and the target electrons, \bar{q}_2 the average ionization state of the target atoms, and

$$A_{12} = \frac{A_1 A_2}{A_1 + A_2} .$$

Meyer-ter-Vehn and Metzler⁽⁷⁾ discussed the minimum impact parameter b_{\min} in $\ln \Lambda$ using the following electronic stopping power equation:

$$\frac{dE}{dX} = \frac{4\pi (q^*)^2 e^4 n}{m v^2} \ln\left(\frac{b_{\max}}{b_{\min}}\right) , \quad (3.9)$$

where $n = (\rho_2 Z_2 / A_2 m_p)$ is the electron density with the mass density ρ_2 , the charge number Z_2 and the mass number A_2 of the target atoms, m_p the proton mass. The minimum and maximum impact parameters are given by

$$b_{\min} = \max \left\{ \frac{q^* e^2}{m v^2} , \frac{\hbar}{mv} \right\}$$

$$b_{\max} = \begin{cases} v/\bar{\omega} & \text{for bound electrons} \\ v/\omega_p & \text{for free electrons,} \end{cases}$$

For the average ionization potential, Meyer-ter-Vehn and Metzler used the expression

$$\hbar \bar{\omega} = 9Z_2 \left(1 + 1.8/Z_2^{1/2} \right) \exp[2.7(q_2/Z_2)^2] \text{ eV.}$$

The dominant stopping mechanisms are energy loss due to binary collisions with electrons at distance $r < r_d$ and due to plasmon excitations at distance $r > r_d$. However, the bound electrons at distance $r > r_d$ also contribute to the energy loss just as the free electrons do. They pointed out that it would be incorrect, for most heavy ion applications, to use the quantum value $b_{\min} = \hbar/(mv)$ which leads to the Bethe stopping formula. The choice for $b_{\max} = v/\bar{\omega}$ (for bound electrons) and $b_{\max} = v/\omega_p$ (for free electrons) in-

cludes binary collisions as well as plasmon excitations.

Furthermore, a similar expression as shown in eq.(3.8) can be written for plasma ion component of the stopping power⁽¹⁾:

$$\left(\frac{dE}{dX}\right)_i = \frac{(q^*)^2 e^2 Z_2}{\beta^2 c^2 A_2} \left(\frac{m}{m_p}\right) \omega_p^2 G(Y_i) \ln \Lambda_i, \quad (3.10)$$

where

$$Y_i = \frac{A_2 E}{A_1 T_i},$$

$$\Lambda_i = b_{\max}/b_{\min},$$

$$b_{\max} = \text{Debye radius} = (T_e / 4 \pi n e^2)^{1/2},$$

$$b_{\min} = \frac{A_{12} \beta_i^2 m_p c^2}{Z_1 Z_2 e^2}$$

and

$$A_{12} = \frac{A_1 A_2}{A_1 + A_2}.$$

This plasma ion contribution to the stopping power becomes appreciable only at high plasma temperatures. For example in the energy deposition of 3.5-MeV α -particles in the compressed core of an ICF pellet, the plasma ion stopping power can play an significant role⁽¹⁾.

Therefore, the total stopping power of projectiles in plasmas can be written by

$$\frac{dE}{dX} = \left(\frac{dE}{dX}\right)_b + \left(\frac{dE}{dX}\right)_f + \left(\frac{dE}{dX}\right)_i. \quad (3.11)$$

According to Meyer-ter-Vehn and Metzler, the total stopping power takes the following form:

$$\frac{dE}{dX} = \frac{1}{\rho} \left(1 - \frac{\bar{q}_2}{Z_2}\right) S_b + \frac{\bar{q}_2}{\rho Z_2} G(v/v_{th}) S_f, \quad (3.12)$$

where $G(x) = [\text{erf}(x) - 2x \exp(-x^2)] / \sqrt{\pi}$ stands for the temperature

dependence of the Coulomb cross section in the case that the thermal electron velocity v_{th} becomes comparable or larger than the ion velocity v . A similar formula is also given by Mehlhorn et al.⁽⁶⁾ in the case of proton stopping power equation as follows:

$$\frac{dE}{dX} = \frac{4\pi N_0 \rho e^4}{mc^2 \beta^2 A_2} [(Z_2 - q_2)L_b + q_2 L_f], \quad (3.13)$$

where

$$L_b = \ln \frac{2mc^2 \beta^2 \gamma^2}{\langle I(q_2 Z_2) \rangle} - \beta^2 - \sum_i \frac{c_i}{Z_2},$$

$$L_f = G(y_e) \ln \frac{E}{\hbar \omega_p}$$

where A_2 is the atomic weight and q_2 is the ionization state of the target atom.

The light-ion energy deposition and implications in the ionized materials for ICF targets are given using the practical scaling formula of the stopping power by Widner et al.⁽²⁾

The individual components (free- and bound-electron contribution) of the total stopping power can be seen in Fig.5, where C ion passes through a partially ionized plasma of Au at $T_e = 200$ eV and 1% of the solid density. The deposition profiles of 10 GeV Bi ions in different materials and at various temperatures relevant to pellet fusion^(7,8) are shown in Figs.6-8. Figure 9 displays the deposition profile of 2 MeV protons in Au as a function of the electron temperature^(1,2). The range of 2 MeV protons in gold at the temperature of 100 eV is only about one half that in the cold target. At higher temperatures, as the free electron component becomes more dominant; the Bragg peak

disappears. As an example of light- and heavy-ion fusions, the dependence of the range of 2 MeV protons and 10 GeV U ions on the density and temperature of an Au-ablator is compared in Figs.10-11. The range lengthening in Fig.10 and conversely, the range shortening in Fig.11 are illustrated. This is because the ion velocity $\beta = 0.065$ for 2-MeV protons is typically less than the electron thermal velocity, while 10-GeV U ions ($\beta = 0.30$) are relatively swift compared to the electrons in the ablator plasmas. As shown in Fig.11, the decrease in the ion range with decreasing the material density at a constant temperature reflects the increase in the degree of material ionization.

§ 4. Stopping Theory due to Dielectric Function Formalism

A charged particle passing through an ionized medium will induce the electric field by polarizing the medium. The induced electric field will then act back on the particle, resisting its motion, and cause it to lose energy. This field is related to the dielectric function $\epsilon(k, \omega)$. Nardi et al.^(9,12), Brueckner et al.⁽¹³⁾ and Mehlhorn⁽²⁾ expressed the energy losses divided into two groups: electrons bound to the plasma ions and free electrons in plasma. These fundamentals of the idea are the same expression described in the previous section: $S = S_b + S_f$. The differences in the stopping power between plasma targets and cold matter targets follow from two factors⁽¹²⁾: (1) The stopping power due to the free electrons in the plasma is different from the stopping power due to the bound electrons in cold matter.

(2) The contribution of the bound electrons in the plasma ions to stopping is different from that of the bound electrons in neutral atoms in cold matter.

Nardi et al.⁽⁹⁾ calculated the energy loss of protons for plasma free electrons in nondegenerate plasmas as follows:

$$\frac{dE}{\rho dx} = \frac{2e^2}{\rho\pi} \int_0^\infty k dk \int_0^1 \mu d\mu \operatorname{Im} \left[\frac{1}{\epsilon(k, \omega = k\mu v)} \right], \quad (4.1)$$

where v is the proton velocity, k is the wave number, ω is the frequency, and $\mu = \cos \theta = \mathbf{k} \cdot \mathbf{v} / kv$.

The dielectric function $\epsilon(k, \omega)$ in the classical form including the effect of collisions is represented by

$$\epsilon(k, \omega) = 1 + 2x^2 [1 + xZ(\zeta)] \omega_p^2 / \omega^2, \quad (4.2)$$

where $\zeta = x + iy$, $x = \omega / kv_{th}$, $y = \nu / kv_{th}$, ν is the collision frequency, v_{th} is the electron thermal velocity, and $Z(\nu)$ denotes the plasma dispersion function.

An upper cutoff wave number k_c has to be introduced in eq.(4.1), if the classical form of $\epsilon(k, \omega)$ is used. Nardi et al. and Mehlhorn used Bethe's cutoff at $k_B^{-1} = e^{-\gamma} \hbar / mv_{th}$, where $\gamma = 0.5772$ in order to avoid divergence at large wave numbers. Furthermore, Nardi et al. used the simplified quantum form for non-collisional plasmas⁽⁴⁰⁾:

$$\begin{aligned} \operatorname{Im}(\epsilon^{-1}) &= -\operatorname{Im}(\epsilon) \\ &= \frac{4\pi^{3/2} ne^2}{\hbar k^3 v_{th}} \exp\left[-\frac{(m\omega + (1/2)\hbar k)^2}{m^2 v_{th}^2}\right] \left[\exp\left(\frac{\hbar k \omega}{k_B T_e}\right) - 1\right] \end{aligned} \quad (4.3)$$

where $\omega = v_{th} \hbar k / 2m$.

The quantum corrections are only important for large wave numbers, where $|\epsilon| \approx 1$ and both the quantum and classical forms

of the dielectric function are valid. In Fig.11, the values of $dE/\rho dx$ of protons obtained by this procedure (curve(c)) and by the use of the non-collisional version ($y=0$) (curve(b)) of eq.(4.2) for gold target (19.0 g/cm^3) are practically equal, which supports the cutoff approximation.

For the contribution of the bound electrons to the energy loss, Nardi et al.^(9,12) used the Bethe collision theory which describes the interaction of short range encounters. Then the average ionization potential based on Bohr's model and the number of the bound electrons based on the Thomas-Fermi model are calculated in the Bethe stopping formula.

Figure 12 shows that the range shortening is caused at higher proton energies, while range the lengthening occurs at lower energies because of the higher thermal velocities of the plasma electrons.

Plasma collisions become significant at the lower portion of energies in the dense target ($\rho=19.0 \text{ g/cm}^3$). For the collective excitation of plasma oscillations, the Pines-Bohm theory⁽⁷⁴⁾ is used:

$$\frac{dE}{\rho dx} = -\frac{e^2 \omega^2}{2\rho v^2} R \ln \left(1 + \frac{2mv^2}{3k_B T_e} \right). \quad (4.4)$$

The values obtained from eq.(4.4) are also given in Fig.12.

Mehlhorn also has compared the results of the binary + collective model in eq.(3.8) to see whether the computationally simpler binary model gives responsible stopping powers for protons in dense Au plasmas ($T_e=1 \text{ keV}$ and $\rho=0.193 \text{ g/cm}^3$) target. Thus the polarization drag and the binary + collective

modes give similar results.

On the other hand, Brueckner et al. derived the energy loss of a fast ion

$$\frac{dE}{dX} = 2 \left[\frac{q^* e}{2\pi} \right]^2 \int dk \int_{-\infty}^{\infty} d\omega \delta(\omega - k_x v) \frac{k_x}{k^2} \text{Im} \left[\frac{1}{\epsilon(k, \omega)} \right] \quad (4.5)$$

$$k^2 = k_x^2 + k_{\perp}^2$$

from

$$\epsilon(k, \omega) = 1 - \frac{\omega_p^2}{\omega(\omega + i\nu_c) - (kv_{th})^2} - \sum_j \frac{\omega_{pl(j)}^2}{\omega(\omega + i\Gamma_j) - \omega_j^2} \quad (4.6)$$

\equiv (plasma free electrons) + (bound electrons to the plasma ions), (4.7)

The effect of collisional damping is included through the collision frequency ν_c , while kv_{th} is the frequency associated with the thermal motion of the plasma electrons, and ω_p denotes the plasma frequency. The dielectric function of the bound electrons, which is calculated using the j -th shell electrons of an atom, experience a harmonic force of the frequency ω_j and a phenomenological damping force Γ_j .

The frequency is written by

$$\omega_{pl(j)}^2 = \frac{4\pi N_a e^2 f_j}{m} \quad (4.8)$$

where N_a is the number density of atoms and f_j is the dipole oscillator strength. Brueckner et al. made the continuum approximation calculation using the Thomas-Fermi model of an atom to estimate the bound electron energies and densities. The oscillator strength with the local density $\rho(r)$ can be expressed by

$$f_j = 4\pi r^2 \rho(r) dr, \quad (4.9)$$

$$\rho(r) = \frac{Z_2^2 \chi(s^2)^{3/2}}{4 \pi b^3 s^2} \quad (4.10)$$

In eq.(4.10), Z_2 denotes the atomic number, $\chi(s^2)$ the function in the Thomas-Fermi equation ; $b \equiv (3 \pi / 4)^{2/3} n^2 / 2me^2$, and $r = s^2 b Z^{-1/3}$.

The plasma frequency can be written by $(Z - Z_{av}) \times$ (the number of ionized atoms of the medium); Z_{av} is the average number of the bound electrons in an ion, i.e.,

$$\omega_p^2 = \frac{4 \pi n e^2}{m} = \frac{4 \pi N_a (Z - Z_{av}) e^2}{m} \quad (4.11)$$

Using these results, we can obtain a complete description of the bound and continuum electrons, including collisional damping.

The cutoff wave number k_c is necessary to prevent the logarithmic divergence when $k^2 = k_y^2 + k_z^2 = \infty$ in eq.(4.5). This divergence is a result of the breakdown of the classical dielectric function at small distances. Since k_c^{-1} is essentially the minimum impact parameter, Brueckner et al. used the k_c value corresponding to the Bohr formula if the Bloch parameter $\xi \equiv q^* e^2 / \pi v_r > 1$ and the k_c value corresponding to Bethe's formula if $\xi < 1$.

They calculated the stopping power using the empirical equations of the effective charge q^* obtained by Nikolaev and Dmitriev⁽⁶⁸⁾, and Brown and Moak⁽⁶⁹⁾ or Betz⁽⁷³⁾.

The evaluation⁽¹³⁾ of dE/dx calculated from these procedures is shown in Fig.13 in comparison with the Northcliffe and Schilling result⁽⁷⁵⁾. The stopping powers for Xe and U ions in Al (a typical low- Z_2 material), and Ag and Au (a typical high- Z_2 material) are given in Figs.14-17.

When the bound electrons are ionized, their contribution to the stopping power increases, provided that the collisional damping is small. The damping is weaker in low- Z_2 materials; hence the stopping power increases with the temperature. For high- Z_2 materials, the collisional damping is more important and the stopping power can be reduced (relative to the cold material) for the temperatures up to several electron volts.

Some aspects of the problems in the energy deposition and bremsstrahlung emission by relativistic electron beams in an Au ablation layer have been discussed in Ref.11, i.e.,

$$\frac{dE}{dX} = \frac{dE}{dX} \Big|_{\text{bound electrons (to the plasma ions)}} + \frac{dE}{dX} \Big|_{\text{free electrons}}. \quad (4.12)$$

The energy loss of the electron beam in collisions with the free electrons in the plasma is given by, using the relativistic Møller cross section,

$$\frac{dE}{\rho dx} = \frac{-2\pi ne^2}{mv^2} \left[\ln\left(\frac{1}{2\epsilon_{\min}}\right) + \frac{1}{8} \left(\frac{K}{K+1}\right) - \frac{2K+1}{(K+1)^2} \ln 2 + 1 - \ln 2 \right], \quad (4.13)$$

where ϵ_{\min} denotes the minimum energy transfer in units of the incident electron energy, K is the kinetic energy in units of the electron rest mass energy, and $\epsilon_{\min}^2 = \lambda / r_D$, λ being the de Broglie wavelength and r_D is the Debye length.

The contribution of the collective plasma oscillation is given by the Pines and Bohm theory⁽⁷⁴⁾. Thus the energy loss as the sum of the Pines-Bohm contribution and binary encounter with the electrons is results identical with those obtained through the more exact plasma dielectric theory. The contribution of the

bound electrons in the ions is evaluated using the Bethe theory.

The number of electrons per unit frequency having a revolution frequency ω of the bound electrons is given by^(10,12),

$$n(\omega) = (32\pi^2\omega^2 / m^2/\hbar^3) \int_0^{r_{\max}(\omega)} r^5 \left[\exp\left(\frac{(\frac{1}{2})m\omega^2 r^2 - eV(r) - H}{k_B T_e}\right) + 1 \right]^{-1} dr$$

$$\omega = (2/m)[E_t + eV(r)]^{1/2}/r, \quad (4.14)$$

where E_t means the total energy at point r (radius of cell), $V(r)$ the potential, H the chemical potential and $r_{\max}(\omega)$ is the radius where an electron with the energy of $\hbar\omega$ becomes free.

In Fig.18, the energy deposition profiles⁽¹⁰⁾ are shown. The plasma effect on the charge state of fast ions traveling through a plasma target under conditions relevant to ion-beam fusion has been calculated by Nardi and Zinamon.^(11,12)

The charge state of the projectile is determined by the competition between electron loss by collisions and capture from the target plasmas. The electron loss process in plasma targets is due to collisions with the ions and also with the free electrons. The capture of free electrons in plasmas takes place in the form of one of the following processes:(1) radiative recombination, (2) three-body recombination, or (3) dielectric recombination.

Collisions with target atoms or ions are given in the binary-encounter approximation(BEA).^(11,12) As shown in Figs.19-21, Nardi and Zinamon calculated the relation of the charge state versus the energy of the projectile as it is slowed down in the

target.

Using the quantum-mechanical form of the dielectric function,⁽⁶⁵⁾ Skupsky^(14,15) obtained the energy loss of ions in a high-density plasma of arbitrary degeneracy.

The logarithmic divergence in a classical plasma, which is expressed by writing the Coulomb logarithm in the form $\ln(b_{\max}/b_{\min})$, results in different kinds of the divergence. One approach is to describe the energy loss by means of two-body collisions using the Rutherford scattering, whereas the second approach treats the plasma as a continuous medium described by a dielectric function. It is necessary to introduce a cutoff parameter in order to prevent the logarithm from divergence. In determination of b_{\min} and b_{\max} , a standard way of combining the close and distant collisions has been briefly discussed by Skupsky.

For a quantum-mechanical plasma (i.e., r in which the inter-electron distance is less than the Bohr radius a_0 , i.e., $((4/3)\pi n)^{-1/3} < \hbar^2/me^2$), the particle-beam interaction can be treated by the random-phase-approximation (RPA). As this formula does not contain any divergent terms, this is valid at any velocity.

Skupsky has extended the dielectric function to arbitrary temperature and degeneracy in a high-density plasma. The energy loss of a charged particle passing through plasma can be represented by the dielectric function $\epsilon(\mathbf{k}, \omega)$ of the medium⁽¹⁴⁾:

$$\frac{dE}{dx} = \frac{Z_1^2 e^2}{2\pi^2 v} \int dk \frac{|\mathbf{k} \cdot \mathbf{v}|}{k^2} \text{Im} \left[\frac{1}{\epsilon(\mathbf{k}, \omega)} \right] . \quad (4.15)$$

The dielectric function in RPA is obtained from quantum-mechanical considerations⁽⁶⁵⁾:

$$\epsilon(\mathbf{k}, \omega) = 1 + \sum_s \frac{4\pi Z_s^2 e^2}{\hbar k^2} \int d\mathbf{v} \frac{f_s(\mathbf{v}) - f_s(\mathbf{v} - \hbar\mathbf{k}/m_s)}{\omega - \mathbf{k}\cdot\mathbf{v} + \hbar k^2/2m_s + i\delta}, \quad (4.16)$$

where the sum is made over all the charged species, and f_s is the single-particle distribution function for the unperturbed plasma. This expression is reduced to the classical form in the limit $\hbar \rightarrow 0$:

$$\epsilon(\mathbf{k}, \omega) = 1 + \sum_s \frac{4\pi Z_s^2 e^2}{m_s k^2} \int d\mathbf{v} \frac{\mathbf{k} \cdot \partial f_s / \partial \mathbf{v}}{\omega - \mathbf{k}\cdot\mathbf{v} + i\delta}. \quad (4.17)$$

The quantum-mechanical expression, eq.(4.16), provides a good description for the linear response of the plasma electrons for all wave number k ⁽⁶⁵⁾ whenever the average interparticle distance is less than the Bohr radius. For a DT plasma whose density is greater than 20 times solid density (10^{24} atoms/cm³)⁽¹⁴⁾, this condition [$((4/3)\pi n)^{-1/3} < a_0$] is satisfied.

Skupsky adopted the Fermi-Dirac distribution function and chose the degeneracy parameter η to satisfy the normalization condition. Skupsky obtained the real and imaginary parts of the dielectric function by means of the expansion of $\epsilon(\mathbf{k}, \omega)$ in the parameter $(\hbar k / 2m) / \langle v_e \rangle$: $\langle v_e \rangle$ is the average electron velocity. The energy loss to electrons finally can be obtained in the form, for small v ($v \ll \langle v_e \rangle$):

$$\frac{dE}{dx} = -\sqrt{E} n \frac{Z_1^2 e^4}{T_e^{3/2}} \left(\frac{m}{M}\right)^{1/2} \sqrt{\pi} \frac{8}{3} \left[\frac{\sqrt{\pi}}{2F_{1/2}(\eta)} \frac{1}{e^{-\eta+1}} \right] \ln \Lambda_{\text{RPA}}, \quad (4.18)$$

where M is the mass of an ion.

The function $F_{1/2}$ is the Fermi integral:

$$F_{1/2}(\eta) = \int_0^\infty \frac{\sqrt{x}}{e^{x-\eta} + 1} dx \quad (4.19)$$

and is related to the electron number density by

$$n = 4 \pi / \hbar^3 (2mT_e)^{3/2} F_{1/2}(\eta).$$

A factor $\ln \Lambda_{\text{RPA}}$ has been separated out to facilitate comparisons with other slowing-down formulas. Skupský formulated $\ln \Lambda_{\text{RPA}}$ for nondegenerate ($\eta < 1$), weak ($\eta \ll 1$) and strong degeneracy ($\eta \gg 1$) plasmas, and for the combinations by an interpolation formula. Figure 22 shows how $\ln \Lambda_{\text{RPA}}$ varies as a function of the temperature for different electron densities⁽¹⁴⁾.

Brysk⁽³⁹⁾ obtained a formula that interpolates between the limits of strong and weak degeneracies⁽¹⁴⁾. However, he had to introduce the Coulomb logarithm in a rather ad hoc manner. Skupský⁽¹⁵⁾ further developed the high density effects on thermonuclear ignition for ICF using his interpolation formula for $\ln \Lambda_{\text{RPA}}$ [see eq.(14) in Ref.(14)].

Dar et al.⁽¹⁶⁾ considered the slowing down of ions by a degenerate ultrahigh-density electron plasma ($n=10^{24}-10^{29} \text{ cm}^{-3}$) by means of RPA and, as a result, obtained the conditions for laser-driven chain-reaction fusion. In the Born approximation, the differential cross section for the ion scattering is given by

$$\frac{d^2\sigma}{d\Delta dk} = \frac{2Z_i^2 e^4 M}{E_i \hbar^3 k^3} S_{-k} \left(\frac{\Delta}{\hbar} \right), \quad (4.20)$$

where the ion initial energy $E_i = Mv^2/2$, the energy transfer

$\Delta = E_i - E_f$, $\hbar k$ is the momentum transfer, and the electron plasma form factor is

$$S_{\mathbf{k}}(\omega) = \int_0^\infty dt e^{i\omega t} \langle \rho_{\mathbf{k}}(t) \rho_{-\mathbf{k}}(0) \rangle. \quad (4.21)$$

Then the energy loss of the ion is given by

$$\frac{dE}{dx} = \frac{1}{V} \int \Delta d\Delta \int \frac{d^2\sigma}{d\Delta dk} dk, \quad (4.22)$$

where V is the volume of the plasma.

The plasma considered here is very dense, i.e.,

$$(4/3) \pi r_s^3 n > a_0^{-3}.$$

It is convenient to express the electron plasma form factor $S_k(\omega)$ in terms of the quantum-mechanical dielectric function $\epsilon(k, \omega)$:

$$S_k(\omega) = \frac{2\hbar v}{v_k} \text{Im} \left[\frac{1}{\epsilon(k, \omega)} \right], \quad (4.23)$$

where $v_k = 4 \pi e^2 / k^2$. $\epsilon(k, \omega)$ is given in eq.(4.17) or the form

$$\epsilon(k, \omega) = 1 - \frac{2v_k}{V} \sum_p \frac{f_{p+k} - f_p}{E_{p+k} - E_p + \hbar\omega} \quad (4.24)$$

(or see (eq.(7) in Ref.(17)),

where $E_p = \hbar^2 p^2 / 2m$ is the electron energy and f_p is the Fermi distribution.

Dar et al. calculated the energy loss for deuterons, tritons and α -particles using eq.(4.23). The results are shown in Fig.23. They have concluded from the slowing-down cross sections displayed in Fig.23 that (1) electrons in plasmas dominate the slowing-down process for densities much below 10^{27} cm^{-3} , but become negligible for densities much above 10^{28} cm^{-3} , and (2) somewhere between these two values lies the critical density for a fusion chain reaction.

On the other hand, Peres and Ron⁽¹⁷⁾ have treated the energy loss due to the ion-ion scattering in a dense plasma. This occurs when the velocities of the electrons are equal to those at

the Fermi surface (for degenerate electrons) or below the thermal velocity of the electrons (if they are nondegenerate). Their approach is due to the Born approximation treated in eqs.(4.20)-(4.24). They evaluated the collective screening effects which make the ion Coulomb cross section finite.

Sayasov^(18,19) calculated the stopping power for nonideal classical and degenerate quantum plasmas on the basis of local field theories. He found that correlational effects leading to a difference between the average field and local field may influence essentially the energy loss in such plasmas. The stopping power increases for both classical and quantum plasmas as a result of local fields effects. The energy loss of an ion using the dielectric function is given by eq.(4.15):

$$\frac{dE}{dx} = \frac{Z_1^2 e^2}{2\pi^2 v} \int dk \frac{\mathbf{k} \cdot \mathbf{v}}{k^2} \text{Im} \left[\frac{1}{\epsilon(\mathbf{k}; kv=\omega)} \right].$$

The longitudinal dielectric function including the influence of the collisional effects can be expressed by^(1,9)

$$\epsilon_L(\mathbf{k}, \omega) = 1 + \frac{k_d^2}{k^2} [1 + sZ(\zeta)] \quad (4.25)$$

$$s = \frac{\omega}{kv_{th}} \quad \zeta = \frac{\omega + i\nu_e}{kv_{th}}$$

where $k_d = 2^{1/2} \omega_p / v_{th}$, $Z(\zeta) = \pi^{-1/2} \int_{-\infty}^{\infty} \frac{e^{-Z^2}}{Z-\zeta} d\zeta$ and $v_{th} = (2T_e k_B / m)^{1/2}$ being the thermal velocity of the plasma electron, ν_e the collision frequency. Here it will be assumed that the projectile ions are swift enough, i.e., $v \gg (m/m_i)^{1/3} v_{th}$; m_i the mass of the plasma ion. This assumption allows to neglect the interaction between the projectile and the plasma ions.

(1) For a classical plasma: the longitudinal dielectric function takes the form:

$$\epsilon_{\ell}(\mathbf{k}, \omega) = 1 + \frac{Q_0}{1 - G(\mathbf{k})Q_0}, \quad (4.26)$$

$$Q_0 = \frac{k_d^2}{k^2} [1 + sZ(s)], \quad s = \frac{\omega}{kv_{th}} \quad (4.27)$$

and the function $G(\mathbf{k})$ is defined by the structure factor $S(\mathbf{q})$. This approach does not take into account the collisional effects. The appearance of the denominator $1 - G(\mathbf{k})Q_0$ in eq.(4.26) takes into account the local field effects. The structure factor $S(\mathbf{q})$ is rewritten by the local field correction as

$$G(\mathbf{k}) = - \int \frac{d\mathbf{q} d\mathbf{k}}{(2\pi)^3 n q^2} [S(|\mathbf{q} - \mathbf{k}|) - 1]. \quad (4.28)$$

Thus the stopping power can be derived from $\text{Im}[\epsilon^{-1}(\mathbf{k}, \omega)]$ in eq.(4.26) as

$$\frac{dE}{dx} = - \frac{4\pi n e^4 Z_1^2}{T} G\left(\frac{v}{v_{th}}\right) \left[1 + 2 \frac{g}{9} H\left(\frac{v}{v_{th}}\right)\right] \ln \Lambda, \quad (4.29)$$

$$g = \frac{1}{\frac{4}{3} \pi r_d^3 n} \quad (\text{plasma parameter}), \quad r_d = \left(\frac{T e}{4\pi n e^2}\right)^{1/2} \quad (\text{Debye-length}),$$

where the forms of the function $H(\xi)$ and the Coulomb logarithm are given in eqs.(20) and (21) in Refs.(18) and (19) by Sayasov.

If the collisional effects are allowed for introducing the collisional integral in the Boltzmann equation, the dielectric function is

$$\epsilon_{\ell} = 1 + \frac{k_d^2}{k^2} \frac{1 + \zeta Z(\zeta)}{1 + iyZ(\zeta)} \quad (4.30)$$

where $\zeta = (\omega + iv_e)/kv_{th}$, $y = v_e/kv_{th}$.

Therefore we obtain

$$\frac{dE}{dx} = - \frac{8 \sqrt{\pi} e^4 z_1^2 n v}{3 T_e v_{th}} \left(\ln \frac{1.2 T_e}{\hbar \omega_p} - \sqrt{\frac{\pi}{2}} \frac{v_e}{\omega_p} \right), \quad (4.31)$$

where

$$\frac{v_e}{\omega_p} = \sqrt{\frac{2}{\pi}} \frac{g}{9} \ln \left[1 + \left(\frac{3}{9} \right)^2 \right]^{1/2}.$$

The total stopping power is given by combination of eq.(4.29) and eq.(4.31).

(2) For a degenerate quantum plasma: the longitudinal dielectric function of an interacting electron gas can be defined as follows,

$$\epsilon_l(k, \omega) = 1 + \frac{Q_0}{1 - G(k)Q_0} \quad (4.32)$$

where Q_0 is the Lindhard polarisability⁽⁶⁷⁾ and $G(k)$ is the local field correction. Substituting eq.(4.32) into eq.(4.15), we can obtain the stopping power

$$\frac{dE}{dx} = - \frac{4 e^4 m^2 z_1^2 v C(r_s)}{3 \pi \hbar^3} \quad (4.33)$$

$$C(r_s) = \int_0^1 \frac{z^3 dz}{[(1 - \chi^2 g(z) f_1(z)) z^2 + \chi^2 f_1(z)]^2}, \quad g(z) = G(z) z^{-2}, \quad (4.34)$$

$$z = \frac{k}{2k_K}, \quad \chi^2 = \frac{e^2}{\pi \hbar v_F} = \frac{r_s}{\pi} \left(\frac{4}{9\pi} \right)^{1/3}$$

where $f_1(z) = 1/2 [1 + (1/2)(1/z) (1 - z^2) \ln \left| \frac{z+1}{z-1} \right|]$ for $z \leq 1$

is the function described in the Lindhard theory (see Ref.65 or Ref.67), $C(r_s)$ = the Lindhard's expression(13) in Ref.67 + the local field correction $G(z)$.

The real field including some local field contribution through the interaction of electrons differs from the average field considered in the Lindhard theory. In Fig.24, the coefficients $C(r_s) = -dE/dx / 4(e^4 m^2 v / 3\pi \hbar^3)$ against $r_s = [3 / (4\pi n a_0^3)]^{1/3}$ are shown along with available experimental values.

Ichimaru et al.⁽²⁰⁾ have treated the theory of interparticle correlations in dense and high-temperature plasmas. The stopping power of a dense two-component plasma has been calculated from the dielectric formulation of eq.(4.15). The static and dynamic local field correlations describing strong Coulomb-coupling effects beyond the RPA are explicitly taken into account.

Cover et al.⁽²¹⁾ examined the effect of the collective excitations to the stopping power of a fast ion in a degenerate electron-ion plasma. Let us assume the ions form a classical plasma at a temperature T_i . Using the energy loss formula, eq.(4.15), described by the longitudinal dielectric function for the low-frequency ion, Cover et al. obtained $(dE/dx)_{co}$ (contribution from collective modes) and $(dE/dx)_{ip}$ (individual-particle contribution). In Fig.25, their calculational results of the ratio $(dE/dx)_{co} / (dE/dx)_{ip}$ vs the density for a 3.5 MeV α -particle incident on a deuterium plasma with an ion temperature of 50 keV are given. The collective contribution to the ion stopping power at densities anticipated in the laser-fusion domain is not significant.

Deutsch et al.⁽²²⁻²⁶⁾ have paid a special attention to the stopping power and straggling of nonrelativistic ions as ICF driver in dense and hot matters. Their approach is based on the RPA with an exact dynamic dielectric function valid at any temperature. The density of the free-electron fluid is given as

$$r_s = [(4/3) \pi n]^{-1/3} a_0^{-1} \leq 1.$$

They have taken advantage of an exact RPA- $\epsilon(k, \omega)$ ⁽²⁴⁾ at any v/v_F ratios, though the works of Arista and Brandt⁽²⁷⁾, and Skupsky⁽¹⁴⁾ were mostly devoted to small v/v_F values. The partial degeneracy effect may be worked out through a simplified⁽⁹⁾ low-frequency form of the RPA- $\epsilon(k, \omega)$.

The stopping power using the Lindhard formula reads

$$\frac{dE}{dx} = \frac{4 \pi Z_1^2 e^4}{m v^2} nL, \quad (4.35)$$

$$L = \frac{6}{\pi X^2} \int_0^{v/v_F} u du \int_0^\infty \frac{z^3 X^2 f_2(u, z)}{[z^2 + X^2 f_1(u, z)]^2 + [X^2 f_2(u, z)]^2} dz \quad (4.36)$$

in terms of the standard dimensionless units

$$z = \frac{k}{2 k_F}, \quad u = \frac{\omega}{k v_F}, \quad X^2 = \frac{\alpha r_s}{\pi} = 0.5211.$$

Maynard and Deutsch⁽²³⁾ generalized eqs.(4.35)-(4.36) to any temperature or degeneracy. The generalization is carried out in eqs.(3),(4),(7) and (8) in Ref.(23), and others.^(21,24-26)

The effect of the temperature is especially noticeable at low velocities, which allow us to visualize the discrepancies of

the complete calculations by Deutsch et al. with respect to the $T=0$ calculations.⁽⁶⁷⁾ The corresponding dE/dx is displayed in Fig.26. The stopping power exhibits the important temperature effects around $T_e \sim 1$ for ions of a few MeV per nucleon, an energy range typical of heavy ions used in ICF.

In Figs.27-28 a few significant examples are displayed, for the range

$$R = \int_0^x dx = \int_{E_0}^{E_0/10} \frac{dE}{\left(\frac{dE}{dx}\right)} \quad (4.37)$$

and for the deposition time

$$t_{\text{deposit}} = \int_{t_0}^{t_1} dt = - \int_{E_0/10}^{E_0} \frac{dE}{\left(\frac{dE}{dx}\right) v} \quad (4.38)$$

where E_0 denotes the projectile incident energy at the pellet.

Arista and Brandt⁽²⁷⁾ and Deutsch et al.⁽²²⁾ have treated the energy loss problem using the following ways: the scattering rate

$$R(\mathbf{k}, \omega) = \left(\frac{4 \pi Z_1^2 e^2}{k^2} \right)^2 \frac{2\pi}{\hbar^2} S(\mathbf{k}, \omega) \quad (4.39)$$

and the dynamic structure factor

$$S(\mathbf{k}, \omega) = \frac{-\hbar k^2}{4\pi^2 e^2} N(\omega) \text{Im} \left[\frac{1}{\epsilon(\mathbf{k}, \omega)} \right] \quad (4.40)$$

where $N(\omega) = [\exp(-\theta \hbar \omega) - 1]^{-1}$ and $\theta = 1/k_B T_e$.

Therefore, the energy loss rate is given by

$$\begin{aligned} \frac{dE}{dt} &= - \int \frac{d\mathbf{p}'}{(2\pi \hbar)^3} \hbar \omega R(\mathbf{k}, \omega) \\ &= \left(\frac{Z e}{\pi} \right)^2 \int d^3 \mathbf{k} \frac{\omega N(\omega)}{k^2} \text{Im} \left[\frac{1}{\epsilon(\mathbf{k}, \omega)} \right] \end{aligned} \quad (4.41)$$

where $\hbar \omega(\mathbf{p}, \mathbf{k}) = E(\mathbf{p}') - E(\mathbf{p}) = \hbar \mathbf{k} \cdot \mathbf{v} + \hbar q^2 / (2M)$ in terms of the incident velocity $\mathbf{v} = \mathbf{p}/M$. For heavy projectiles $M \gg m$, the recoil effects are small and we can expand eq.(4.41) in terms of $\Delta\omega = \hbar k^2 / 2M$ to obtain

$$\frac{dE}{dt} = \left(\frac{dE}{dt}\right)_0 + \left(\frac{dE}{dt}\right)_1 + \dots, \quad (4.42)$$

where

$$\left(\frac{dE}{dt}\right)_0 = - \left(\frac{Ze}{\pi}\right)^2 \int d^3k \frac{\omega N(\omega)}{k^2} \text{Im} \left[\frac{1}{\epsilon(\mathbf{k}, \omega)} \right] \Big|_{\omega = \mathbf{k} \cdot \mathbf{v}}. \quad (4.43)$$

Finally the stopping power S is

$$\begin{aligned} S &= - \frac{dE}{dX} \simeq - \frac{1}{V} \left(\frac{dE}{dt}\right)_0 \\ &= - \frac{2}{\pi} \left(\frac{Ze}{V}\right)^2 \int_0^\infty \frac{dk}{k} \int_0^\infty d\omega \omega \text{Im} \left[\frac{1}{\epsilon(\mathbf{k}, \omega)} \right]. \end{aligned} \quad (4.44)$$

For nondegenerate plasmas, $k_B T_e \gg \hbar \omega$, they made an approximation to S and $\Omega^{\frac{1}{2}}$:

$$\Omega^2(V, n, T_e) \simeq 2k T_e S(V, n, T_e). \quad (4.45)$$

Brandt⁽²⁸⁾ reviewed a series of problems in low-velocity stopping power physics in 1981. He concentrated on three topics of them: (1) the material dependence of low-velocity stopping powers, (2) the effective charge q^* of atomic projectiles as defined by the stopping power of matter, (3) the change of stopping powers in the transition from degenerate to nondegenerate plasmas. This change will occur in controlled fusion devices.

Measurements⁽²⁹⁾ of energy losses $\Delta E_{\text{He}} / \Delta E_{\text{D}}$ of ${}^2_1\text{D}$ and ${}^4_1\text{He}$ ions in solids, covering their entire range of r_s values, reveal

the pronounced target effects that diminish with increasing the ion velocity (see Fig.1 in Ref.(29) or Fig.3 in Ref.(28)).

Schulz and Brandt⁽³⁰⁾, and Brandt⁽³¹⁾ derived the effective charge fraction,

$$\zeta \equiv \frac{q^*}{Z_1} \approx \frac{1}{Z_1} \left(\frac{S}{S_p} \right)^{\frac{1}{2}} \quad (4.46)$$

in a dielectric response approximation and tested the predictions on new low-velocity precision experiments and high-velocity channeling experiments. Brandt obtained ζ in the form:

$$\zeta(v_r) \approx q(v_r) + C(r_s) \left[1 - q(v_r) \right] \ln \left[1 + \left(\frac{4\Lambda(v_r)^2}{r_s} \right) \right], \quad (4.47)$$

where

$$V_r(v, V_F) = \begin{cases} \frac{3}{4} V_F \left(1 + \frac{2}{3} V^2/V_F^2 - \frac{1}{15} V^4/V_F^4 \right) & \text{for } v \leq V_F \\ v \left(1 + \frac{1}{5} V_F^2/v^2 \right) & \text{for } v_F \leq v, \end{cases} \quad (4.48)$$

$$\Lambda(v_r) \approx \frac{[1 - q(v_r)]^{2/3}}{2 Z_1^{1/3} \left\{ 1 - \frac{1}{7} [1 - q(v_r)] \right\}} \quad (4.49)$$

$C(r_s) \approx 0.5$ for most metals and

$q(v_r) = Q(v_r)/Z_1$; $q = Q/Z_1$, if the ion carries N electrons, the ionic charge $Q = Z_1 - N$.

The effective charge of slow ions in solids with a mean relative velocity between the ion and electron was represented by Kreussler et al.⁽²⁹⁾ On the other hand, a general expression for the effective charge of slow ions in dilute plasmas at the temperature T was obtained by Arista and Brandt.⁽³³⁾ For swift ions

in condensed matters, Brandt and Kitagawa⁽³²⁾ also calculated the effective charge based on a dielectric-response approximation. According to the theory of Arista and Brandt, the effective charge of slow ions in dilute plasma, for all ions with $Z_1 \geq 5$, can be obtained from

$$q^* = Z_1 (1 - e^{-bx}) \quad (4.50)$$

with $x = (3k_B T_e / m)^{1/2} Z_1 v_0$, v_0 the Bohr velocity and $b=3.5$ for $v < v_{th}$.

Moreover, they discussed the charge dependence of the energy loss of slow ions with velocities $v < v_{th}$ and the charge Ze ($Z \leq Z_1$, Z_1 is the atomic number) in a plasma, using a quantum-mechanical treatment. The ion velocity v is replaced by a mean relative velocity between the ion and the electrons. The relative velocity is given by the thermal electron velocity $v_{th} = (3k_B T_e)^{1/2}$, since $v < v_{th}$.

The energy loss is given in the form:

$$\frac{dE}{dx} = \frac{16\sqrt{\pi}}{3} \frac{n Z_1^2 e^4 v}{m} \left(\frac{m}{2k_B T_e} \right)^{3/2} L(n, T_e, Z) \quad (4.51a)$$

for the collision logarithm

$$L(n, T_e, Z) = \ln \left[\frac{4 (k_B T_e)^{3/2}}{Z e^2 m^{1/2} e^{1/2} \omega_p} \right] - 2\gamma - \frac{1}{2} - \frac{1}{2} e^\gamma E_1(\gamma) \quad (4.51b)$$

Here $E_1(\gamma)$ is the exponential integral of argument

$$\gamma = \left(\Gamma Z_1 e^2 / \hbar v_e \right)^2 = \Gamma^2 Z_1^2 m v_0^2 / 2 k_B T_e, \quad v_e = (2/3)^{1/2} v_{th},$$

$$\gamma = 0.577, \quad \Gamma = e^\gamma = 1.78, \quad \text{and} \quad \omega_p = (4\pi n e^2 / m)^{1/2}.$$

In the limit of high temperatures ($k_B T_e \gg Z^2 m e^4 / \hbar^4$), L becomes independent of the ion charge, i.e.,

$$L_{\text{QMPT}}(n, T_e) = \ln\left(\frac{k_B T_e}{\hbar \omega_p}\right) + \frac{1}{4} \quad (4.52)$$

where quantum-mechanical perturbation theory (QMPT) is applied under the condition $\xi \equiv q^* e^2 / \hbar v_{\text{th}} \ll 1$. This result follows from eq.(4.51) for $y \rightarrow 0$, the exponential integral $E_1(y) = -\Upsilon - \ln y$ and the approximation $(3/2)\ln 2 - (1/2)\Upsilon - (1/2) \approx 1/4$.

This is also in an exact agreement with the result obtained from the $\mathcal{E}(k, \omega)$ formalism for a nondegenerate quantum plasma (see eq.(23) in Ref.(27)). In the classical limit $\xi \equiv q^* e^2 / \hbar v_{\text{th}} \gg 1$, (i.e. $k_B T_e \ll Z_1^2 m e^4 / \hbar^2$), we then obtain

$$L_{\text{CL}}(n, T, Z) = \ln\left[\frac{4(k_B T_e)^{3/2}}{Z_1 e^4 m^{1/2} \omega_p}\right] - 2\Upsilon - \frac{1}{2} \quad (4.53)$$

Arista and Brandt discussed the transition between the classical and quantum-mechanical approximation and explained physically its condition. The transition will take place when $L_{\text{CL}}(n, T_e, Z) = L_{\text{QMPT}}(n, T_e)$ at the temperature $T_c = 2.82 Z^2 m e^4 / \hbar^2 k_B = Z^2 \times 10^6$ K. They have obtained the effective charge in the form

$$q^* = Z_1 f(t) \quad (4.54)$$

$$f(t) = 1 - \exp(-at^{1/2}),$$

where $a = \sqrt{3} b \cong 6$ and t is a reduced variable defined as $t = k_B T_e / Z_1^2 m v_0^2$ with $k_B T_0 = m e^4 / \hbar^2 = 1$ a.u., ($T_0 = 27.2$ eV/ $k_B = 3.16 \times 10^5$ K). Setting $Z = q^* = Z_1 f(t)$, they found a useful scaling of eq.(4.51) in terms of t :

$$L(n, T, Z) = L_{\text{QMPT}}(n, T) + \Delta L(t), \quad (4.55)$$

$$L(t) = \ln[4t^{1/2}/f(t)] - 2\Upsilon - 3/4 - (1/2)e^y E_1(y) \quad (4.56)$$

with $y = \Gamma^2 f^2(t)/2t$. For fully stripped ions, then $Z=Z_1$ by setting $f(t)=1$.

Values of collision logarithm $L(n, T_e, Z)$ as calculated by eqs.(4.55) and (4.56), are shown in Fig.29.

The application of Lindhard's dielectric theory to real solids becomes a formidable task since the direct numerical integration of the Lindhard stopping formula is slow and cumbersome due to the presence of singularities in the integrand. Numerical evaluation of Lindhard's theory of stopping power for a charged particle in a free-electron gas was first made by Iafrate and Ziegler⁽³⁴⁾.

For an ion of charge $Z_1 e$ (bare nuclear point charge) moving with velocity v in a medium of uniform density n , the energy loss due to electron excitation can be written in the form^(65,67)

$$-\frac{dE}{dx} = \frac{4\pi}{m} \left(\frac{Z_1 e^2}{v} \right)^2 nL(n, v), \quad (4.57)$$

where L is called the stopping number. In the dielectric formalism, L is written as

$$L = \frac{i}{\pi \omega_p^2} \int \frac{dk}{k} \int_{-kv}^{kv} \omega d\omega \left[\frac{1}{\epsilon(k, \omega)} - 1 \right], \quad (4.58)$$

where $\omega_p^2 = 4\pi n e^2/m$.

Lindhard obtained the dielectric function for a free-electron gas within the first-order perturbation theory.

The Lindhard stopping number can be written in the form

$$L = \frac{6}{\pi} \int_0^{v/v_F} u du \int_0^\infty \frac{z^3 f_2(u, z) dz}{[z^2 + \chi^2 f_1(u, z)]^2 + [\chi^2 f_2(u, z)]^2} \quad (4.59)$$

where the parameter $\chi^2 = v_0 / \pi v_F$, the reduced variables $z = k / 2k_F$ and $u = \omega / kv_F$, and for $f_1(u, z)$ and $f_2(u, z)$ and the method of derivation of equations, see eqs.(1)-(11) in Ref.34, or Ref.35, or also eqs.(4.1)-(4.12) in Ref.(65).

In Fig.30, the calculational results in stopping number with the electron density and energy are shown.

Moreover, Iafrate et al.⁽³⁵⁾ evaluated the Lindhard dielectric theory of stopping power within the local density approximation of Lindhard and Scharff⁽⁶⁴⁾ and the concept of the effective charge.

In the local density approximation, each volume element of the solid is considered to be an independent plasma of uniform density, so that the total electronic stopping power is given by

$$-\frac{dE}{dx} = \frac{4\pi}{m} \left(\frac{Z_1 e^2}{v} \right)^2 \int_0^\infty n(r) L(n, v) 4\pi r^2 dr, \quad (4.60)$$

where $n(r)$ is the spherical averaged charge density of the target atom. They used the spherically averaged solid-state charge densities in evaluating eq.(4.60). Inspection of Figs.31-32 shows that the stopping number integrand of eq.(4.60) approximately follows the radial charge density in spatial variation. It should be noted that the low-energy (100 keV/amu) projectile stopping number is influenced mainly by the outer shell electron charge distribution, whereas the high-energy projectile (10000 keV/amu) stopping number is dependent on the inner electron shells as well (see Fig.2 in Ref.(24)).

When the projectile is an ionized atom with an intrinsic electronic charge distribution, the question of the net charge of

the projectile arises.

Ziegler⁽³⁷⁾ made the effective charge q^* in the form

$$\frac{q^*}{Z_1} = 1 - [\exp(-A)] [1.034 - 0.1777 \exp(-0.08114 Z_1)], \quad (4.61)$$

where

$$\begin{aligned} A &= B + 0.0378 \sin \frac{1}{2} \pi B \\ B &= 0.886(40E/M)^{1/2} / Z_1^{2/3}, \end{aligned} \quad (4.62)$$

where the ion energy E is in MeV, and the ion mass M is in amu.

Ziegler⁽³⁶⁾ calculated the stopping power of energetic ions in matter (energies above 200 keV/amu) using the method in the preceding discussions. He also presented new calculations for mean ionization potentials, $\langle I \rangle$, and correction parameter, λ , for the traditional $\langle I \rangle$ in comparison with experiments. The mean ionization potential is expressed in the local density approximation in the form:

$$\ln \langle I \rangle = \frac{1}{Z_2} \int_0^v n_c \ln(\lambda \hbar \omega_p) dV, \quad (4.63)$$

where Z_2 is the total electron charge, and λ is some constant of the order of unity, i.e., $\lambda = 1 \sim \sqrt{2}$, and n_c the charge density. Table 1 in Ref.(36) shows calculations of the mean ionization potential, $\langle I \rangle$, for solid density and gases $Z=1-92$, using eq.(4.63) and average values of λ .

Sigmund and Fu⁽³⁸⁾ evaluated the energy loss straggling of a point charge penetrating a free-electron gas based on the Lindhard dielectric function. With regard to straggling, Bonderup's formula has been partially confirmed, but it was found

that this correction is important in numerical applications. The correction is substantial for ion velocity v which approaches v_F , in particular at high electron densities, i.e., for

$$\chi^2 = e^2 / (\pi n v_F) \ll 1.$$

§ 5. Theory of Stopping Power based on Kinematic Description

In order to calculate the energy loss of a projectile as it passes through a plasma, it is necessary to specify the distributions of various plasma species, i.e., how many particles at point r and time t have velocity v . The time evolution of the distribution function is described by a kinetic equation whose collision term is appropriate for the plasma conditions under consideration.

Expressions were derived by Brysk⁽³⁹⁾ for the stopping power of a fast ion in a plasma from the kinematic description of an elastic collision between two bodies. The kinematic basis use the Rutherford cross section. The energy loss was calculated in full degeneracy ($T_e \rightarrow 0$) using the Fermi distribution and in the opposite limit using the Maxwell distribution.

For ICF-plasma, the application of the Lenard-Balescu equation^(76,77) or a quantum-mechanical version was proposed by Gould and Dewitt⁽⁷⁸⁾. The quantum Lenard-Balescu equation can be interpreted as a Boltzmann equation describing collision between two quasiparticles which interact via the dynamically shielded

Coulomb potential. It treats both close and distant collisions correctly, and requires no ad hoc cutoffs.

By the use of the Lenard-Balescu kinematic equation, Lampe⁽⁴⁰⁾ treated the number and mean energy loss of electrons scattered through small angles for a tenuous monoenergetic electron beam incident on a quiescent plasma.

Sigmar and Joyce⁽⁴²⁾ developed a formalism for a tenuous energetic test-particle (species) with a multispecies of high temperature plasma. Their calculations contain suitable quantum corrections for large angle scattering, i.e., for close collisions. The theory was applied to the slowing down of fusion-born α -particles in a mirror-confined plasma ($T_i=100$ keV, $T_e=50$ keV, $n=10^{14}$ cm⁻³). Then the theory and numerical results were compared to the α -particle slowing down in Tokamak electron-deuteron plasma ($T_i=4$ keV, $T_e=6$ keV, $n=10^{14}$ cm⁻³) and the injected proton slowing down in Tokamak electron-proton plasma ($T_i=0.5$ keV, $T_e=1$ keV, and $n=5 \times 10^{13}$ cm⁻³).

On the other hand, Payne and Perez⁽⁴¹⁾ derived an expression for the energy loss of a beam of particles passing through an inhomogeneous plasma which includes the effects of departures from local equilibrium due to gradients in the plasma.

A combination of the test-particle approximation with the Lenard-Balescu collision term and the Bhatnagar-Gross-Krook(BGK) approximation⁽⁷⁹⁾ for the plasma kinetic equation is used. Calculations for an α -particle beam with energies from 0.5 to 4.5 MeV in a fully ionized hydrogen plasma were presented.

The effects due to temperature gradients produce a sizeable

change in plasma stopping power. The largest changes are found at high temperatures ($\gtrsim 1$ keV) and at low α -particle energies ($\lesssim 1$ MeV) (see Fig.4 in Ref.(41)). These nonequilibrium conditions can be directly observed if the energy loss of a probe beam is measured at various angles with respect to the plasma gradients.

§ 6. Collective, Vicinage and Beam-Density Effects in Stopping Power by Ion Clusters

Efficient coupling of beam energy to a target medium is of crucial importance to the viability of ICF. The energy deposition enhancements are attributed to several phenomena: (a) the increase of effective path length in the target by applied or self-generated fields, (b) collective beam-target interactions,^(80,81) (c) modification of the single-particle deposition rate because of the finite target temperature,^(1,3,10) and (d) beam-density effect.⁽⁸²⁾

The origin of the beam-density effect is the two particle vicinage, or proximity, contribution to energy loss.

Rule and Crawford⁽⁴⁵⁾ presented an analytic expression for nonrelativistic vicinage function and showed that it would have a dipolelike behavior for large separations between beam particles (Z_i, Z_j). A pair of particles separated by R_{ij} have total energy loss per unit path length W_{ij} which can be written as the sum of the usual single-particle terms $W_s = Z^2 S$ plus the vicinage term $W(R_{ij})$:

$$W_{ij} = Z_i^2 S_p + Z_j^2 S_p + W(R_{ij}) \quad (6.1)$$

where Z_i , and Z_j are the nuclear charge and S_p is the stopping power of a proton.

Let us consider the i -th particle in a beam consisting N particles, then the total energy loss by these particles is

$$W = W_s + W_B, \quad (6.2)$$

where

$$W_B = \frac{1}{2} \sum_{j=1}^N W(R_{ij}), \quad j \neq i \quad (6.3)$$

is the contribution from cooperative energy loss, or the beam-density term⁽⁸²⁾, i.e., W_B is the proximity, or vicinage term for loss by a pair of relativistic particles.⁽⁴³⁾

Figure 33 shows the ratio of the beam-density contribution W_B to single-particle energy loss W_s versus the distance of a beam particle from the beam front on the beam axis. The curves were calculated for a 5-MeV proton beam of 10 kA with a Gaussian radial profile.

The total energy loss is also written by the resonant term plus the nonresonant term:

$$W = W_R + W_N, \quad (6.4)$$

(see eqs.(12) and (13) in Ref.(45)).

Rule and Cha⁽⁴³⁾ derived the collective effects in energy loss by relativistic clusters of charged particles using a classical description . Extension of Fermi's method in it for deriving the density effects is used^(43,45).

Basbas and Ritchie⁽⁴⁴⁾ analyzed theoretically the vicinage effects for ion diclusters penetrating an electron gas and in collision with single atoms. They discussed similarities between

the vicinage function for energy loss of a swift cluster in an electron gas and that for the same cluster colliding with a system of noninteracting atoms at condensed-matter density.

§ 7. Experiments and Model Calculations of Stopping Power and Effective Charge

Knowing the effective charge of the projectile ion is very important for the stopping power calculations in heavy-ion driven ICF target.

The stopping power of a medium for a point-like projectile of the charge $Z_1 e$ may be expressed as

$$\frac{dE}{dx} = nZ_2 \frac{4 \pi Z_1^2 e^4}{mv^2} L(Z_1, Z_2, v). \quad (7.1)$$

For partially stripped, high-energy heavy ions, Z_1 in the dE/dx formula should be replaced by an effective charge q^* .

Both the density effect and plasma temperature effect in its charge arise through changes in charge-changing cross sections.

Cowern⁽⁴⁷⁾ determined the effective stopping power charge q^* for partially stripped ions by a balance of the electron capture and loss cross sections within the stopping medium. The density effect on charge-changing process is discussed by the genuine gas-solid density effects. The limiting cases of a low-density target ($n \rightarrow 0$) "gas target" and high density target ($n \rightarrow \infty$) "solid target" are assumed in the evaluation of charge-changing cross section.

In measurements on stopping power for 0.5-10 MeV/amu heavy ions in solids and gases, Geissel et al.⁽⁴⁸⁾ demonstrated some characteristics of the effective charge, which is defined by

$$S_{HI,v,Z_2} = (q^*)^2 S_{p,v,Z_2} \quad (7.2)$$

where S_{HI,v,Z_2} and S_{p,v,Z_2} are the stopping powers of heavy ions and protons at the same velocity v in the same medium Z_2 .

The effective charge characterizes the average equilibrium charge of an ion during its slowing down process, implying that q^* should be equal to the root-mean-square of the average equilibrium charge distribution

$$\bar{q} = [(\sum_i \phi_i q_i)^2]^{1/2}, \quad (7.3)$$

where ϕ_i is the fraction of the ions in charge state q_i .

The basic assumption in this statement is that the partially stripped heavy ion interacts with the target electrons as a point charge. This assumption has been supported by data in gases, but for solid targets \bar{q} has been found to be larger than q^* .

Figures 34 and 35 show that the stopping powers and the effective charge extracted from measured stopping powers of heavy ions depend clearly on the stopping medium. Figure 36 shows a comparison of the experimental values of q^* and \bar{q} for 1.4 MeV/amu Kr, Xe, Pb, and U ions in Ar. It is demonstrated that the agreement for relatively light ions, Kr, is good, whereas for the heavier projectiles, \bar{q} is larger than q^* . For U and Pb ions, the difference is about 15%. Stopping power of (0.5-1.3) MeV/amu Pb, Xe, and Kr ions in solids and gases are shown in Fig.3 in Ref.48(1982).

Stopping power calculations for heavy ions of (1-100) GeV energy and results of 1D and 2D simulations of the stretched target cylinders heated by intense heavy ion beams have been presented by Arnold and Meyer-ter-Vehn⁽⁴⁹⁾. Such experiments in the hot dense matters are planned at GSI.

Anthony and Lanford⁽⁵⁰⁾ measured the stopping powers of several heavy ions (C, Si, Cl, Ti, Fe, Ni, Ge, Br, Nb, and I) in elemental targets (C, Al, Cu, Ag, and Au) at energies near the maximum in the stopping power versus energy curve (see Figs.3-7 in Ref.(50)). From these measurements, the effective charges of ions are examined. Both of the magnitude and the target dependence of the effective-charge expression:

$$\frac{\bar{q}}{z_1} = 1 - A \exp\left(\frac{-\lambda v}{v_0 z_1^\gamma}\right), \quad \gamma = \frac{2}{3} \quad (7.4)$$

are consistent with average equilibrium charge state measurements made in gases (see the effective charge parameter A and λ of Table II in Ref.(50)).

Bailey et al.^(51,52) presented the time dependent charge state of a heavy projectile traversing a finite temperature plasma target by means of the average-atom model to integrate the rate equation.

The charge state of the projectile is determined by the competition between electron loss by collisions and capture from the bound electrons in the target atom^(11,51) listed as follows:

Electron Rates: bound-bound excitation and de-excitation
 bound-free ionization
 radiative recombination
 3-body recombination

Ion Rates: bound-bound excitation and de-excitation
 bound-free ionization.

The result of solving the rate equations for various projectile ions with an energy of 46 MeV/amu (corresponding to 9 GeV for an Au-ion) is shown in Fig.37(a) for electron-ion excitation and in Fig.37(b) for ion-ion excitation for a target ion with a q^* of 10. For such fast ions, the equilibrium charge state is very close to the fully stripped ion in all cases, although the time to reach equilibrium increases with projectile Z_1 . The equilibrium time decreases for the ion-ion case (Fig.(37b)). The equilibrium charge is almost identical to the electron-ion case.

Brice⁽⁵³⁾ made a formalism of the electronic stopping cross section over low-high energy ranges using three adjustable parameters, i.e., one from the modification of the Firsov formalism and two from the extension to higher velocities.

$$S_e(u) = (Z_1 + Z_2) S'_e(u) f(u)$$

$$S'_e(u) = \frac{4\hbar^2}{5m} \left[\sqrt{\epsilon} \left(\frac{30\epsilon^3 + 80\epsilon^2 + 74\epsilon + 21}{3(1+\epsilon)^3} \right) + (10\epsilon + 1) \cdot \tan^{-1} \sqrt{\epsilon} \right] \quad (7.5)$$

$$\epsilon = (u/2v_0Z)^2 \quad (7.6)$$

$$f(u) = [1 + (au/v_0)^n]^{-1}, \quad (7.7)$$

where the parameter is given by $a=v_0T/\ell$. Since v_0T and ℓ are of the order of the length of the atomic dimensions it is expected that $a \cong 1$. The parameters a and n appearing in $f(u)$ and the parameter Z (nuclear effective charge) in $S'_e(u)$ are considered as adjustable parameters to be determined by experiment (see Tables

I and II in Ref.(53)).

Recently Grygoriev et al.⁽⁵⁴⁾ proposed a model which accounts for three proton mechanisms, i.e., energy losses due to strongly bound electrons, excitation of collective free electron oscillations, and individual collisions with weakly bound electrons.

The total stopping cross section S_{tot} consists of two independent subsystems: inner-shell electrons (core electrons) S_c and free electrons forming a dense plasma S_f .

$$S_{tot} = S_c + S_f. \quad (7.8)$$

It is assumed that the value of S_c is the sum of electronic stopping powers for different subshells,

$$S_c = \sum_{n,l} \omega_{nl} S_{nl}, \quad (7.9)$$

where ω_{nl} is the number of electrons with the quantum numbers n, l in an atom:

$$S_{n,l} = 4\pi \int_0^\infty v_{n,l} |\Psi_{nl}(v_{nl})|^2 dv_{nl} \int_{U_{nl}}^{E_{max}} \frac{d\sigma}{d(\Delta E)} \Delta E d(\Delta E), \quad (7.10)$$

where v_{nl} is the electron velocity, $\Psi_{nl}(v_{nl})$ the electron wave function in momentum representation, $d\sigma/d(\Delta E)$ the cross section for transfer of energy E from a proton moving with velocity v to an electron with velocity v_{nl} .

The stopping cross section for an electron plasma is given by

$$S_f = S_{eh} + S_{pl}, \quad (7.11)$$

where the energy loss S_{eh} is due to the electron-hole generation

$(-dE/dx)_{eh}$ and S_{pl} due to plasmon excitation $(-dE/dx)_{pl}$.

In studying different processes accompanying the ion penet-

ration in matter, Burenkov et al.⁽⁵⁵⁾ proposed a model based on the first principle calculation of the inelastic energy loss of heavy ions in different targets for any nonrelativistic projectile energy. Two stopping mechanisms were taken into account: (1) Energy loss to excitation or ionization of the target electrons by the partially screened field of the moving ion nucleus is calculated in BEA. (2) Energy to electron exchange is calculated on the basis of the modified Firsov theory taking into account the electron-electron scattering. Figure 38 shows the calculated stopping cross sections and the contribution of electrons in the medium. Figure 39 presents the calculated results for the stopping cross sections, together with experimental data.

Ferrariis and Arista⁽⁵⁶⁾ calculated the energy loss of charged particles in nondegenerate plasmas using the classical and quantum-mechanical approximations. They considered the classical binary collisions between the test particle and the particle in the plasma, and obtained the energy transferred as a function of the relative velocity. Furthermore, they used the quantum-mechanical analysis of the scattering of partial waves to find the transport cross section for a screened potential, and introduced analytical approximations to calculate the phase shifts. Their study yielded a simple expression for the energy loss in terms of the velocity and charge of the particle and of the density and temperature of the plasma.

For ions with high velocities, $v \gg v_{th} (= [2k_B T_e / m]^{1/2} = \text{electron thermal velocity})$, the plasma stopping power is given by

$$-\frac{dE}{dx} = \frac{4\pi n Z_1^2 e^4}{mv^2} \ln \Lambda(v, Z_1) \quad (7.12)$$

and for low velocities, $v \ll v_{th}$,

$$-\frac{dE}{dx} = \frac{16\sqrt{\pi} n Z_1^2 e^4 \sqrt{m} v}{3(2k_B T_e)^{3/2}} \ln \Lambda(v_{th}, Z_1). \quad (7.13)$$

Simple expressions for the velocity-dependent collision logarithm $\ln \Lambda$ can be given in each case using either the classical or quantum-mechanical (plane wave) approximation. In particular, in the impact-parameter description the result is given in Table I in the form $\ln \Lambda = \ln(b_{max}/b_{min})$.

Treatments of the maximum and minimum impact parameters have been discussed in detail (see eqs.(3)-(6) in Ref.(56)).

Tahir and Long⁽⁵⁷⁾ considered various aspects of heavy ion-beam ICF. They used an energy deposition code GORGON which has been written based on the macroscopic interactions responsible for the slowing down of ions in materials. Some details of this code have been described.^(9,10,57) The formulae depend on the shape factor and range, but do not in turn depend on temperature and density, as it would do in more detailed calculations.

Wright et al.⁽⁵⁸⁾ developed a model to study two loss mechanisms during the propagation of high-power beams of C-ions in the current-carrying air-plasma channels. Such channels can provide the necessary standoff between the diode and the target in light-ion-driver ICF. They considered that particle energy losses are due to the radial charge-exchange diffusion across the channel magnetic field and the collisions with target particles.

Semiempirical charge exchange cross sections were derived

from literature sources and used in a 3-D Monte Carlo transport code with the energy loss modeled in the continuous slowing down approximation. They concluded that the charge exchange losses would probably not be of major concern for light-ion-beam ICF reactor configurations using channel transport, whereas the collisional energy loss could be detrimental to the ICF reactor if the plasma channel density is too large.

Santarius and Callen⁽⁵⁹⁾ solved the bounce averaged Fokker-Planck equation for α -particles slowing down in a background plasma of electrons and ions in the central cell of a tandem mirrors.

The density-effect correction for the ionization energy loss of charged particles has been evaluated⁽⁶⁰⁾ as a function of the particle velocity for total of 278 substances in ATOMIC DATA AND NUCLEAR DATA TABLES. In the calculations, the up-to-date values of $\langle I \rangle$ and the atomic absorption edges $h\nu_i$ were employed as input data for the general equations of the density effect correction.

Beynon⁽⁶¹⁾ presented a formalism for obtaining the energy deposition distribution function for an ICF target irradiated with multiple ion beams. In evaluating the target performance, Beynon concluded that the geometry of the multiple beam, i.e., "beamlet" geometry might be as important as the detailed description of the slowing down processes contained in the stopping power of the medium.

A few-beam irradiation produces rapidly fluctuating energy deposition profiles, which are significantly smoothed when more than about 20 beams are used, as is in the HIBALL target design.

Sugiyama⁽⁶²⁾ expressed the formalism of heavy ion stopping power as the sum of a modified Bethe formula and a modified LSS formula. The theory is made to satisfy the requirement at intermediate energies: (a) The formula is in accord with the Bethe-Bloch formula at high energies. (b) Some of the inner-shell electrons of both projectile and target atom has the possibility of forming a quasi-molecule at the collisions. (c) The formula is proportional to projectile velocity at low energies, or does not contradict with the Firsov theory (see eqs.(2)-(7) for the modified Bethe formula and the modified LSS formula in Ref.(62)).

Acknowledgements

The authors would like to express their sincere thanks to the members of the Study Group on Atomic Processes in Hot, Dense Plasmas for their useful and critical comments to this work.

Glossary

The following is a brief list of the most important symbols which have been consistently used throughout all sections of this article.

- S: Stopping power
- S_b : Stopping power due to contribution of electrons bound to plasma ion
- S_f : Stopping power due to contribution of plasma free electrons
- E: Projectile energy
- E_f : Fermi energy
- T: Plasma temperature
- T_e : Plasma electron temperature
- T_i : Plasma ion temperature
- n: Target electron number density
- ρ : Target mass density
- Z_1 : Atomic number of projectile ion
- Z_2 : Atomic number of target atom
- m: Electron mass
- M: Projectile mass
- q_2 : Ionization state of target atom
- \bar{q}_2 : Average ionization state of target atom
- q^* : Effective charge of projectile ion
- R: Range derived from stopping power
- t: Time
- v: Projectile velocity
- v_{th} : Thermal electron velocity($=[2k_B T_e / m]^{1/2}$)
- k_B : Boltzmann constant

N_0 : Avogadro number
 v_F : Fermi velocity = $\frac{\hbar}{m}(3\pi^2 n)^{1/3}$
 a_0 : Bohr radius ($\hbar / (me^2) = 5.291 \times 10^{-9}$ cm)
 v_0 : Bohr velocity ($e^2 / \hbar = 2.188 \times 10^8$ cm/sec)
 k : Wave number vector
 ω : Frequency
 ω_p : Plasma frequency
 r_d : Debye length = $(T / (4\pi ne^2))^{1/2}$
 g : Plasma parameter = $[1 / ((4\pi / 3)r_d^3 n)]$
 r_s : One-electron radius = $[1 / (4\pi / 3)na_0^3]^{1/3}$
 $\epsilon(k, \omega)$: Dielectric function

References

- (1) T.A.Mehlhorn: A finite material temperature model for ion energy deposition in ion-driven inertial confinement fusion targets: J.Appl.Phys. 52(1981)6552, and Report Sand 80-0038(1980).
- (2) M.M.Widner, T.A.Mehlhorn, F.C.Perry, E.T.J.Burns, and A.V Farnsworth, Jr: Light-ion energy deposition and implications for inertial confinement targets: Comments Plasma Phys. Controlled Fusion 7(1982)37-45.
- (3) F.C.Young, D.Mosher, S.J.Stephanakis, S.A.Goldstein and T.A.Mehlhorn: Measurements of enhanced stopping power of 1-MeV deuterons in target-ablation plasmas: Phys.Rev.Lett. 49(1982)549.
- (4) J.Peek: Free-electron-gas approximation for the stopping power of ionic targets: Phys.Rev. A 26(1982)1030.
- (5) E.J.McGuire, J.M.Peek, and L.C.Pitchford: Phys.Rev.

A26(1982)1318.

(6) T.A.Mehlhorn, J.M.Peek, E.J.McGuire, J.N.Olsen, and F.C.Young: Current status of calculations and measurements of ion stopping power in ICF plasma: SAND 83-1519(1983).

(7) J.Meyer-ter-Vehn and N.Mezler: Target design for heavy ion beam fusion: MPQ 48(1981).

(8) J.Meyer-ter-Vehn: ICF-target studies for heavy ion fusion: MPQ 64(1982).

(9) E.Nardi, E.Peleg, and Z.Zinamon: Energy deposition by fast protons in pellet fusion targets: Phys. Fluids, 21(1978)574.

(10) E.Nardi and Z.Zinamon: Energy deposition by relativistic electrons in high-temperature targets: Phys. Rev. A18(1978)1246.

(11) E.Nardi and Z.Zinamon: Charge state and slowing of fast ions in a plasma: Phys. Rev. Lett. 49(1982)1251.

(12) E.Nardi and Z.Zinamon: Plasma effects in ion beam interaction: J.Phys. (Frs.)C8,44(1983)93.

(13) K.A.Brueckner, L.Senbetu and N.Metzler: Stopping power for energetic ions in solids and plasmas: Phys. Rev. B25(1982)4377.

(14) S.Skupsky: Energy loss of ions moving through high-density matter: Phys. Rev. A16(1977)727.

(15) S.Skupsky: High density effect on thermonuclear ignition for inertially confined fusion: Phys. Rev. Lett. 44(1980)1760.

(16) A.Dar, J.Grunzweig-Genossar, and A.Ron: Slowing down of ions by ultrahigh-density electron plasma: Phys. Rev. Lett. 32(1974)1299.

(17) A.Peres and A.Ron: Plasma screening effect in ion-ion scattering: Phys. Rev. A13(1976)417.

- (18) Yu.S.Sayasov: Swift ion energy losses in dense plasma: J.Phys. (Frs.) C8,44(1983)1.
- (19) Yu.S.Sayasov: On the energy losses of slow ions in an interacting degenerate electron gas:Z.Phys. A313(1983)9.
- (20) S.Ichimarū, S.Mitake, S.Tanaka, and X.Z.Yan: Theory of interparticle correlations in dense, high-temperature plasmas I. General Formalism, II. Correlation Functions, III. Thermodynamic Functions: to be published in Phys Rev. A(1985).
- (21) R.A.Cover, G.Kalman and B.J.Smirnoff: Collective contribution to the energy loss of a fast ion in a degenerate electron-ion plasma:Phys. Rev. A13(1976)490.
- (22) C.Deutsch, G.Maynard and H.Minoo: Ion stopping in dense and hot matter: Proc. Sym. on Accelerator Aspects of Heavy Ion Fusion (West Germany, 1982).
- (23) G.Maynard and C.Deutsch: Energy loss and straggling of ions with any velocity in dense plasma at any temperature: Phys. Rev. A26(1982)665.
- (24) C.Gouedard and C.Deutsch: Dense electron-gas response at any degeneracy : J.Math. Phys. 19(1978)32.
- (25) C.Deutsch: Atomic physics for beam-target interactions: INS International Sym. on Heavy Ion Accelerators and Applications to Inertial Fusion (1984, Tokyo).
- (26) C.Deutsch, H.Minoo, and G.Naouri: Renormalization group approach to ionization in dense plasmas. I. General, II. Line Shifts in Partially Ionized H, He, and Ne: J.Phys.(Frs.)C8,44(1983).
- (27) N.R.Arista and W.Brandt: Energy loss and straggling of charged particles in plasmas of all degeneracies: Phys. Rev.

A23(1981)1898.

(28) W.Brandt: Modern problems of low-velocity stopping powers: Nucl. Instrum. Methods, 191(1981)453.

(29) S.Kreussler, C.Varalás, and W.Brandt: Target dependence of effective projectile charge in stopping powers: Phys. Rev. B23(1981)82.

(30) F.Schulz and W.Brandt: Effective charge of low-velocity ions in matter: A comparison of theoretical predictions with data derived from energy-loss measurements: Phys. Rev. B26(1982)4864.

(31) W.Brandt: Effective charges of ions and the stopping power of dense media: Nucl. Instrum. Methods, 194(1982)13.

(32) W.Brandt and M.Kitagawa: Effective stopping-power charges of swift ions in condensed matter: Phys.Rev. B25(1982)5631.

(33) N.R.Arista and W.Brandt: Effective charge and collision logarithm for slow ions in fusion plasmas: Phys. Rev. A30(1984)630.

(34) G.J.Iafrate and J.F.Ziegler: Numerical evaluation of Lindhard's theory of stopping power for a charged particle in a free-electron gas: J. Appl. Phys. 50(1979)5579.

(35) G.J.Iafrate, J.F.Ziegler and M.J.Nass: Application of Lindhard's dielectric theory to the stopping of ions in solids: J. Appl. Phys. 5(1980)984.

(36) J.F.Ziegler: The stopping of energetic ions in solids: Nucl. Instrum. Methods, 168(1980)17.

(37) J.F.Ziegler: The electronic and nuclear stopping of energetic ions: Appl. Phys. Lett. 31(1977)544.

(38) P.Sigmund and De-Ji Fu: Energy loss straggling of a point

- charge penetrating a free-electron gas: Phys. Rev. A25(1982)1450.
- (39) H.Brysk: Electron-ion equilibration in a partially degenerate plasma: Plasma Phys. 16(1974)927.
- (40) M.Lampe: Multiple scattering and energy loss of a fast test electron beam in a plasma: Phys. Fluids, 13(1970)2578.
- (41) G.L.Payne and J.D.Perez: Stopping power of a nonequilibrium plasma: Phys. Rev. A21(1980)976.
- (42) D.J.Sigma and G.Joyce: Plasma heating by energetic particles : Nucl. Fusion, 11(1971)447.
- (43) D.W.Rule and M.H.Cha: Collective effects in energy loss by relativistic clusters of charged particles: Phys. Rev. A24(1981)55. .
- (44) G.Basbas and R.H.Ritchie: Vicinage effects in ion-cluster collisions with condensed matter and with single atoms: Phys. A25(1982)1943.
- (45) D.W.Rule and O.H.Crawford: Nature of the beam-density effect on energy loss by nonrelativistic charged-particle beams: Phys. Rev. Lett.52(1984)934.
- (46) C.C.Sung and R.H.Ritchie: The energy-loss spectra of fast charged particles passing through a metallic film: J.Phys.C14(1981)2409.
- (47) N.E.B.Cowern: Effective charge of energetic heavy ions, gases, solids and plasmaa: J.Phys.(Frs.)C8,44(1983)107.
- (48)H.Geissel, Y.Laichter, W.F.W.Schneider and P.Armbruster: On the effective charges from stopping powers of 0.5-10 MeV/u. Heavy ions: Phys. Lett. A99(1983)77, and : Observation of a gas-solid difference in the stopping powers of (1-10) MeV/u heavy ions: Phys.Lett. A88(1982)26.

- (49) B.Arnold and J.Meyer-ter-Vehn: Heavy ion beam heated cylinders Planning for hot dense matter experiments at GSI: J.Phys.(Frs.)C8,44(1983)137.
- (50) J.M.Anthony and W.A.Lanford: Stopping power and effective charge of heavy ions in solids: Phys. Rev. A25(1982)1868.
- (51) D.Bailey, Y.T.Lee, and R.M.More: Abinitio calculations of the charge state of a fast heavy ion stopping in a finite temperature target: Proc. of Sym. on Accelerator Aspects of Heavy Ion Fusion (West Germany,1982)pp.571.
- (52) D.Bailey, Y.T.Lee, and R.M.More: see Ref.(51): J.Phys.(Frs.)C8,44(1983)149.
- (53) D.K.Brice: Three parameter formula for the electronic stopping cross section at nonrelativistic velocities: Phy. Rev. A6(1972)1791.
- (54) V.G.Grygoriev, F.G.Neshov, A.A.Puzanov, and A.R.Urmanov: Effects of electronic structure on ion stopping cross-section in solids: Phys. Stat. Sol. 83(1984)573.
- (55) A.F.Burenkov, F.F.Komarov and M.M.Temkin: Semiclassical theory for energy loss of heavy nonrelativistic ions in matter: Radiat. Eff. 46(1980)59.
- (56) L.Ferrariis and N.R.Arista : Classical and semiclassical treatments of the energy loss of charged particles in dilute plasma : Phys. Rev. A29(1984)2145.
- (57) N.A.Tahir and K.A.Long: Target design studies for a heavy ion-beam driven inertial confinement fusion reactor: Atomkernerenergie Kerntechnik, Bd.40(1982)157.
- (58) T.P.Wright, T.A.Green, and A.Mehlhorn: Charge exchange and energy loss of carbon ions in air-plasma channels: J.Appl.Phys. 52(1981)147.

- (59) J.F.Santarius and J.D.Callen: Alpha particle loss and energy deposition in tandem mirrors: Phys. Fluids, 26(1983)1037.
- (60) R.M.Sternheimer, M.J.Berger, and S.M.Seltzer: Density effect for the ionization loss of charged particles in various substances: At.Data Nucl.Data Tables, 30(1984)261.
- (61) T.A.Beyon: Energy deposition distributions for multiple ion-beam irradiation of ICF targets: J.Phys.(Frs.)C8,44(1983)123.
- (62) H.Sugiyama: Electron stopping power formula for intermediate energies: Radiat.Effects, 56(1981)205.
- (63) H.Bethe: On the theory of the passage of fast particle beams through matter: Ann. Phys.5(1930)325.
- (64) J.Lindhard and M.Scharff: Energy loss by fast particles of low charge: K.Dan.Vidensk.Selsk.Mat.Fys.Medd, 27, No 15(1953).
- (65) J.Lindhard: On the properties of a gas of charged particles: K.Dan.Vidensk.Selsk.Mat.Fys.Medd. 28, No 8(1954).
- (66) J.Lindhard, M.Scharff, and H.E.Schiott: Range concepts and heavy ion ranges. (Notes on atomic collisions. II): K.Dan.Vidensk. Selsk.Mat.Fys.Medd. 33, No 14(1963).
- (67) L.Lindhard and A.Winther: Stopping power of electron gas and equipartition rule: K.Dan.Vidensk.Selsk.Mat.Fys.Medd. 34, No 4(1964).
- (68) V.S.Nikolaev and I.S.Dmitriev: On the equilibrium charge distribution in heavy element ion beams: Phy.Lett. 28A(1968)277.
- (69) M.D.Brown and C.D.Moak: Stopping powers of some solids for 30-90-MeV ²³⁸U ions: Phys.Rev.B6(1972)90.
- (70) J.F.Ziegler: Stopping Cross-Sections for Energetic Ions in all Elements: (Pergamon, New York, 1980)vol.5.
- (71) J.D.Jackson: Classical Electrodynamics: (Wiley, New York,

1975)pp.643.

(72) B.S.Yarlagadda, J.E.Robinson and W.Brandt: Effective-charge theory and the electronic stopping power of solids: Phys. Rev. B17(1978)3473.

(73) H.D.Betz: Charge state and charge-changing cross sections of fast heavy ions penetrating through gaseous and solid media: Rev. Mod. Phys. 44(1972)465.

(74) D.Pines and D.Bohm: A collective description of electron interactions; II. Collective vs individual particle aspects of the interactions: Phys. Rev. 85(1954)338.

(75) L.C.Northcliffe and R.F.Schilling: Range and stopping-power tables for heavy ions: Nucl. Data Tables, 7(1970)233.

(76) A.Lenard: On Bogoliubov's kinetic equation for a spatially homogeneous plasma: Ann. Phys.3(1960)390.

(77) R.Balescu: Irreversible processes in ionized gas: Phys.Fluids, 3(1960)52.

(78) H.A.Gould and H.E.Dewitt: Convergent kinetic equation for a classical plasma: Phys. Rev. 155(1967)68.

(79) P.L.Bhatnagar, E.P.Gross, and M.Krook: A model for collision processes in gases. I. Small amplitude processes in charged and neutral one-component systems: Phys. Rev. 94(1954)511.

(80) K.Imasaki, S.Miyamoto, S.Higaki, S.Nakai, and C.Yamanaka: Evidence of anomalous interaction between a relativistic electron beam and a solid target: Phys. Rev. Lett. 43(1979)1937.

(81) K.Imasaki, S.Miyamoto, S.Higaki, S.Nakai, K.Nishihara, and C.Yamanaka: Energy absorption and transport in layered targets

irradiated by a relativistic electron beam: Appl. Phys. Lett.
37(1980)533.

(82) R.A.McCorkle and G.J.Iafrate: Beam-density effect on the
stopping of fast charged particles in matter: Phys. Rev.
Lett.39(1977)1263.

Table I. Velocity-dependent collision logarithm in the classical and quantum-mechanical approximation method.

	classical approximation: $\xi \gg 1$	quantum-mechanical approximation $\xi \ll 1$
$v \gg v_{th}$	$b_{min} \approx \frac{Z_1 e^2}{mv^2}$ $b_{max} \approx \frac{v}{\omega_p}$ $\ln \Lambda \approx \ln \left(\frac{1.123 mv^3}{Z_1 e^2 \omega_p} \right)$	$b_{min} \approx \frac{\hbar}{mv}$ $b_{max} \approx \frac{v}{\omega_p}$ $\ln \Lambda \approx \ln \left(\frac{2mv^2}{\hbar \omega_p} \right)$
$v \ll v_{th}$	$b_{min} \approx \frac{Z_1 e^2}{mv_e} = \frac{Z_1 e^2}{2k_B T}$ $b_{max} \approx \left(\frac{k_B T}{4\pi n e^2} \right)^{\frac{1}{2}} = \frac{v_{th}}{\omega_p}$ $\ln \Lambda \approx \ln \left(\frac{4(k_B T)^{3/2}}{Z_1 e^2 p m^{\frac{1}{2}}} \right) - 2\gamma - \frac{1}{2}$	$b_{min} \approx \frac{\hbar}{mv_{th}}$ $b_{max} \approx \left(\frac{k_B T}{4\pi n e^2} \right)^{\frac{1}{2}} = \frac{v_{th}}{\omega_p}$ $\ln \Lambda \approx \ln \left(\frac{k_B T}{\hbar \omega_p} \right) + \frac{1}{4}$

The Debye screening length = $r_d = (k_B T / 4\pi n e^2)^{\frac{1}{2}}$, plasma frequency = $\omega_p = (4\pi n e^2 / m)^{\frac{1}{2}}$, $e^{\gamma} = 1.78$, the Bloch parameter = $\xi = b_{CL} / b_{QM} = Z_1 e^2 / \hbar v_r$, where v_r denotes a mean relative velocity between a projectile ion and electron (in particular $v_r = v$ if $v \gg v_{th}$, and $v_r = v_{th}$ if $v \ll v_{th}$), CL represents the classical approximation and QM the quantum-mechanical approximation.

Table II Key Theories of Stopping Power for charged Particles over a wide range of energy, density and temperature

Reference	Subjects	Energy, Density, Temperature
(A) Mehlhorn ⁽¹⁾	$S = S_b + S_f + S_{ion}$. $S_b = \min. (S_{Bethe}, S_{LSS})$. $S_f = \text{binary} + \text{collective}$. ICF target deposition profiles.	2-MeV protons and 10-GeV U ions in Au (19.3 and 0.193 g/cm ³).
Widner et al. ⁽²⁾	$S = S_b + S_f$. S and R of proton for ICF.	proton. $T_e \text{ (eV)} < 545E \text{ (MeV)} / A$ (atomic mass).
Young et al. ⁽³⁾	$S = S_b + S_f$. scaling formula for $\langle I(Z,q) \rangle$ ICF target design. proton range, radial charge density profiles.	$E = 1-10^5$ keV proton in Au, Au ¹⁰⁺ , Au ²⁰⁺ , and Au ³⁰⁺ plasma. $E = 1$ MeV deuterons in target-ablation plasma. cold target.
Peek ⁽⁴⁾	$\langle I(Z,q) \rangle$ based on FEG theory and quantum mechanical definition.	Al ^{q+} , Au ^{q+} .
McGuire et al. ⁽⁵⁾	Generalized-oscillator-strength formulation of plane-wave Born approximation, individual subshell ionization and excitation to proton S. $\langle I(Z,q) \rangle$ and oscillator strength.	$E = 0.1-100$ MeV protons in Al ^{q+} ($0 \leq q \leq 11$).
Mehlhorn et al. ⁽⁶⁾	see Ref. (3). models of $\langle I \rangle$.	

Meyer-ter
-Vehn (7)

$S = S_b + S_f + S_{\text{plasma ion}}$
ion target design for ICF.
deposition profiles.

$209_{\text{Bi}} (10 \text{ GeV}) + 208_{\text{Pb}}$
 $209_{\text{Bi}} (10 \text{ GeV}) + 7_{\text{Li}}$
for any T.

J. Meyer
-ter-Vehn (8)

see Ref. (7)

(B)

Nardi
et al. (9)

ϵ -method.
 $S = S_b + S_f$.
dense and collisional plasma
via polarization response
 $\epsilon(k, \omega)$.
 $\epsilon(k, \omega)$ of collisional form.
 S_b : Bethe theory.
<I>: T-F model.
: L-S model.
conditions relevant to pellet
fusion (deposition, temperature
and pressure profile).

low T, high- Z_2 -target and
high T, high- Z_2 -target.

$E = 1-10 \text{ MeV}$ protons
 $\rho = 0.19 \text{ g/cm}^3$,
 $\rho = 19.0 \text{ g/cm}^3 \text{ Au}$.

Nardi
et al. (10)

relativistic Møller theory and
Bohm-Pines theory (collective
plasma oscillations).
n and I by T-F model.

$E = 400 \text{ keV}$ electrons in
cold and 1 keV Au target.
 $\rho = 0.19 \text{ g/cm}^3$,
 $\rho = 19.0 \text{ g/cm}^3$.

Nardi
et al. (11)

electron loss process by using
BEA.
ionization of projectile by the
plasma free electron.
electron capture process from
bound electrons in the plasma
ion (Bell theory, 1953).
capture by projectile of free
plasma electrons by the radiative
recombination, the dielectronic
recombination and three-body

$E = 0-54 \text{ MeV}$ Al ion
 $E = 0-12 \text{ MeV}$ C ion.
 $\rho = 10^{-2} \text{ g/cm}^3$.
 $T = 25 \text{ eV}, 100 \text{ eV}$ for
C-target.
 $T = 25 \text{ eV}$ for fully ionized
Li-target.
 q^* of C-ion with $E=12 \text{ MeV}$.

	<p>recombination process. energy deposition profile (C → Li and Al → C). q^* of Al-ion in fully ionized target, 2-bound electrons in target, cold target. Betz formula.</p>	
Nardi et al. (12)	<p>$\epsilon(k, \omega)$-method. I: Bethe theory. plasma effects on S. plasma effects on charge state of fast ions. plasma opacity effects.</p>	<p>$\rho = 2.78 \times 10^{-2} \text{ g/cm}^3$. $kT = 0.05\text{-}0.20 \text{ keV}$ $E < 600 \text{ keV}$ of deuterons in CD_2 target.</p>
Brueckner et al. (13)	<p>$\epsilon(k, \omega)$-method. $\epsilon = \epsilon_f$ (contribution of plasma free electrons) + ϵ_b (contribution of bound electrons). ϵ_b: T-F model. q: Nikolaev-Dmitriev, and Betz. comparison with Northcliffe and Schilling's result and cutoff wave number in classical and quantum k_c^{-1}.</p>	<p>low Z material. Xe (0-15 MeV/amu) + Al ($0.1x\rho_s, 1x\rho_s, 3x\rho_s$) (T = 0-1290 eV). high Z-material Xe (0-15 MeV/amu) + Au ($0.1x\rho_s, 1x\rho_s, 3x\rho_s$) (T = 0-1568 eV).</p>
Skupsky (14)	<p>$\epsilon(k, \omega)$-method. = $\epsilon_1 + i\epsilon_2$. by Lindhard's no-collisional formula. in Λ_{RPA} via Te. in Λ_{RPA} for nondegenerate plasma, weak degeneracy, strong degeneracy, and Sommerfeld formula.</p>	<p>$n = 10^{25}, 10^{26}, 10^{27} \text{ cm}^{-3}$. $T = 10^6 - 10^9 \text{ }^\circ\text{K}$</p>

Skupsky ⁽¹⁵⁾	<p>in Λ_{RPA}.</p> <p>energy reflection depends on the ratio of mean free path for 90° scattering and that for energy loss λ_E.</p>	<p>$E = 3.5$ MeV α-particle in high-Z, Fermi-degenerate shell (Au-tamper, $n = 5 \times 10^{27} \text{ cm}^{-3}$, $T = 1$ keV).</p>
Dar et al. ⁽¹⁶⁾	<p>$\epsilon(k, \omega)$-method.</p> <p>form factor $S_k(\omega)$ by means of RPA.</p> <p>slowing-down cross section of deuteron, triton and α.</p>	<p>$n = 10^{24} - 10^{29} \text{ cm}^{-3}$.</p> <p>$E = 0.01 - 10$ MeV.</p> <p>$T_e = 0$.</p>
Peres et al. ⁽¹⁷⁾	<p>$\epsilon(k, \omega)$-method.</p> <p>form factor $S_k(\omega)$ by means of RPA.</p> <p>plasma collective screening effect in ion-plasma ion scattering.</p> <p>small angle ion-ion scattering.</p> <p>electron loss efficiency for stopping heavy charged particle in high-n, T plasma.</p>	<p>high density and high T plasma.</p>
Sayasov ⁽¹⁸⁾	<p>$\epsilon(k, \omega)$-method</p> <p>no collisional and collisional effects.</p> <p>average field (for $r_s \ll 1$) and local field effects.</p>	<p>$r_s < 6.03$.</p> <p>DT plasma.</p> <p>classical plasma.</p> <p>degenerate quantum plasma.</p>
Sayasov ⁽¹⁹⁾	<p>$\epsilon(k, \omega)$-method.</p> <p>energy loss of slow ions in an interacting electron gas.</p> <p>see Ref. (18).</p>	<p>$v \ll v_F$.</p> <p>degenerate electron gas.</p>
Ichimaru et al. ⁽²⁰⁾	<p>hot and dense plasmas.</p> <p>correlation function.</p> <p>local field effect.</p>	

Cover et al. (21)	(dE/dx) (collective excitation of ion wave) / (dE/dx) (individual ion-ion collision) * $\epsilon(k, \omega)$ -method.	$n = 10^{28} - 10^{33} \text{ cm}^{-3}$. $E = 3.5 \text{ MeV } \alpha$ -particle incident on degenerate electron-deuterium plasma with $T_i = 50 \text{ keV}$.
Deutsch et al. (22)	$\epsilon(k, \omega)$ -method. Lindhard's dimensionless variable and other dimensionless parameters. partially degenerate electron fluid. $\epsilon(k, \omega)$ at low T and high T limit.	$n = 10^{25} \text{ cm}^{-3}$. $T_e = 0 - 4.68 \times 10^6 \text{ K}$, and $E = 0.1 - 100 \text{ MeV/amu}$ for heavy ions used in ICF. $n = 10^{27} \text{ cm}^{-3}$. $T_e = T_F$, and $E = 3.5 \text{ MeV}$ α -particle in Al plasma.
Maynard et al. (23)	$\epsilon(k, \omega)$ -method. exact RPA ϵ .	$r_s < 1$. any velocity ratio v/v_F . $n = 10^{25} - 10^{29} \text{ cm}^{-3}$. $E = 0.1 - 100 \text{ MeV/amu}$. $T = 0 - 10^6 \text{ K}$.
Gouedard et al. (24)	exact expression for the linear response function of dense electron gas at any T in RPA.	$T \rightarrow 0$ and $T \rightarrow \infty$.
Deutsch et al. (25)	$\epsilon(k, \omega)$ -method. linear response theory. RPA at any T.	$n = 10^{25} - 10^{29} \text{ cm}^{-3}$ vs. T.
Deutsch et al. (26)	renormalization group approach to ionization: I. General II. Line shifts in partially ionized H, He, and Ne.	dense plasma
Arista et al. (27)	$\epsilon(k, \omega)$ -method. $\epsilon = \epsilon_1 + i\epsilon_2$. expansion of dE/dt and $S \approx -1/v(dE/dt)_0$. low-frequency approximation for $\epsilon(k, \omega)$.	$n = 10^{25} \text{ cm}^{-3}$. $\theta = kT/E_F = 0.1 - 50$. $v/v_F = 0.1, 0.5, 1$, and 10.

Brandt (28)	<p>material dependence of S: variations of mean valence-electron densities. validity of q^*-theory: linear response approximation. Z_2 oscillations of S. effective stopping power charge fraction. S for proton in the reduced form. energy loss in plasmas of all degeneracies.</p>	$v_r / (v_0 Z_1^{2/3}) = 0 - 1.6$ $v_1 / v_F = 0.1.$ $kT / E_F = 0.1 - 50.$ r_s : solid.
Kreussler et al. (29)	<p>test of q^*. relative velocity $v_r = v_r(v_e, v)$. strong material dependence of q^*.</p>	He^+ and D^+ in Au ($r_s = 1.49$), C (1.66), Al (2.12), and Cs (5.88).
Schulz et al. (30)	<p>theory and experiment: effective charge fraction ζ_{expt}. ζ_{expt}: linear-response theory on the basis of a statistical model of ions of given v-dependent degree of ionization.</p>	$v/v_0 = 0.47 - 1.28.$ $Z_1 = He, N, Ar.$ $Z_2 = C, Al, Au.$
Brandt (31)	<p>$\epsilon(k, \omega)$-method. Thomas-Fermi model. Z_2 oscillations of S.</p>	S versus Z_2 (25 - 200 keV). relative effective charge $(q^*/Z)/q$ versus reduced relative velocity $v_r / v_0 Z_1^{2/3}$ (0.1-1.0).
Brandt (32)	<p>q^* in condensed matters.</p>	$5 \leq Z_1 \leq 92.$ $T_e = 10^4 - 10^9$ K. $n = 10^{13} \text{ cm}^{-3}.$ $v < v_{\text{th}}.$
Arista et al. (33)	<p>general expression for q^* of slow ions in dilute plasma at T. classical and quantum transition. collision logarithm $L(n, T, Z)$.</p>	$5 \leq Z_1 \leq 92.$ $T_e = 10^4 - 10^9$ K. $n = 10^{13} \text{ cm}^{-3}.$ $v < v_{\text{th}}.$

Iafrate et al. (34)	<p>$\epsilon(k, \omega)$-method. Lindhard's S $S = (4\pi/m_e) (Z_1 e^2/v)^2 nL(n, v)$</p>	<p>$n = 10^{22} - 10^{32} \text{ cm}^{-3}$. $E = 100, 1000, 10000$ keV/amu.</p>
Iafrate et al. (35)	<p>$\epsilon(k, \omega)$-method. spherically average charge density model. charge density (Herman-Skillman, 1963) and (Moruzzi-Janak- Williams, 1978). Lindhard formalism.</p>	<p>$E = 100, 1000, 10000$ keV/amu.</p>
Ziegler (36)	<p>$\epsilon(k, \omega)$-method. Lindhard's theory. local density approximation. free electron gas model. new calculation I . q_{HI}^* (heavy ion)/q_H^* (hydrogen)</p>	<p>$E > 200 \text{ keV/amu}$.</p>
Ziegler (37)	<p>electronic contribution to $T=0$. stopping by use of scaling from proton stopping powers. S of empirical formula.</p>	
Sigmund et al. (38)	<p>$\epsilon(k, \omega)$-method. Lindhard's theory. expansion of $\epsilon(k, \omega)$ and L(stopping number of Lindhard).</p>	<p>high electron density $x^2 = e^2/\pi V_F \ll 1$. high velocities.</p>
(C) Brysk (39)	<p>kinematic basis of collisions between two bodies. electron distribution function f and temperature in f. energy loss rate (density and temperature contribution).</p>	

Lampe (40)

quantum Lenard-Balescu equation.
collision frequency γ_{coll} of
electrons and ions in plasma is
larger than the appropriate
instability growth rate γ .

low density.

e.g. $T = 2500 \text{ }^\circ\text{K}$
 $n = 10^{12} \text{ cm}^{-3}$
 $E = 50 \text{ eV}$.

Payne
et al. (41)

Lenard-Balescu collision term
and Bhatnagar-Gross-Krook
approximation (BGK model).
the effects of departures from
local equilibrium due to
gradients in the plasma.
 α -particle S in a homogeneous and
inhomogeneous plasmas.

$E = 0.5 - 4.5 \text{ MeV}$. (α) in
a fully ionized hydrogen
plasma.
 $n = 10^{19} - 10^{23} \text{ cm}^{-3}$.
 $T = 50 - 1000 \text{ eV}$.

Sigma
et al. (42)

Lenard-Balescu kinetic equation.
collective effects through
 $\epsilon(k, \omega)$.
quantum correction for close
collisions (large angle
scattering)

α -particle slow down in
electron-deuteron plasma:
($T_i = 100 \text{ keV}$, $T_e = 50$
 keV , $n = 10^{14} \text{ cm}^{-3}$),
($T_i = 4 \text{ keV}$, $T_e = 6 \text{ keV}$,
 $n = 10^{14} \text{ cm}^{-3}$), and
protons slow down in
electron-proton plasma:
 $T_i = 0.5 \text{ keV}$, $T_e = 1 \text{ keV}$,
 $n = 5 \times 10^{13} \text{ cm}^{-3}$.

(D)

Rule
et al. (43)

classical $\epsilon(k, \omega)$ of medium to
which the particles lose
energy in distant collision.
extension of Fermi's method for
deriving the density effect.
proximity function.
new expression collective energy
loss for clusters in the
non-relativistic limit.

Basbas
et al. (44)

$\epsilon(k, \omega)$ -method.
configuration effect on
integrations of clusters with
an electron gas and with single
atoms (vicinage effect) and,
similarly, with a system of
noninteracting atoms at
condensed matter.
classical harmonic oscillator
model and quantum mechanical
perturbation theory.
spatial configuration of ions
making up the cluster.
S of a di-cluster in a valence
electron gas.
fluctuations in cluster energy
loss.

Rule
et al. (45)

analytic expression for the
vicinage function.
two particle vicinage
contribution to S.
dipole-like behavior for large
separations between beam
particles.
beam-density effect on energy
loss.

Sung
et al. (46)

Landau transport theory to
include the quantum mechanical
transition effect.
general approach developed
 $\epsilon(k, \omega)$ -method.
energy loss spectrum of a cluster
of correlated charged particles.
number operator formulation.

$$n > \frac{N}{\pi} \frac{\omega^2}{v^3} \left(\frac{z_1 z_2 e^2}{2fMR_0^3} \right)^{1/2}$$

n = density of gas atom.

z_1, z_2 = ion charges

M = reduced mass of the
di-cluster.

n: typical condensed
matter density for

$$N = 10^3 \text{ cm}^{-3}, 14 \text{ eV},$$

$$z_1 = z_2 = 1, R_0 = 1 \text{ \AA}$$

$$v = 5 v_0 \text{ and } f = 0.1.$$

E = 5 MeV - proton with
beam density $n_b = 6.44 \times 10^{14} \text{ cm}^{-3}$ in weakly
ionized H_2 ($n = 2.67 \times 10^{19} \text{ cm}^{-3}$, $n = 1.11 \times 10^{15}$, $\times 10^{16} \text{ cm}^{-3}$, $kT = 0.75 \text{ eV}$).

(E)

Cowern (47)

charge-changing cross sections
and q^* .
charge fraction.

limit $n \rightarrow 0$ and
 $n \rightarrow \infty$.

Geissel
et al. (48)

q^* for Z_1 (0.6 MeV/amu) $\rightarrow Z_2$
 $Z_1 = Kr, Xe, Pb, U$ -ions in Ar
gas (1.4 MeV/amu)
 $S_{HI, v, Z_2} = (q^*)^2 S_{p, v, Z_2'}$
where S_{HI, v, Z_2} and S_{p, v, Z_2}
are the stopping powers of heavy
ions and protons at the same
velocity (v) in the same medium
(Z_2).

Z_2 : solid
0.5-10 MeV/amu heavy ion

S versus q .

observation of a gas-solid
difference in the stopping
powers of (1-10) MeV/amu heavy
ions.

Arnold
et al. (49)

heavy ion beam heated cylinders
experiments
ion-beam energy deposition.
density profile.
temperature profile.

hot dense matters

Anthony
et al. (50)

experiment.
empirical formula of q/Z_1 , and
 (q^*/Z_1) .
S for $Z_1 = C, Si, Cl, Ti, I, Fe,$
 $Ge, Br, Nb.$
 $Z_2 = C, Al, Cu, Ag, Au.$

E: at energies near
maximum in S.

(F)

Bailey
et al. (51)

average atom model to integrate
the rate equations.

E = 1-100 MeV/amu.
T = 1, 100, 300 eV.

	<p>electron rates for bound-bound excitation, bound-free ionization, radiative recombination and 3-body recombination.</p> <p>ion rates for bound-bound excitation, de-excitation and bound-free ionization.</p> <p>stripping rate.</p> <p>q^*/Z.</p>	<p>$n = 6 \times 10^{23} \text{ cm}^{-3}$.</p> <p>fully ionized Al.</p>
Bailey et al. (52)	see Ref. (51).	
Brice (53)	three parameter semi-phenomenological manner. modified Firsov formalism.	low and high energies
Grygoriev et al. (54)	<p>$S = S$ (core electron) + S_f</p> <p>$S_f = S$ (electron-hole generation) + P_{pl}.</p> <p>$v \lesssim v_0$: elastic collision</p> <p>$v \gg v_0$: ionization</p> <p>modified Firsov's theory.</p> <p>Bonderup statistical model.</p> <p>Brandt-Reinheimer formalism.</p> <p>role of different electronic subshells in a solid for proton energy loss.</p>	<p>$E = (200-400) \text{ keV-proton} \rightarrow Z_2$ for S.</p> <p>$E = (50-500) \text{ keV-proton} \rightarrow {}^{29}\text{Cu}, {}^{27}\text{Co}, {}^{23}\text{V}$ for S.</p>
Burenkov et al. (55)	<p>semiclassical theory for energy loss of heavy nonrelativistic ions.</p> <p>BEA.</p> <p>modified Firsov theory.</p>	<p>$E = 0.01-12 \text{ MeV/amu}$</p> <p>$Z_1 = \text{F, Mg, S}$</p> <p>$Z_2 = \text{Ne, Ni, Fe, Ag}$.</p> <p>$Z_1 = \text{S}$</p> <p>$Z_2 = \text{Ne, Ar-gas}$.</p>
Ferrariis et al. (56)	<p>nondegenerate plasma</p> <p>BEA between test particle and particles in plasma.</p>	<p>$T = 10^4 - 10^8 \text{ K}$.</p> <p>$v = 0.1 - 100 \text{ a.u.}$</p>

	quantum mechanical analysis of the scattering of partial wave. energy loss (v , q , n , T).	
Tahir et al. (57)	energy deposition code GORGON also see Ref. (9), (10), and Long and Tahir: Nuclear Research Centre Karlsruhe Report (1981) KfK 3232. Long: GSI Report (1981) 81-3. p.19.	heavy ion beam Pb in LiPb, DT. $\rho = 10^{-2} - 10^4$ (g/cc) $T = 1$ eV - 10 keV $P = 10^{-4} - 10^8$ (MB)
Wright et al. (58)	charge exchange and energy loss of C ions. semiempirical charge exchange cross section. 3-D Monte Carlo transport code. $-dE / dx \approx 6 \text{ keVcm}^{-3} / \text{g}$ (density in g/cm^3) for C in N_2 -gas.	light ion-beam for ICF. $E = 0.5-2.0$ MeV/amu
Santarius et al. (59)	bounce averaged Fokker-Planck equation for α -particle slow- ing down in electron and ion plasma.	$T_e = 300$ keV. electro-static potential: 100 keV.
Sternheimer et al. (60)	numerical evaluation of the density effect. fitting formula. Bethe's stopping power formula ionization potential I and S.	$Z = 1-98$. chemical compounds and substances of biological interest.
Beyon (61)	formalism of energy distribution function for ICF target.	
Sugiyama (62)	modified Bethe formula. modified LSS formula.	$E = 0.04-5$ MeV/amu.

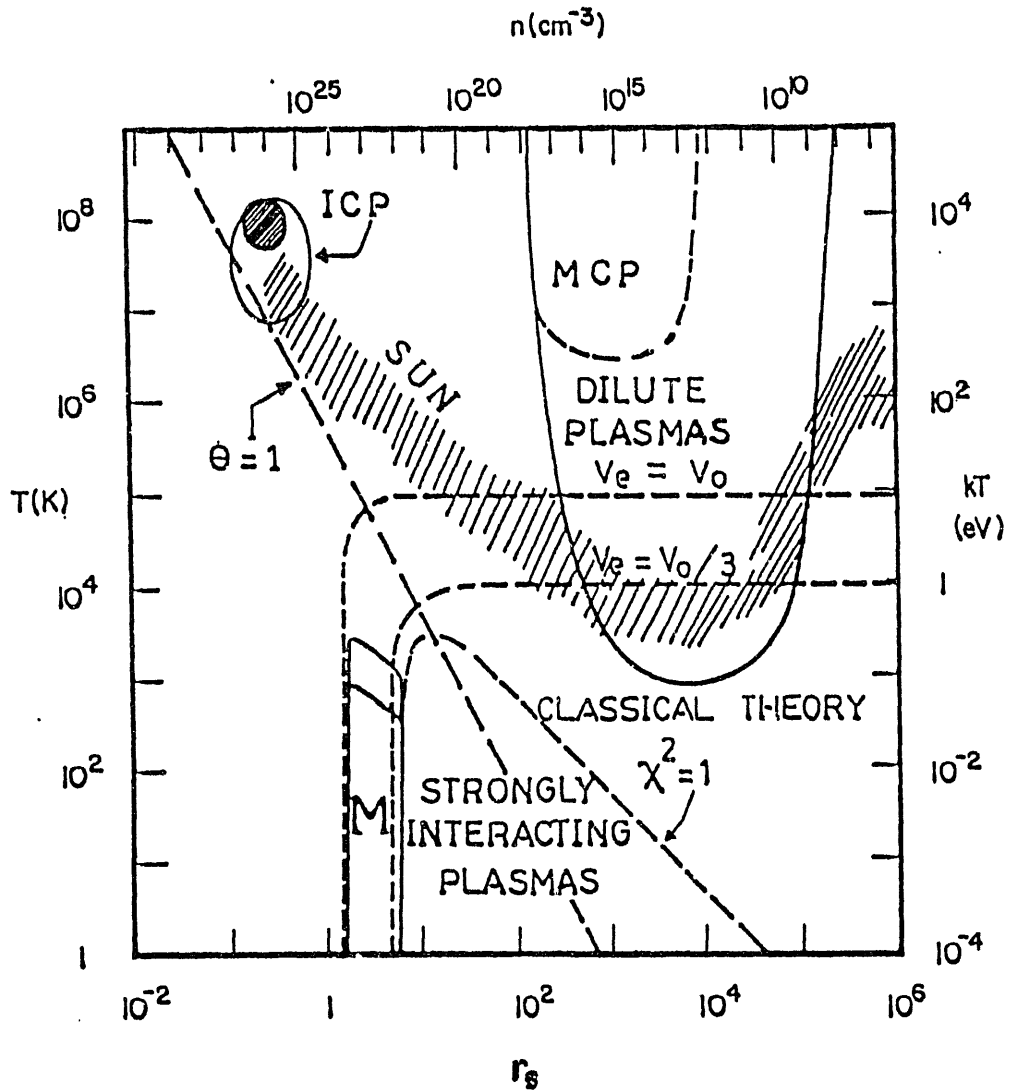


Fig.1 Plasma conditions. The ordinates represent the electron plasma temperature T and the abscissa displays the one-electron radius r_s (a.u.), related to the electron density n (upper scale) as $(4\pi/3)/r_s^3 = 1/na_0^3$. The line $\chi^2 = 1$ separates the conditions in strongly interacting plasmas from those in weakly interacting plasmas. The lines $v_e = v_0$ and $v_e = v_0/3$ indicate the transition region between the plasma where classical theories describe the energy loss (lower right-hand quadrant) and all other plasmas where quantum-mechanical descriptions are appropriate. Below the line $\theta \equiv kT/E_F = 1$, the plasmas are degenerate or cold, whereas above the line they are nondegenerate or hot.

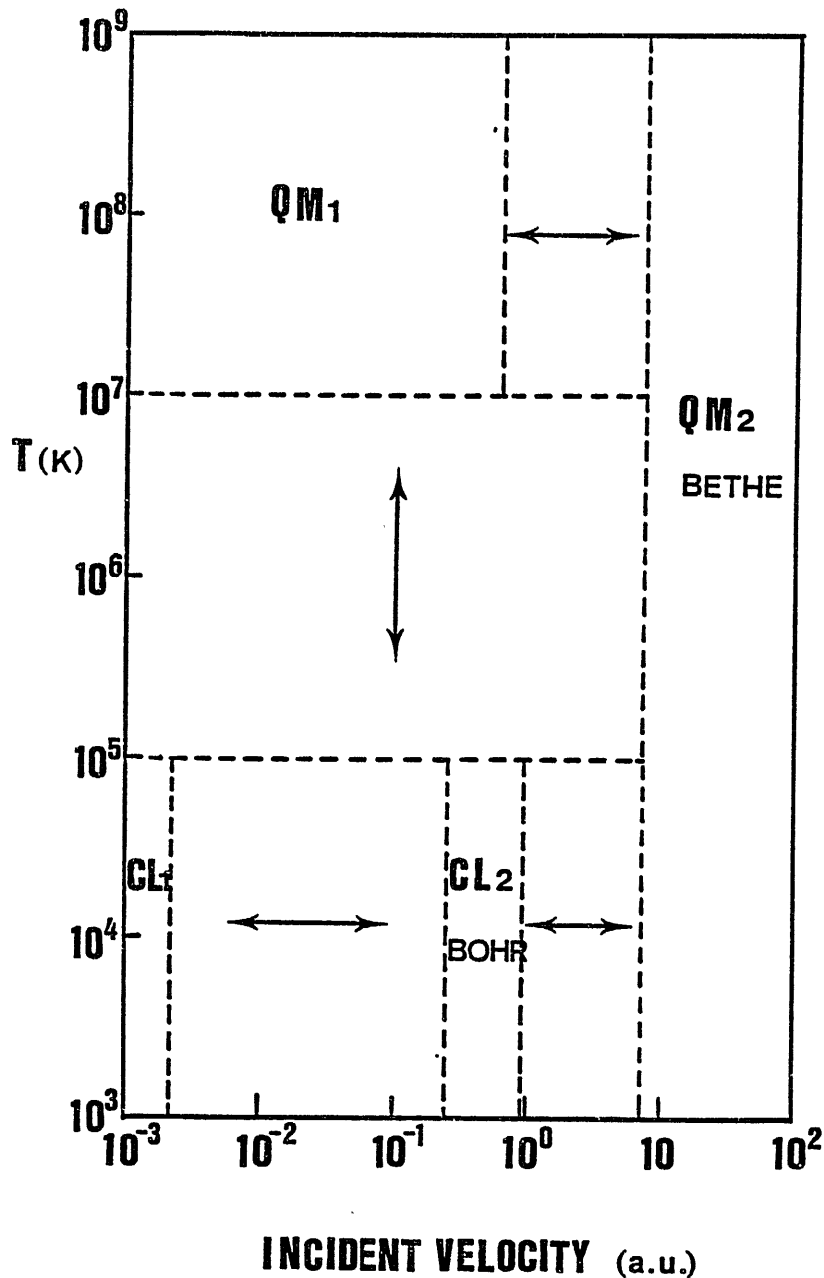


Fig.2 Summary⁽⁵⁶⁾ of the theories of the stopping power of ions in an electron plasma, based on the description of the collision logarithm $\ln\Lambda$. For $\ln\Lambda$, CL₁ and CL₂ represent the cases of low velocities ($v < v_{th} < Z_1 v_0$) and intermediate ($v_{th} < v < Z_1 v_0$) at low temperatures in the classical approximation, respectively. QM₁ and QM₂ represent the cases of low ($v < Z_1 v_0 < v_{th}$) and high velocities ($v > v_{th} > Z_1 v_0$) at high temperatures in the quantum-mechanical approximation, respectively. The Bohr theory corresponds to CL₂ limit and the Bethe theory corresponds to QM₂. Arrows indicate the directions of increasing (\uparrow , \rightarrow) (or decreasing, \downarrow , \leftarrow) ion velocity or increasing (or decreasing) plasma temperature. These regions are described as "transition region".

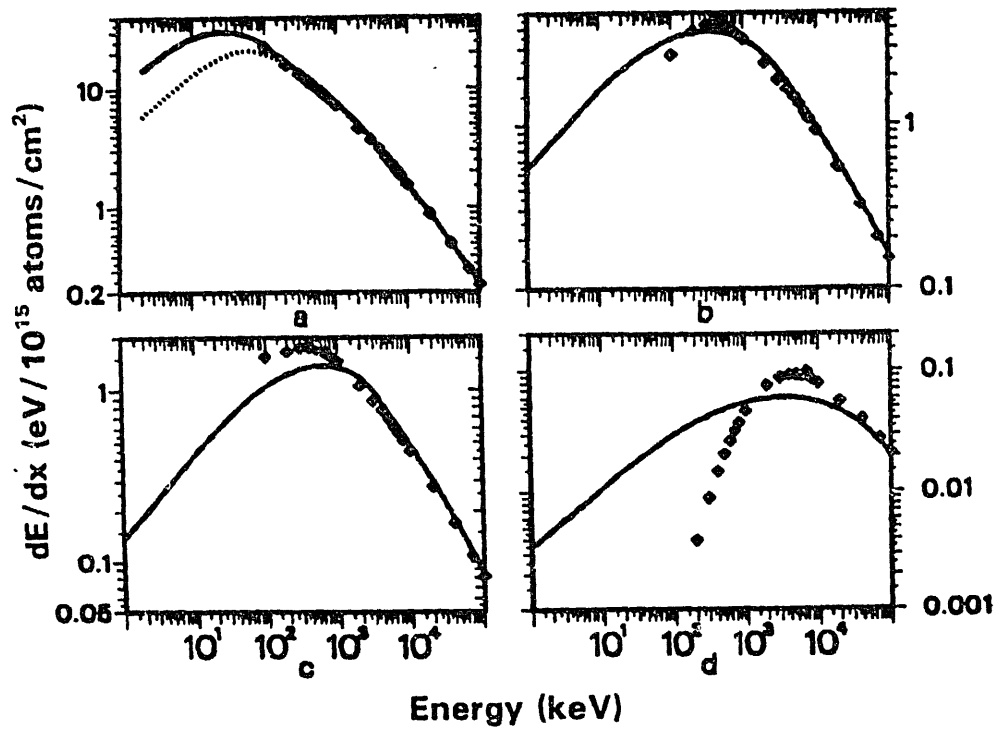


Fig.3 Comparison of proton stopping power in Al as a function of energy: augmented-LOM model (solid line), GOS model (diamond), Ziegler's analytic fit to experiment (dotted line). Plot a is for neutral Al, b for Al³⁺ plasma, c for Al⁷⁺, and d for Al¹¹⁺ plasma, respectively.

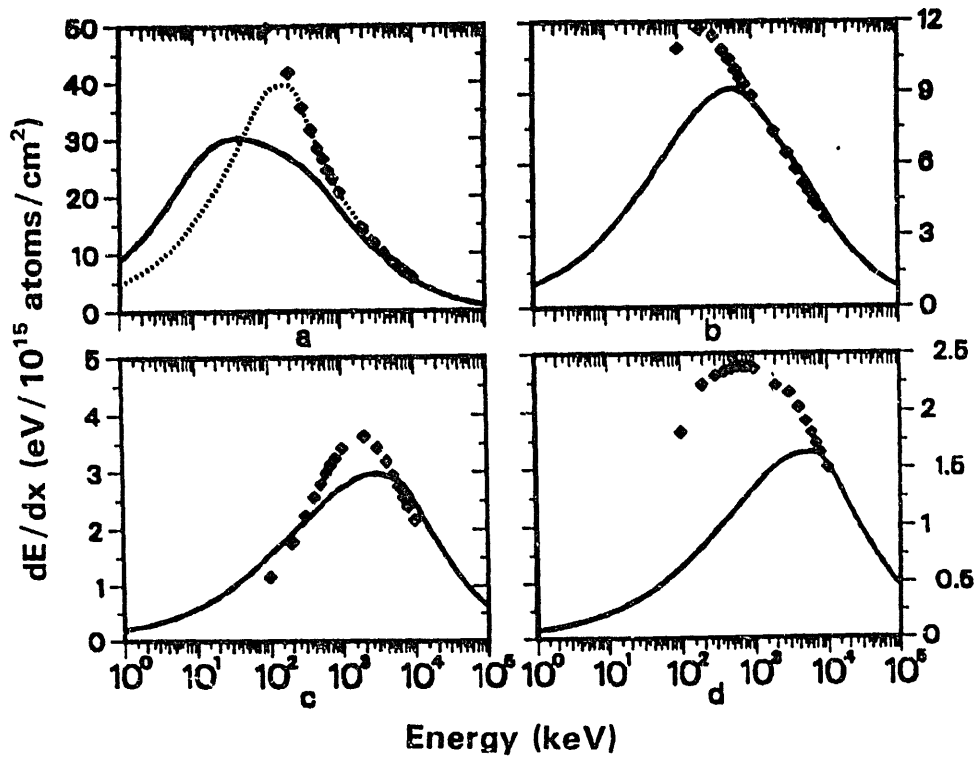


Fig.4 Comparison of proton stopping power in Au as a function of energy: augmented-LOM model (solid line), GOS model (diamonds), Ziegler's analytic fit to experiment (dotted line). Plot a is for neutral Au, b for Au¹⁰⁺ plasma, c for Au²⁰⁺, and d for Au³⁰⁺ plasma, respectively.

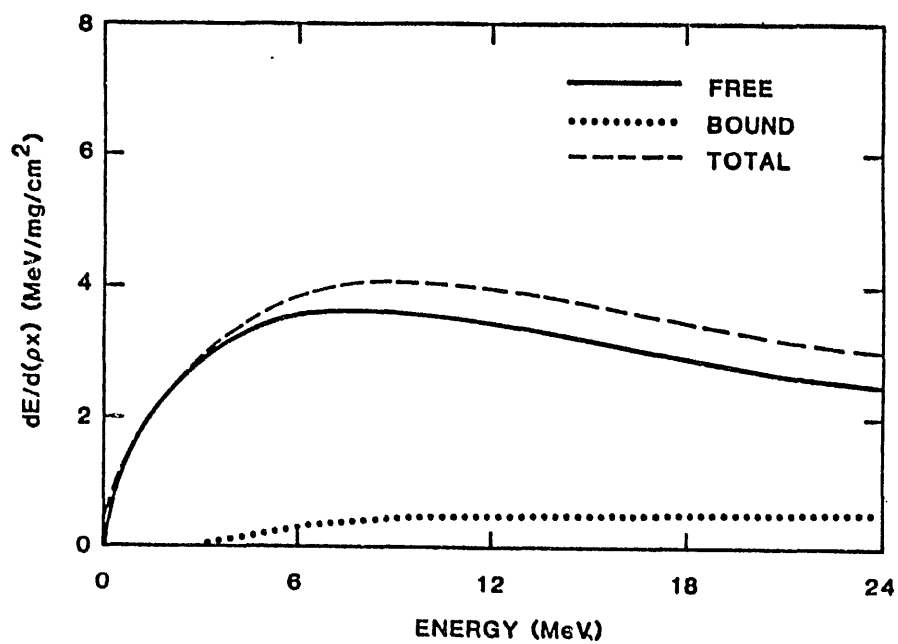


Fig.5 Stopping power of $0.01 \rho_0$
 Au at $T_e = 200$ eV for C ions.

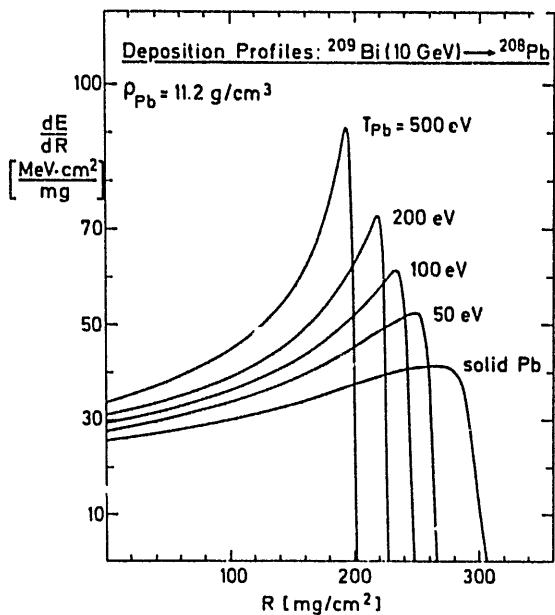


Fig. 6 Stopping power as a function of range for Bi ions on Pb for different target temperatures.

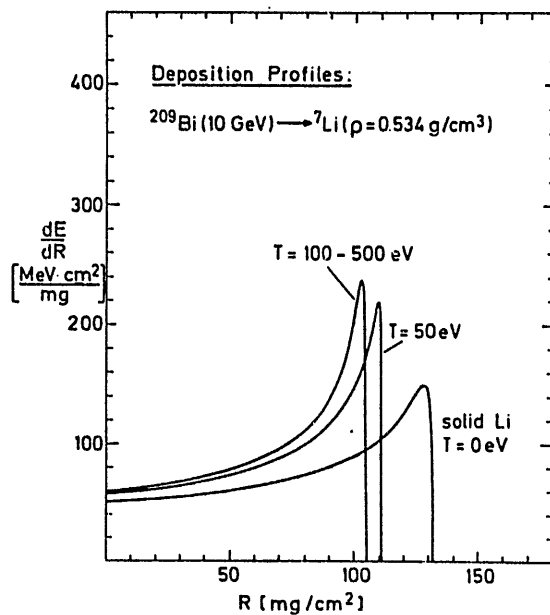


Fig. 7 Stopping power as a function of range for Bi ions on Li for different temperatures.

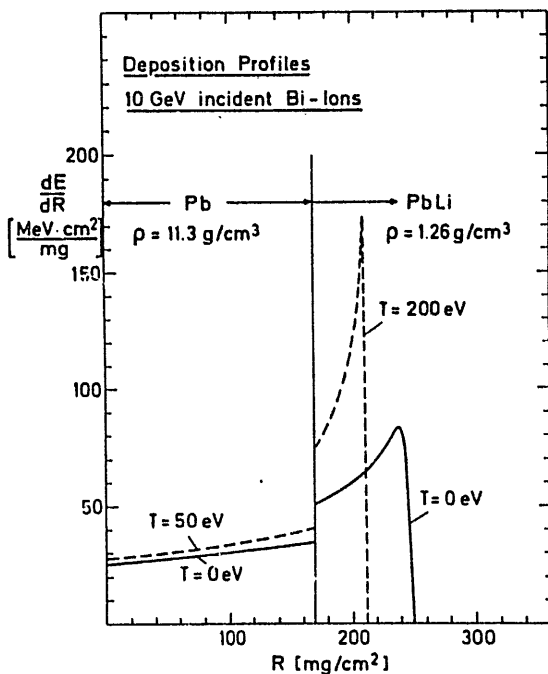


Fig. 8 Energy deposition of 10-GeV Bi ions in the absorption layers of HIBALL pellet. Solid line is for cold target, broken line for typical temperatures during implosion.

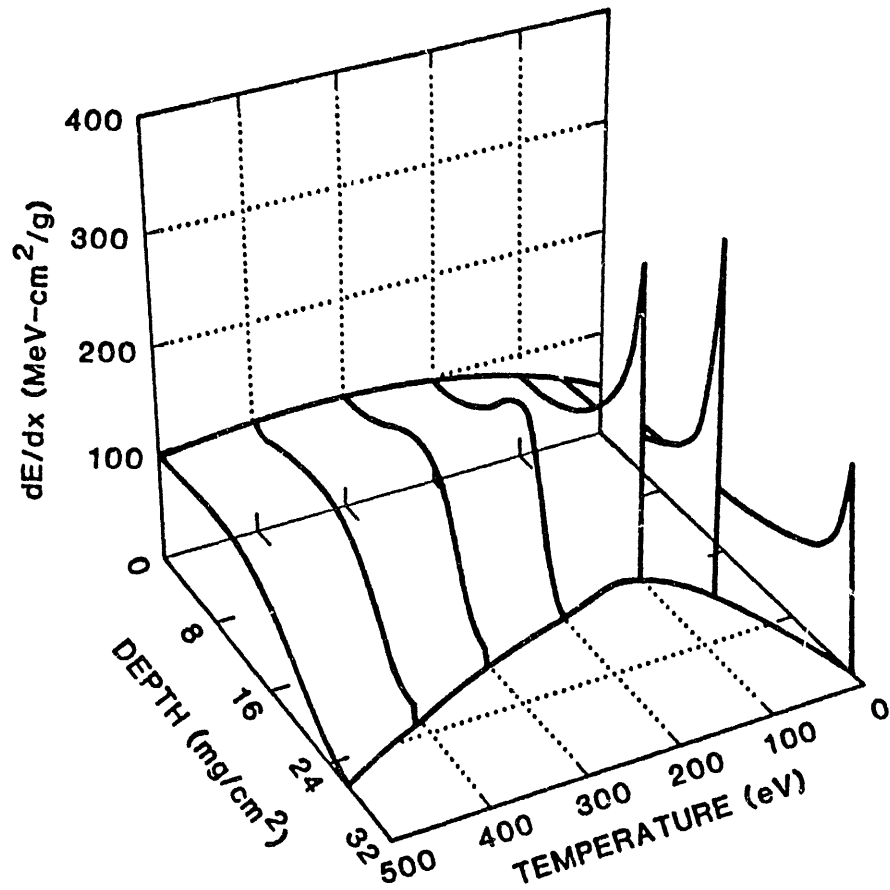


Fig.9 Deposition profiles for 2-MeV protons in Au at a density of 0.193 g/cm³ as a function of temperature.

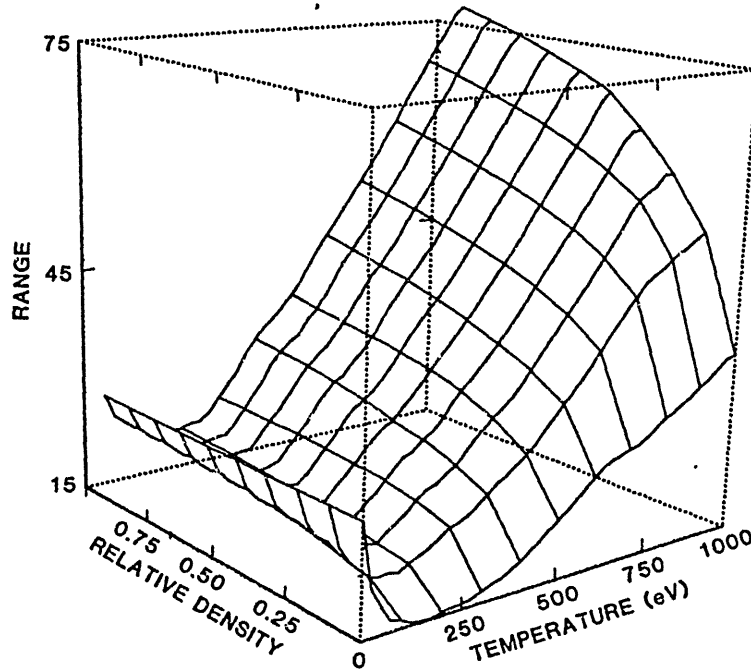


Fig.10 Variation of the range of 2-MeV protons in Au as a function of density and temperature.

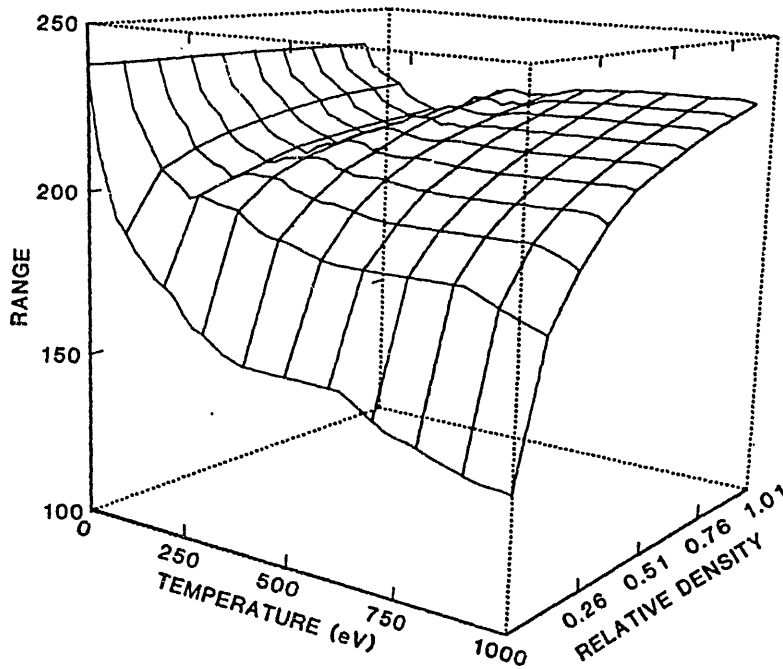


Fig.11 Variation of the range of 10-GeV U ions in Au as a function of density and temperature.

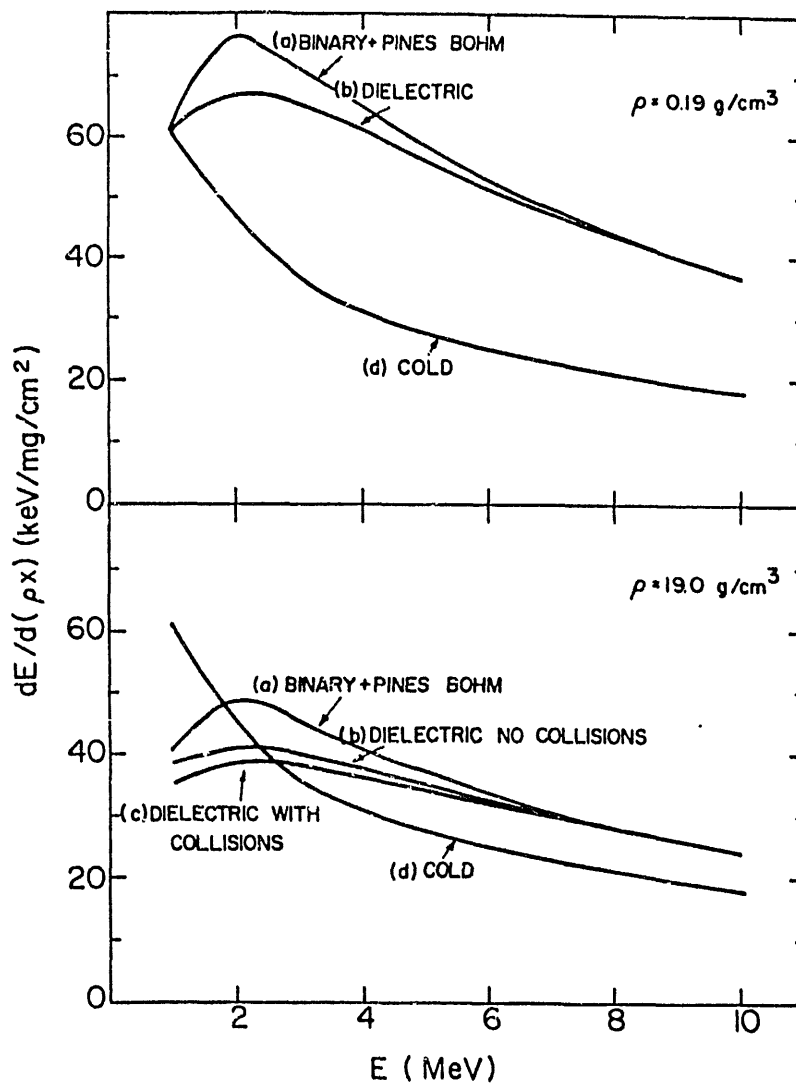


Fig.12 Energy loss as a function of proton energy in Au targets at the temperature of 1 keV. Free electron contribution is estimated according to; (a) Binary collision theory with plasma oscillations, (b) Dielectric function without plasma collisions, quantum form (collisional effects are negligible in the low density case), (c) Dielectric function with plasma collisions, classical form with cutoff at k_B , (d) Experimental energy loss in a cold target.

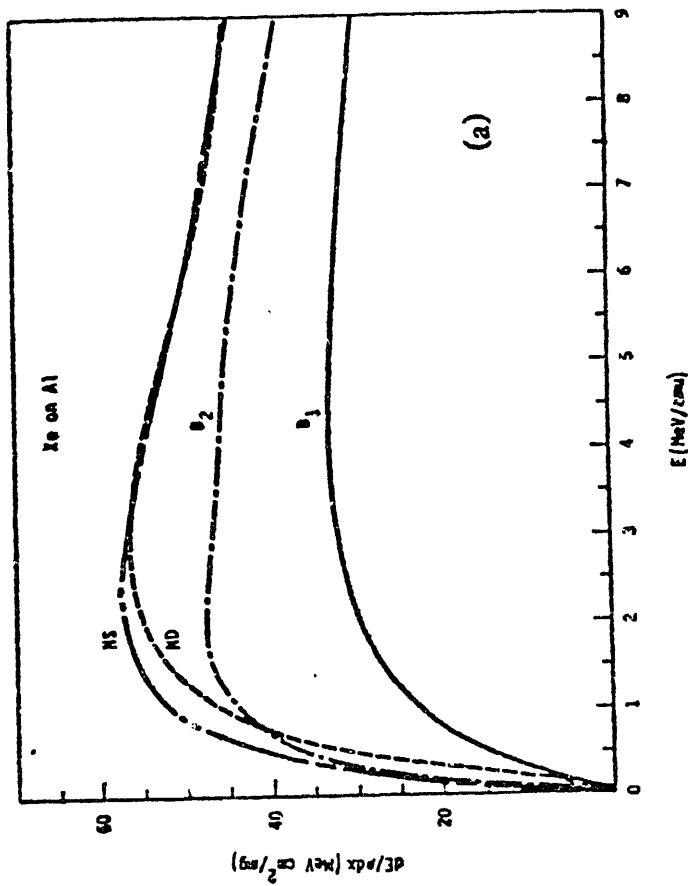
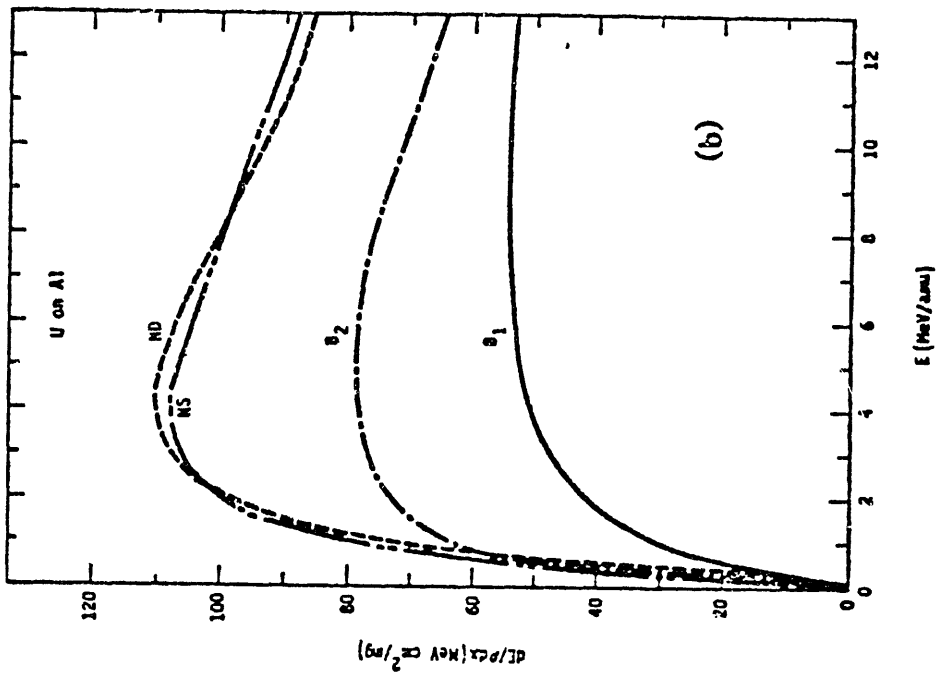


Fig. 13 The cold stopping powers for (a) Xe ions and (b) U ions on Al. (curve B₁) using Betz's q^* and the classical q_m^{-1} if $\xi = q^* e^2 / v > 1$ and quantum q_m^{-1} if $\xi < 1$; (curve B₂) using Betz's q^* and the quantum q_m^{-1} ; (curve ND) using Nikolaev and Dmitriev's q^* ; (curve NS) Northcliffe and Schilling's result.

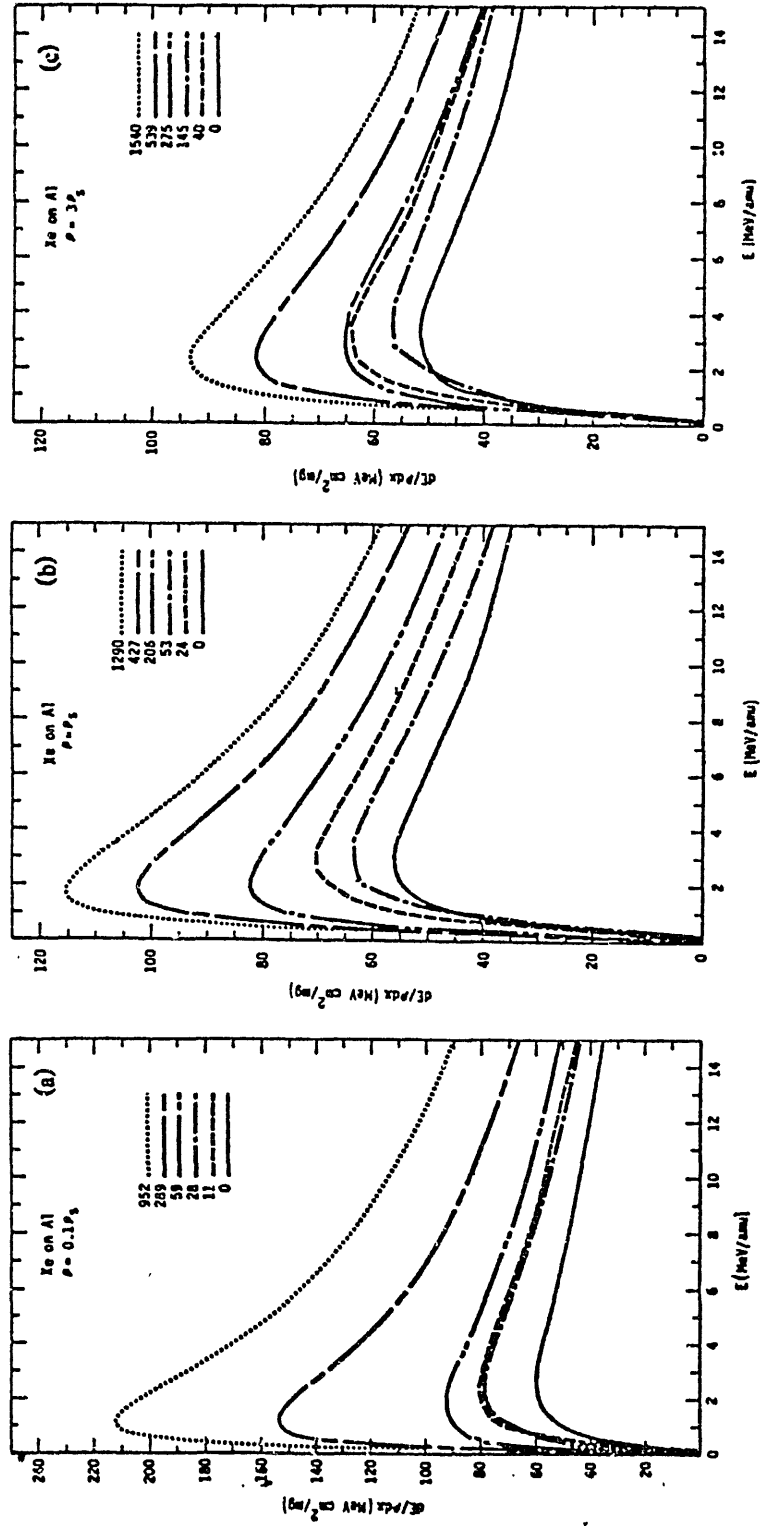


Fig.14 The stopping power for Xe on Al at (a) 0.1 solid density, (b) solid density, and (c) three times solid density, as a function of the energy per amu. The curves are labeled by the corresponding temperatures T in eV.

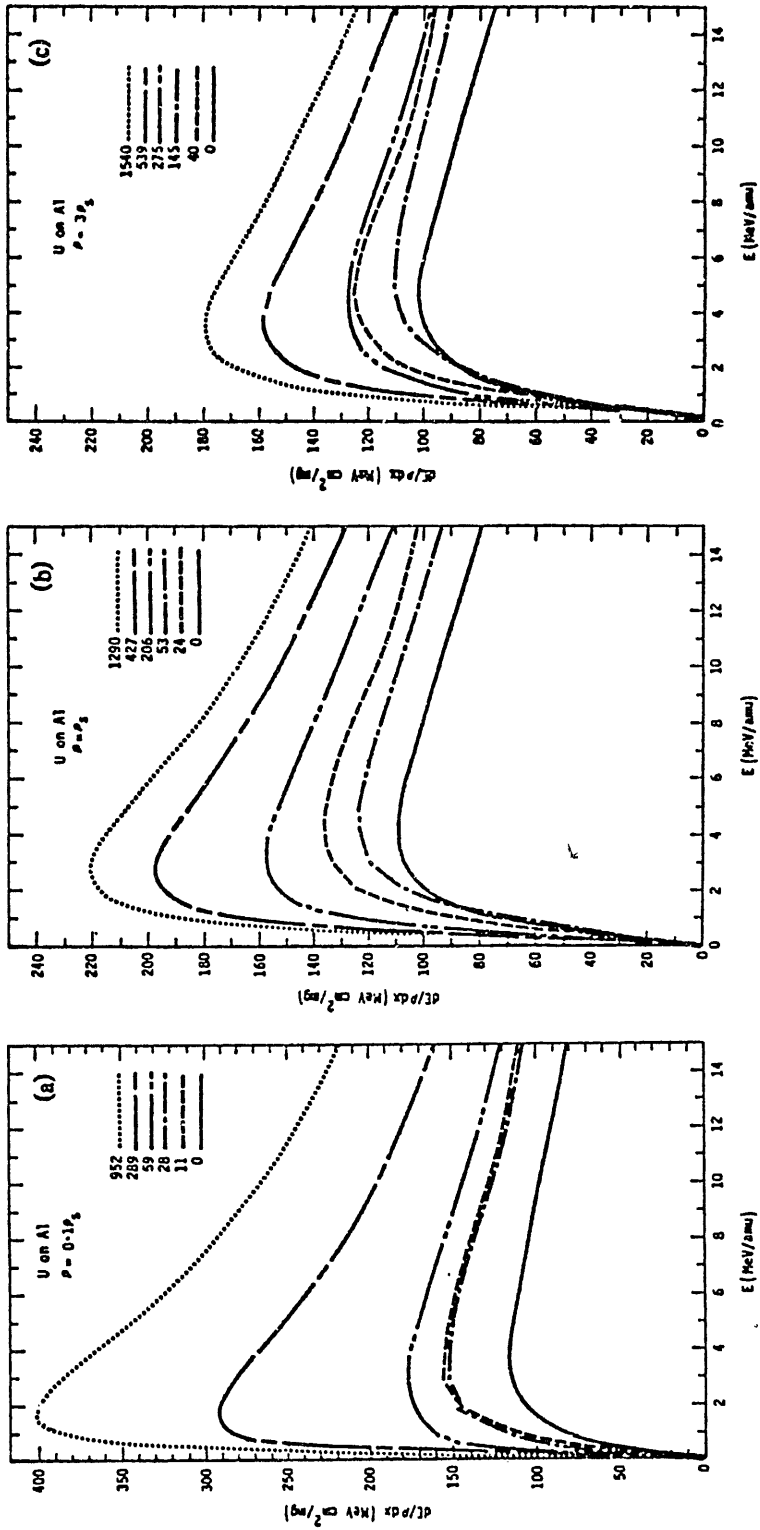


Fig.15 The stopping power for U on Al at (a) 0.1 solid density (b) solid density, (c) three times solid density, as a function of the energy per amu. The legend for each curve is the temperature in eV.

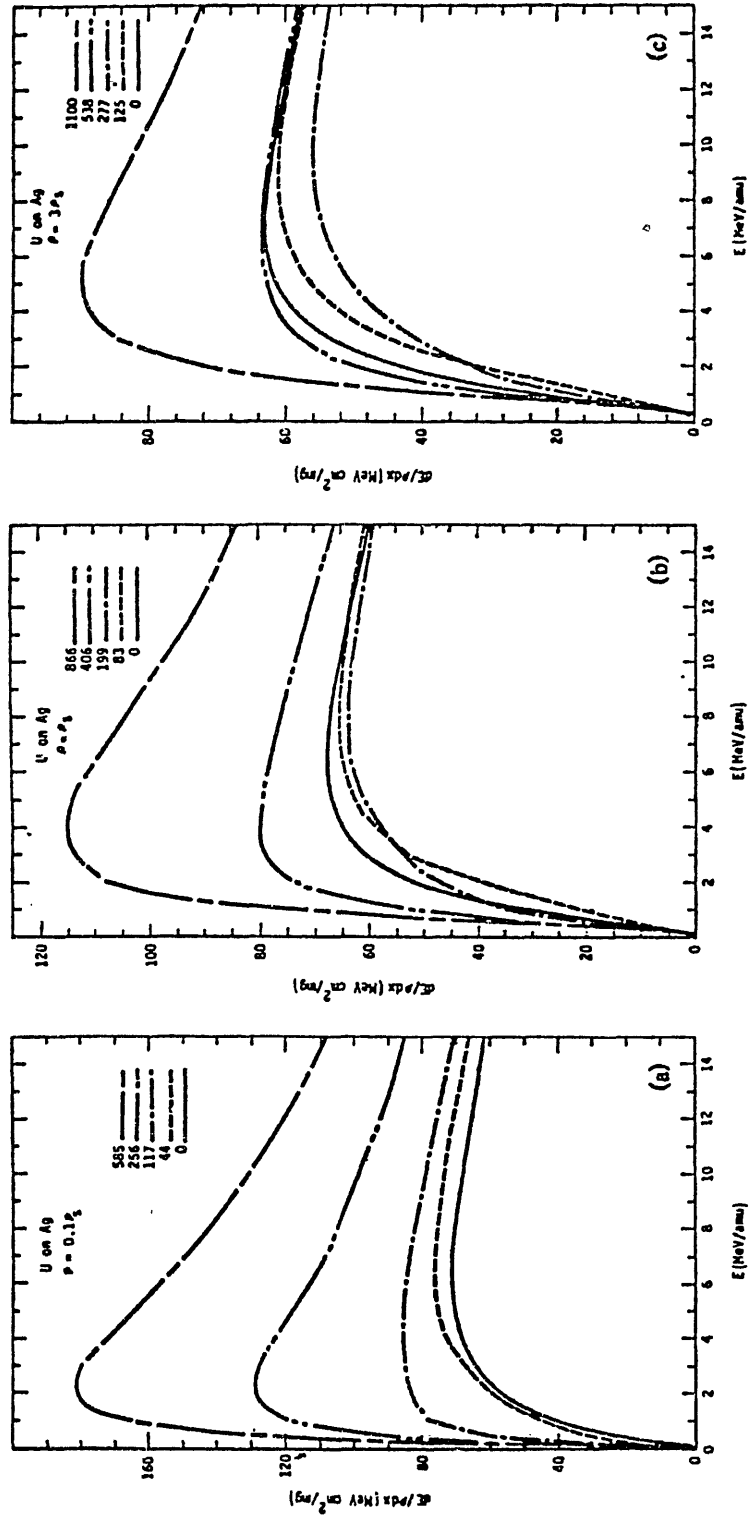


Fig.16 The stopping power for U on Ag at (a) 0.1 solid density, (b) solid density, and (c) three times solid density, as a function of the energy per amu. The legend for each curve is the temperature in eV.

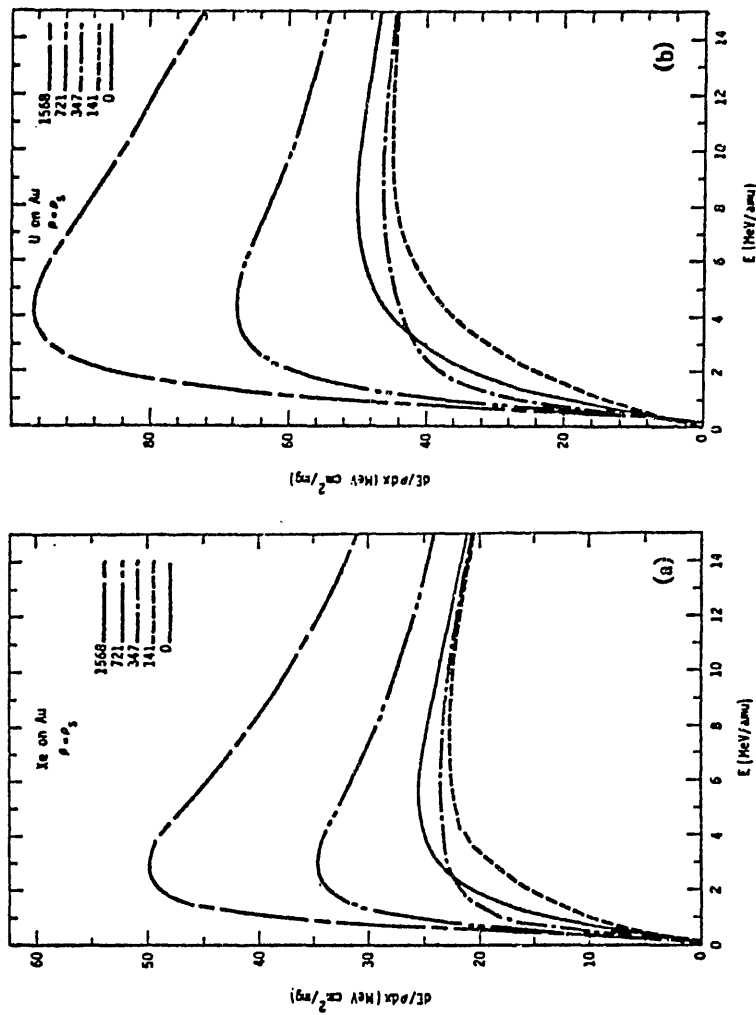


Fig.17 The stopping power as a function of the energy per amu for (a) Xe on Au, and (b) U on Au. All cases are at solid densities and the legend for the curves is the temperature in eV.

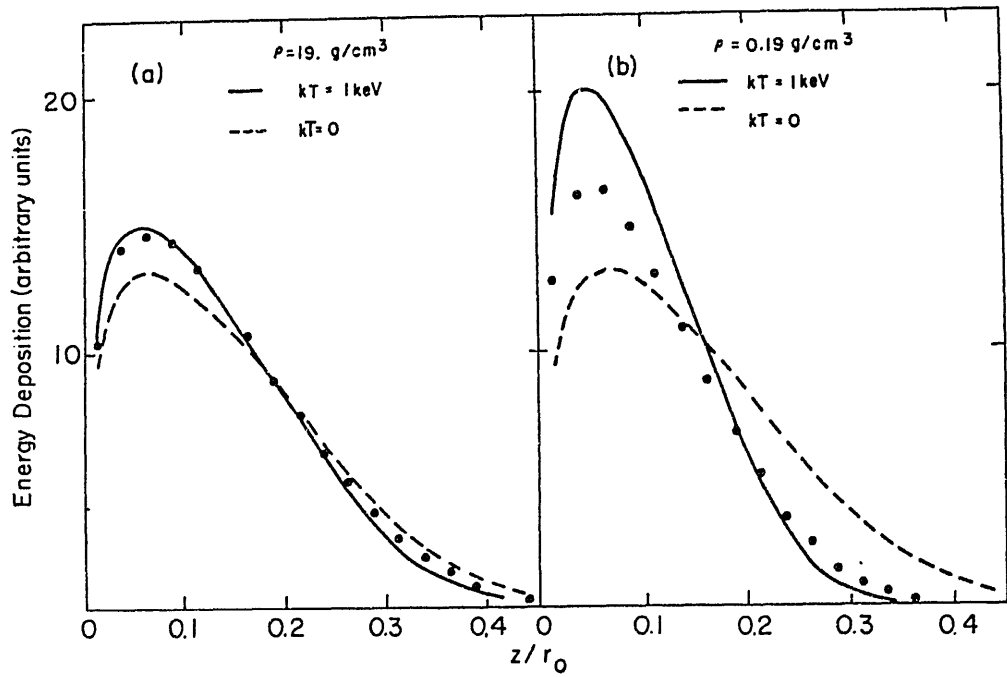


Fig.18 Deposition profiles of 400-keV electrons in cold and 1-keV Au targets. (a) $\rho = 19.0 \text{ g/cm}^3$, and (b) $\rho = 0.19 \text{ g/cm}^3$. Dots represent results with cold multiple scattering.

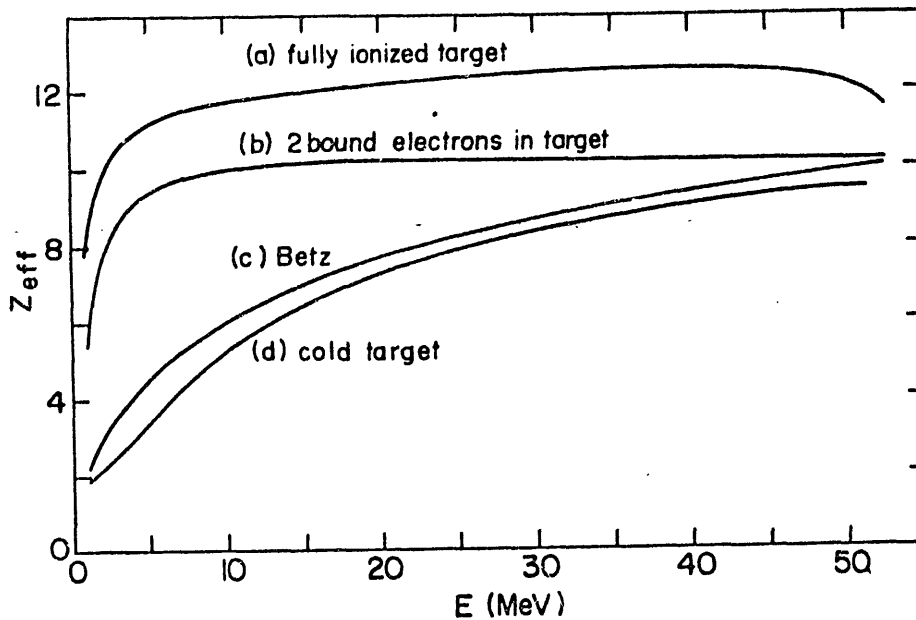


Fig.19 The charge state Z_{eff} of an Al ion with the initial energy of 54 MeV as a function of its energy as it is slowed in C targets at various temperatures. The transition from $Z=3$ is very fast and not shown. The empirical curve of Betz is shown for comparison.

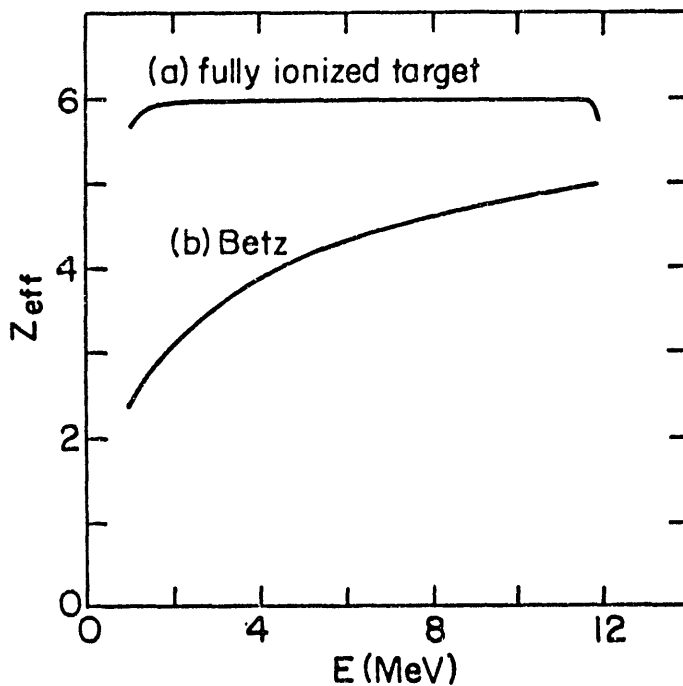


Fig.20 The charge state q^* of C ions with initial energy of 12 MeV as a function of its energy as it is slowed in a fully ionized Li target as compared with the empirical curve of Betz for a Au target.

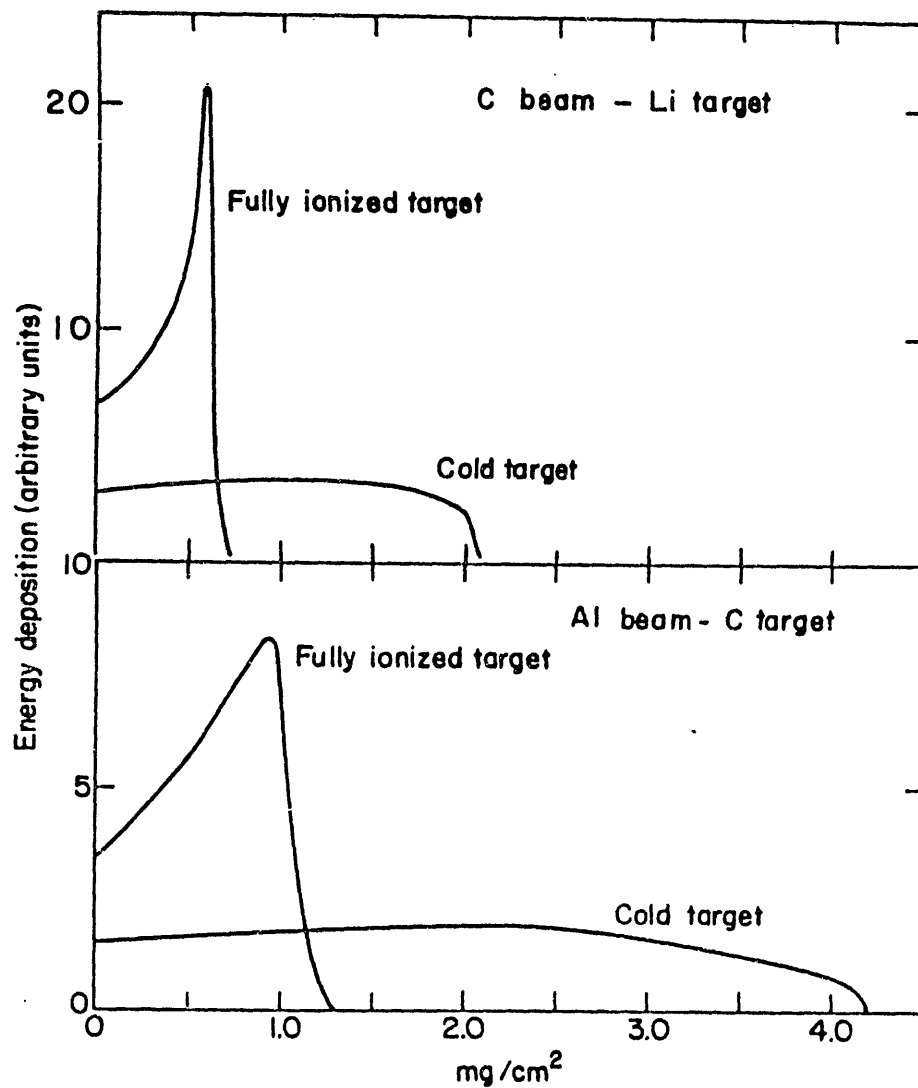


Fig.21 Energy deposition profiles. Top: 12-MeV C beam in fully ionized and in cold Li targets. Bottom: 54-MeV Al beam in fully ionized and in cold C targets.

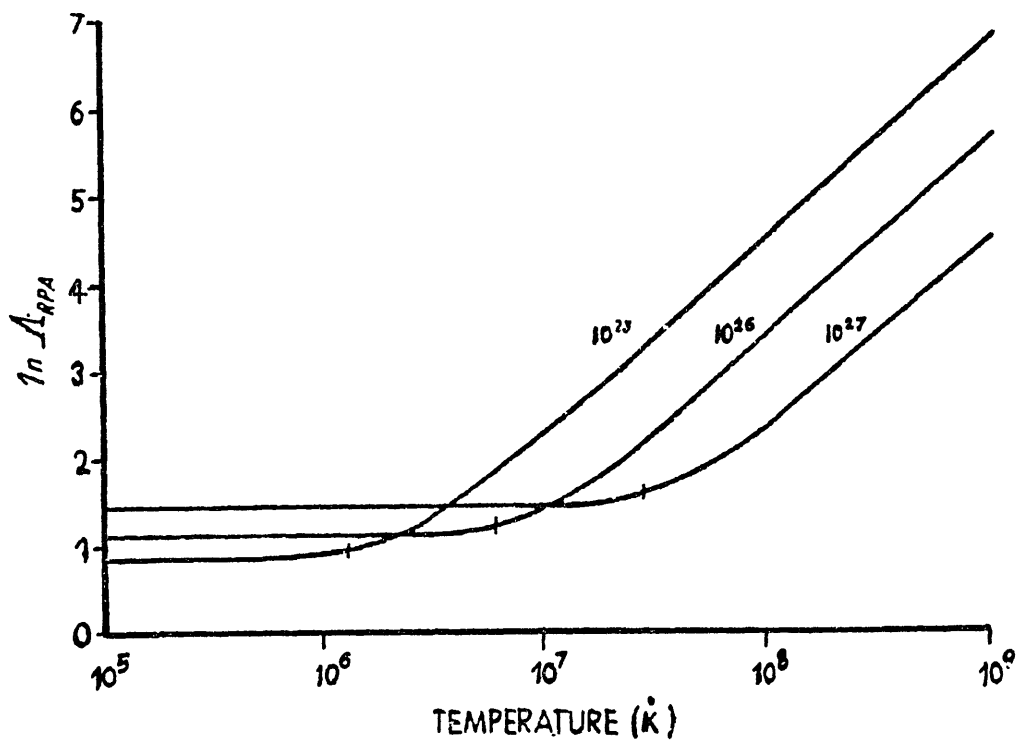


Fig.22 RPA Coulomb logarithm as a function of the temperature for different electron densities. The vertical line on each curve indicates the Fermi temperature.

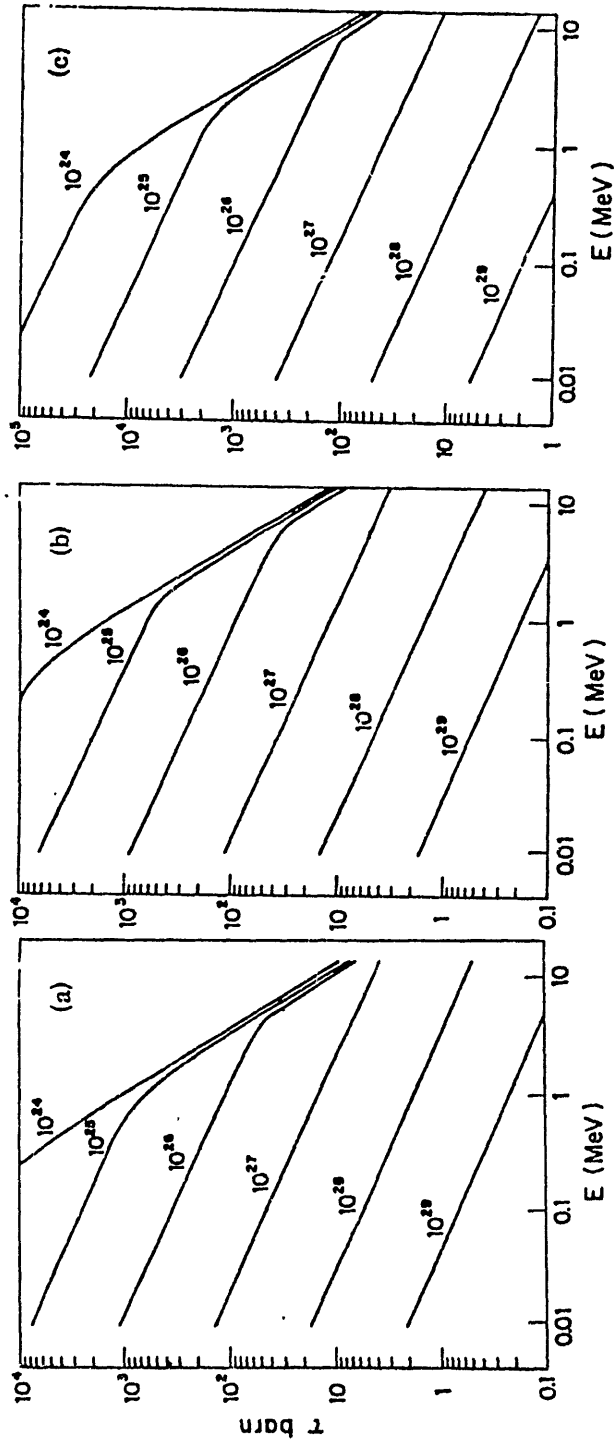


Fig.23 Slowing-down cross section τ as a function of ion energy E , for $n_e = 10^{24}$ to 10^{29} cm $^{-3}$, for (a) deuterons, (b) tritons, and (c) α -particles.

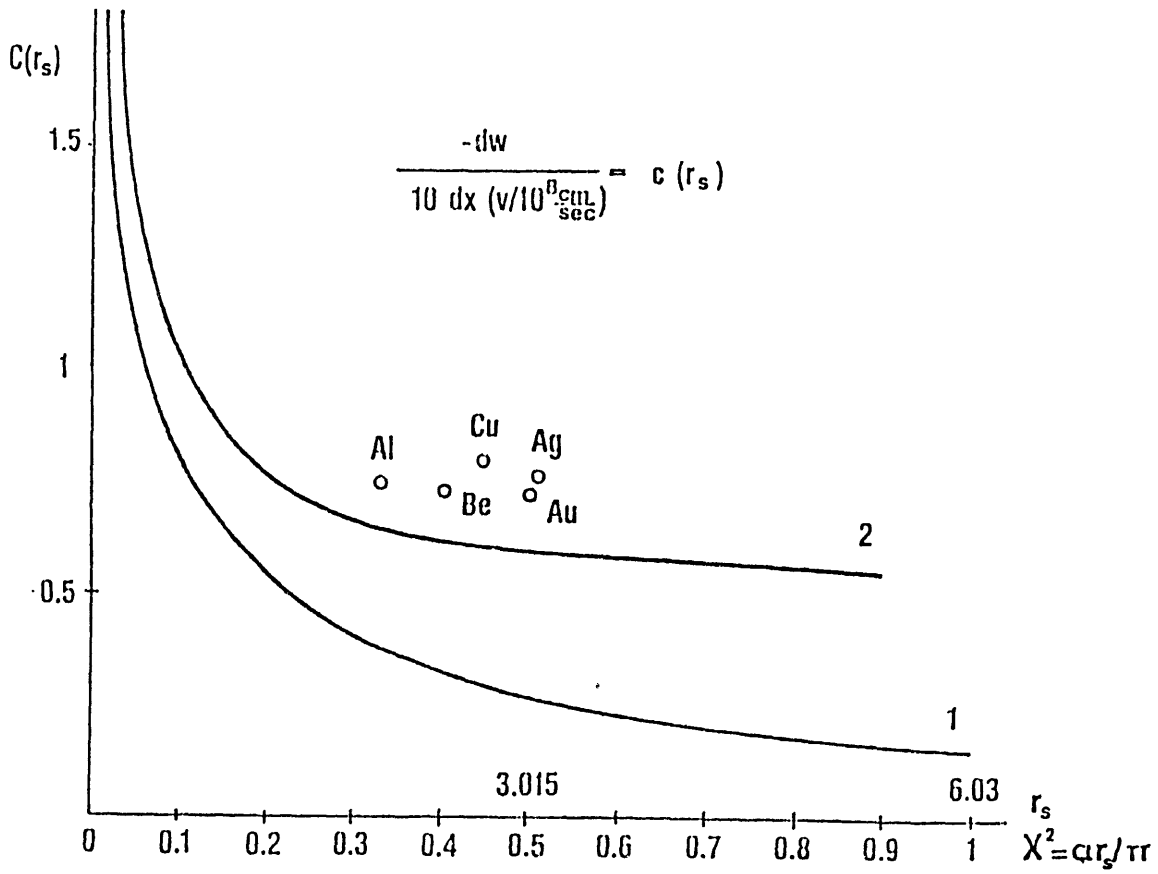


Fig.24 Curve 1: Lindhard approximation corresponding to assumption $G=0$ in the formula (4.34); curve 2: formula (4.34). Open circles are experimental values. Energy losses dE/dx are expressed in units of $\text{eV}/\text{\AA}$ ($Z=1$).

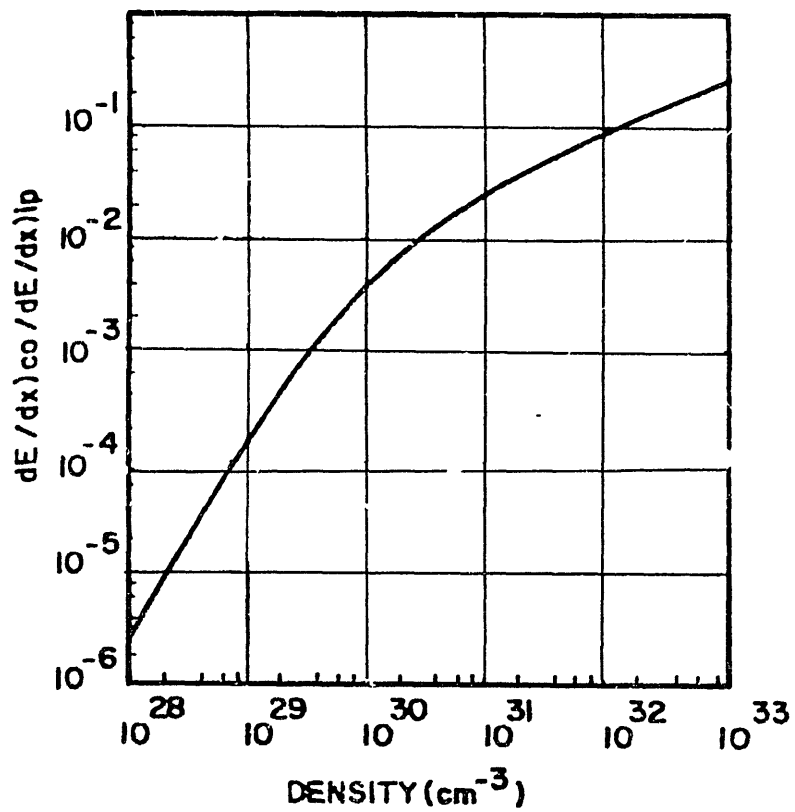


Fig.25 Ratio $(dE/dx)_{co} / (dE/dx)_{ip}$ vs density for 3.5-MeV α -particles incident on degenerate electron-deuterium plasmas with $T_i = 50$ keV.

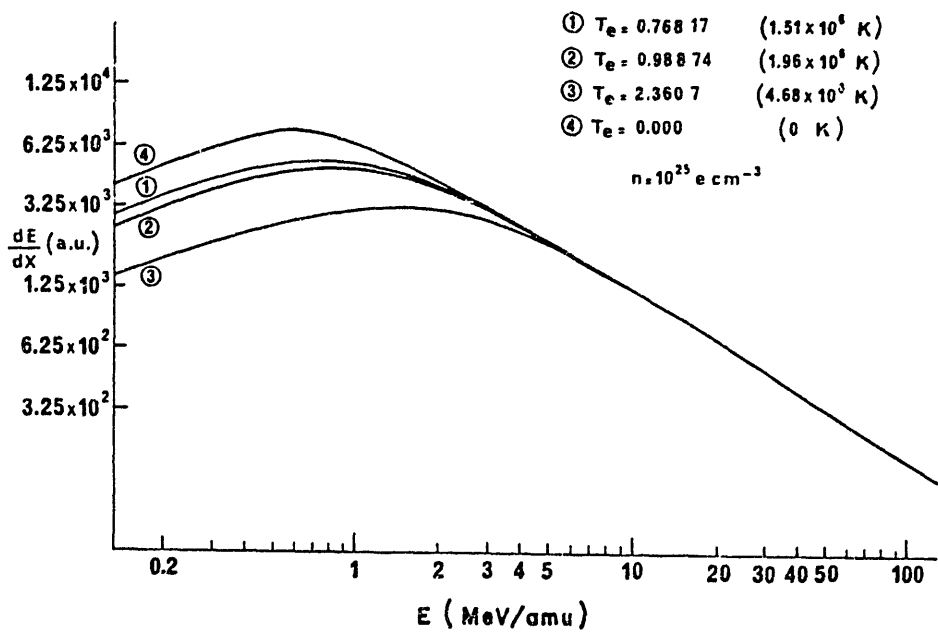


Fig.26 Stopping power dE/dx (a.u.) at $n = 10^{25}$ cm $^{-3}$ and various temperatures.

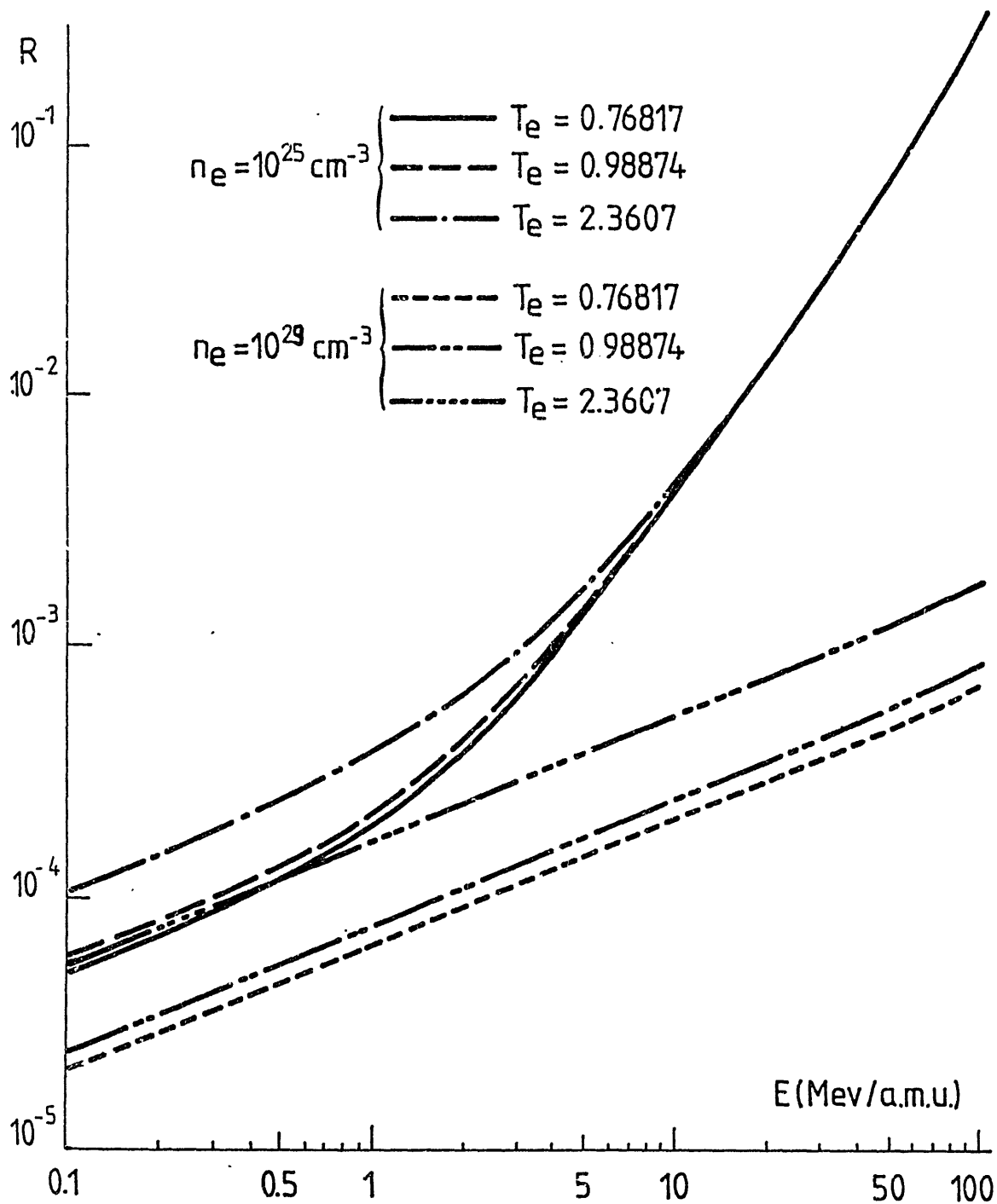


Fig.27 Ranges at $n = 10^{25}$, and 10^{29} cm^{-3} and various temperatures.

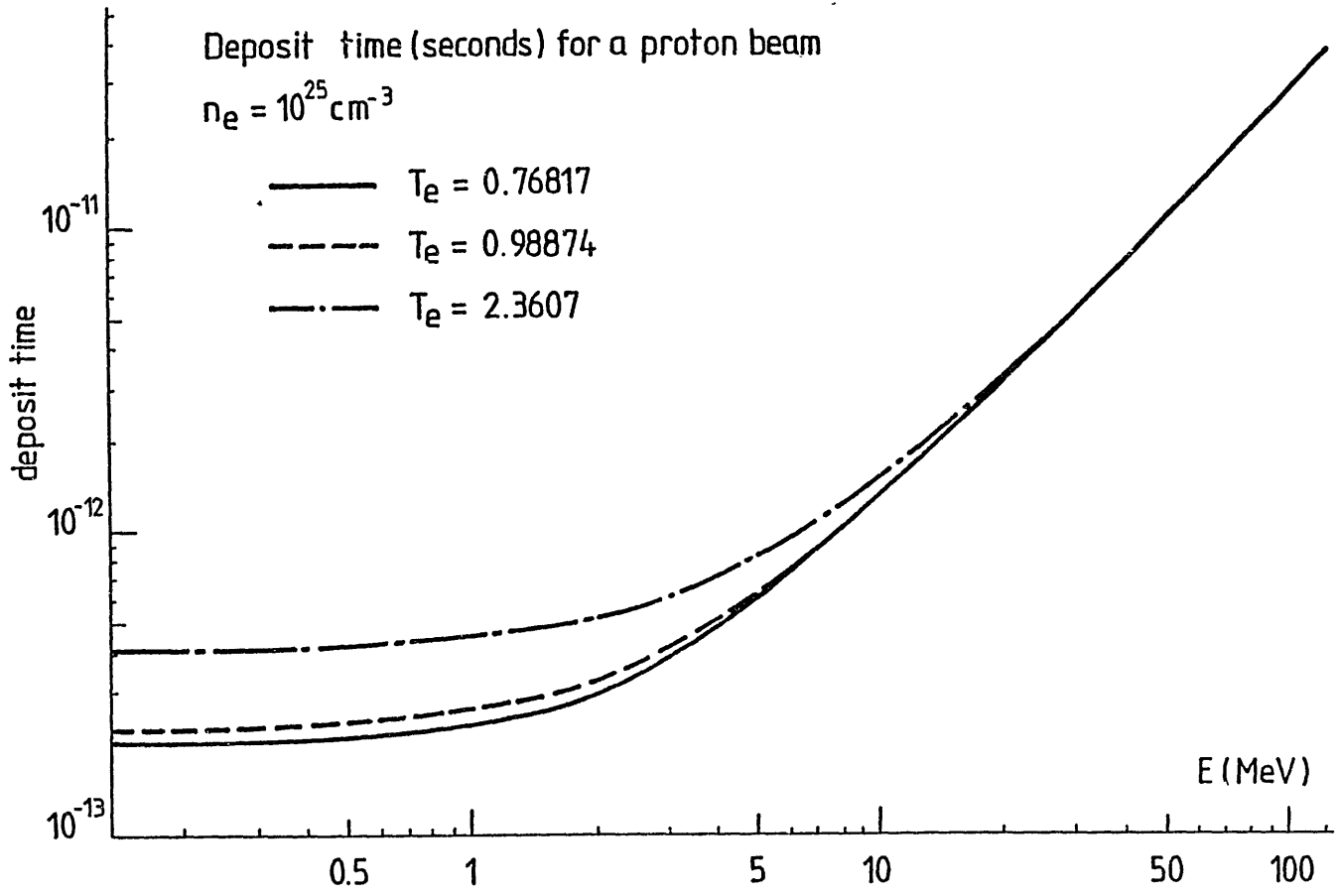


Fig.28 Deposit time (sec) at $n = 10^{25} \text{ cm}^{-3}$ and various temperatures as a function of proton beam energy (MeV).

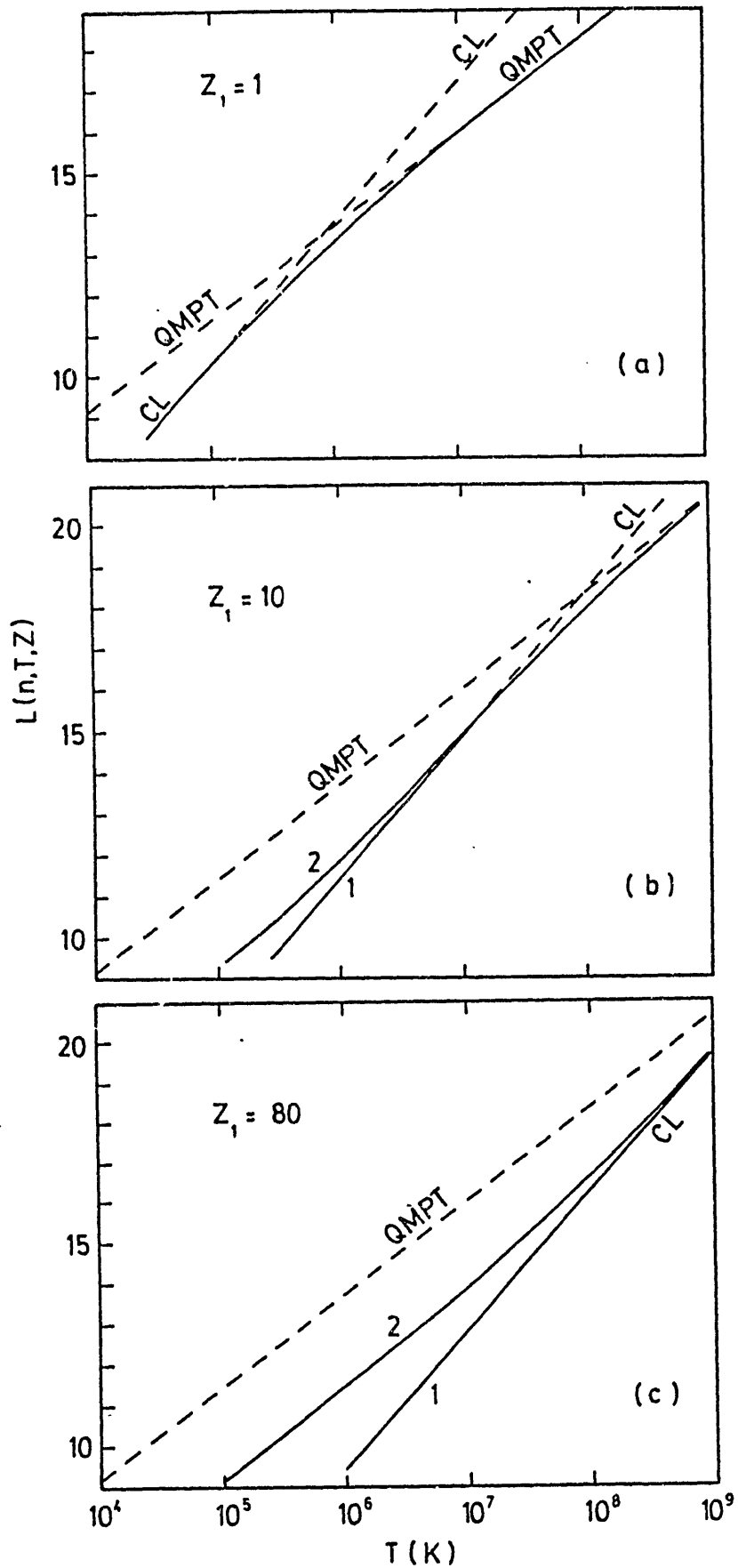


Fig.29 Values of the collisional logarithm $L(n, T, Z)$ for electron density $n = 10^{13} \text{ cm}^{-3}$, for protons ($Z=Z_1=1$), and for light and heavy ions ($Z_1=10, Z_1=80$). The lines labeled 1 and 2 correspond to $Z=Z_1$ and $Z=q^*$, respectively.

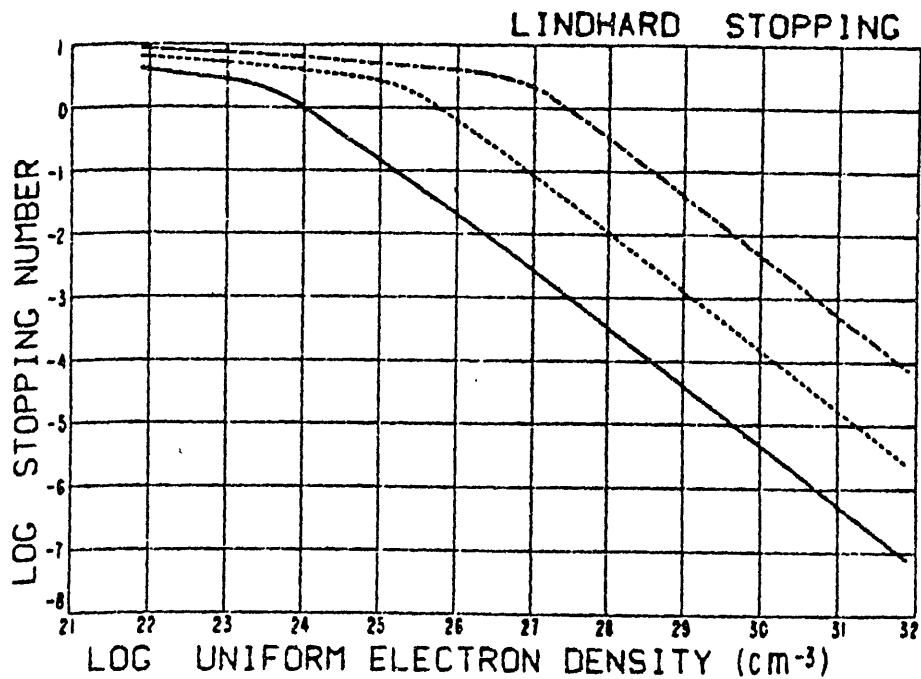


Fig.30 Plot of variation in stopping number with electron density for selected projectile energies. ((—)100 keV/amu; (---)1000 keV/amu; (---)10000 keV/amu).

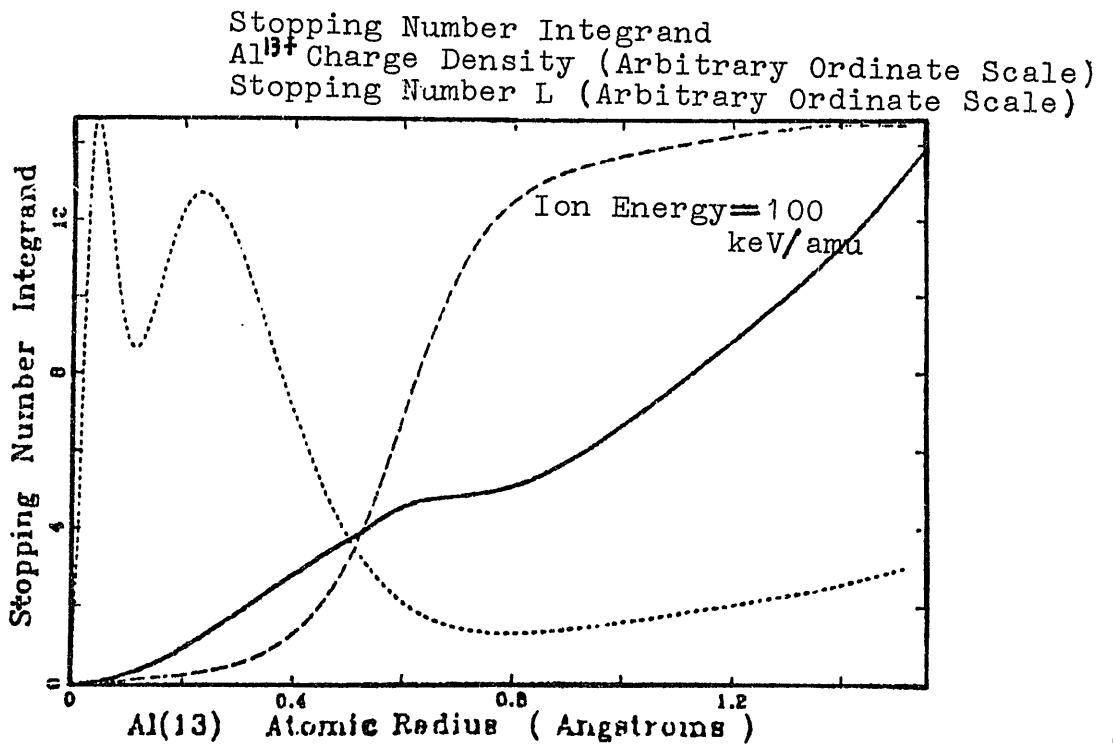


Fig.31 Comparison of spatial variation in the stopping number integrand of eq. (4.60), and the solid-state radial charge density for Al (V.L. Moruzzi, J.F. Janak, and A.R. Williams: Calculated Electronic Properties of Metals (Pergamon, New York, 1978)) with ion energy of 100 keV/amu.

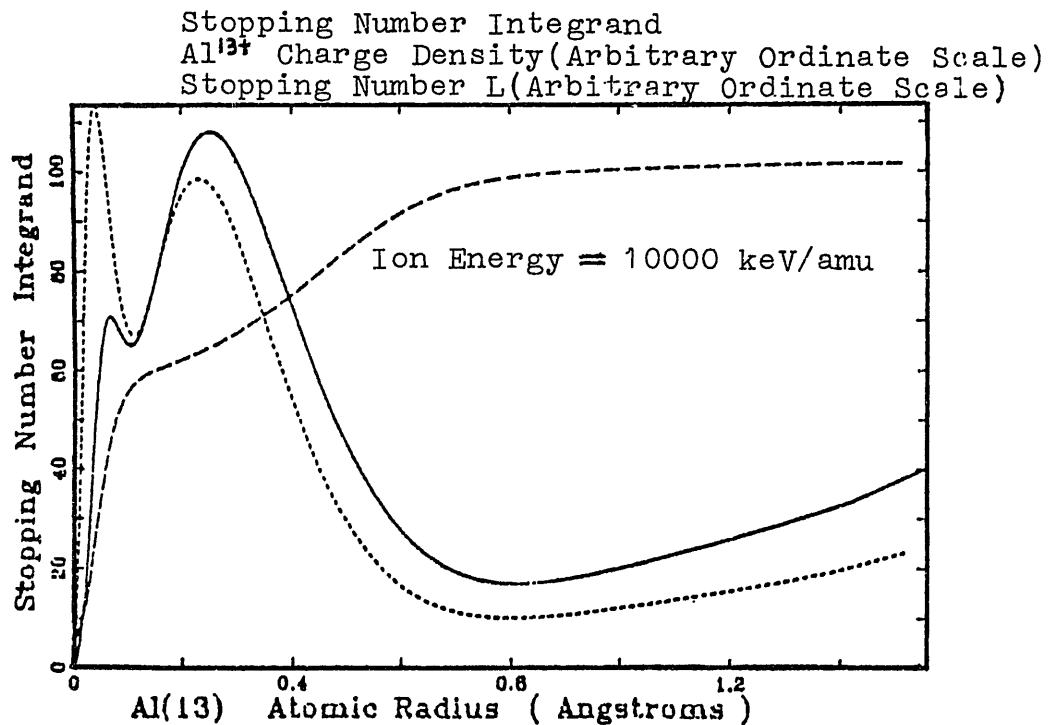


Fig.32 Comparison of spatial variation in the stopping number integrand of eq. (4.60), the stopping number of eq. (4.60), and the solid-state radial charge density for Al (see the reference in in Fig.31) with ion energy of 10000 keV/amu.

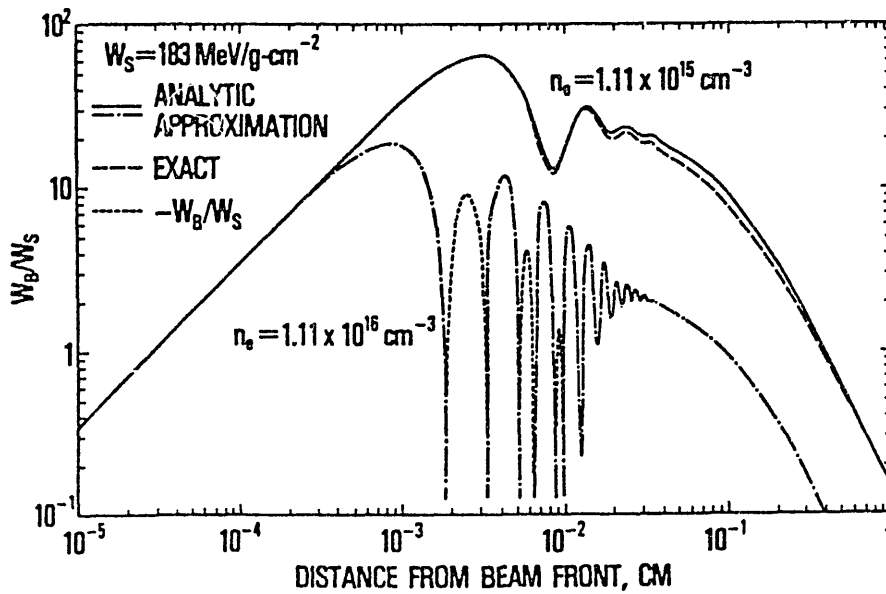


Fig.33 The ratio of the beam-density contribution W_B to the single-particle energy loss W_S vs the distance of a beam particle from the beam front. The curves were generated for a 5-MeV proton beam with beam density $n_b = 6.44 \times 10^{14} \text{ cm}^{-3}$ interacting with partially ionized H_2 containing n free electrons per cubic centimeter.

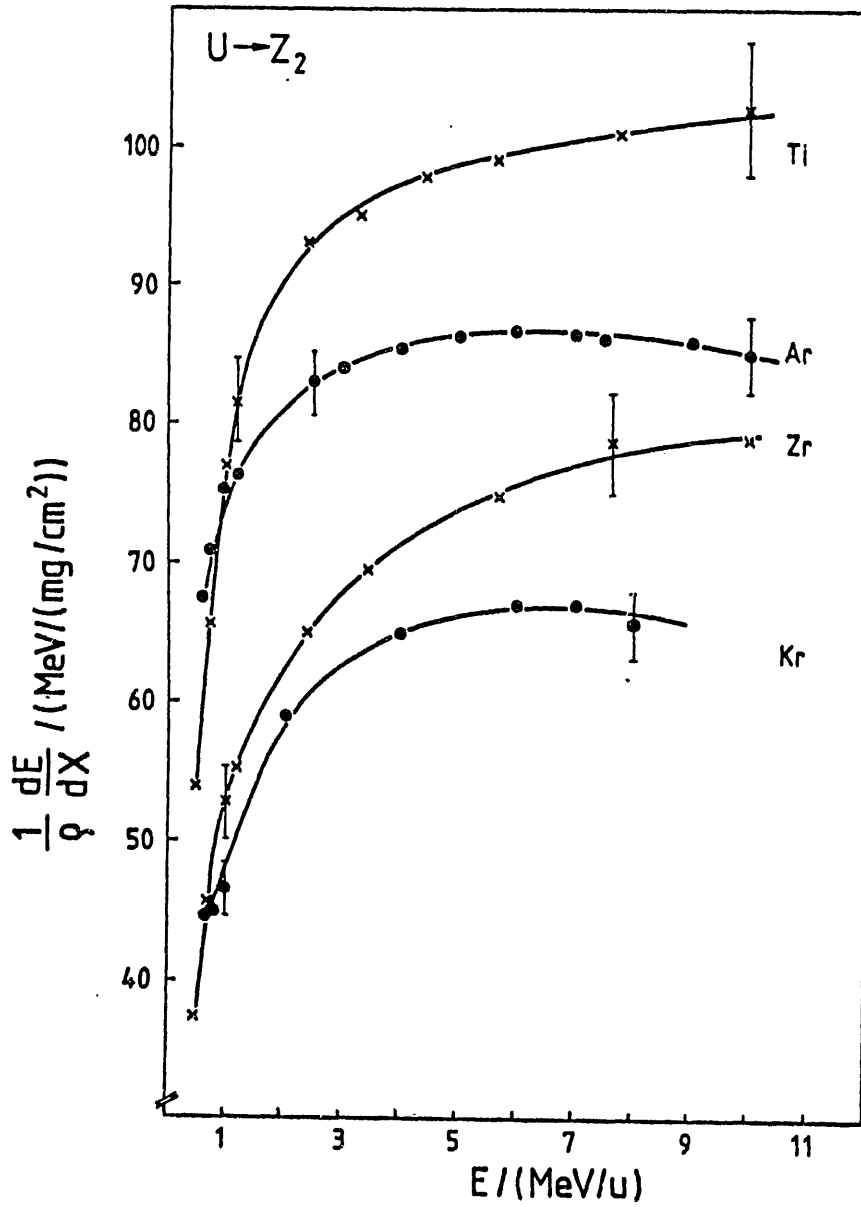


Fig.34 Stopping powers of (0.5 ~ 10) MeV/amu U ions in solids and gases.

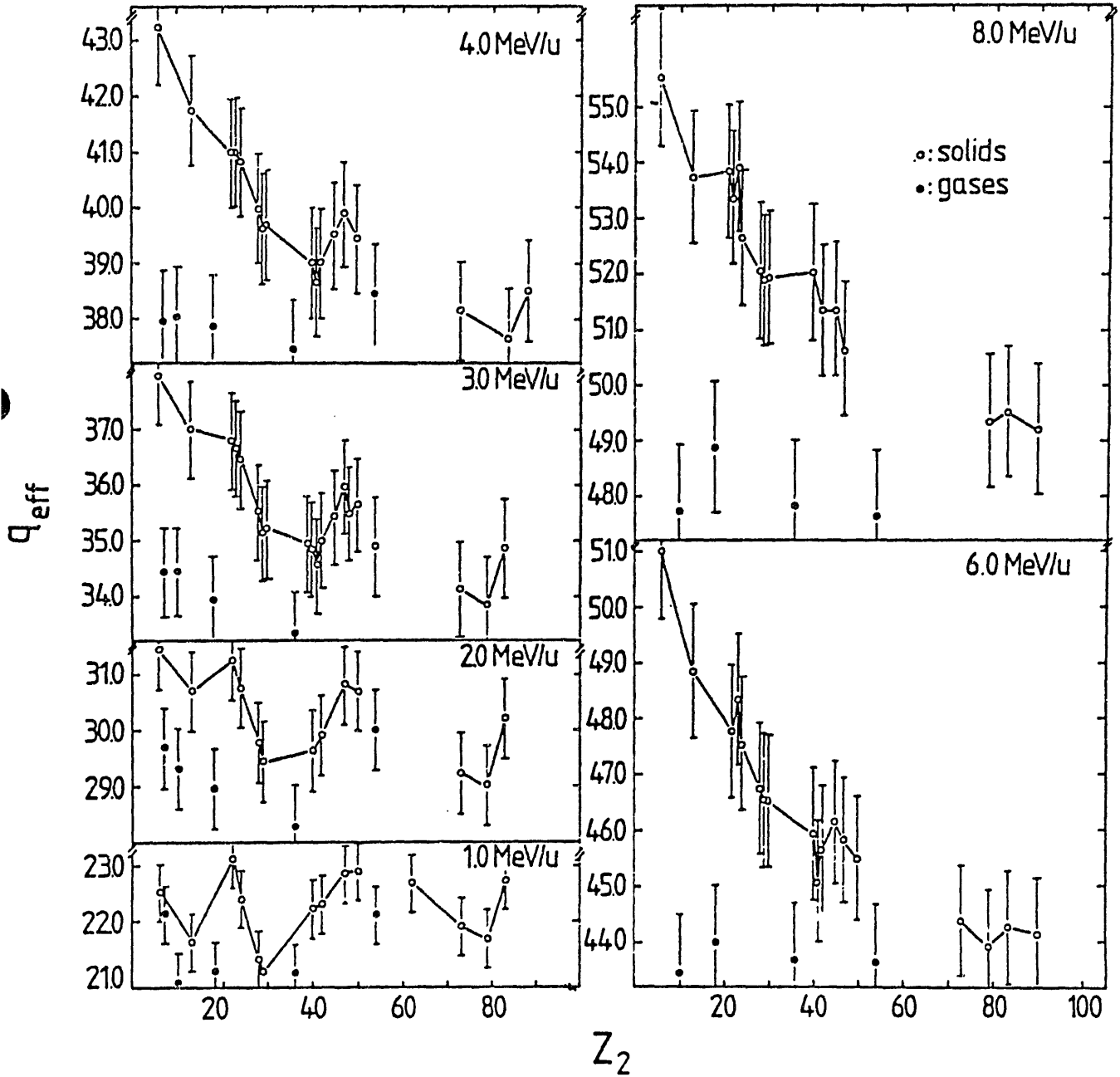


Fig.35 Effective charge q^* for U-ions in gases and solids at different energies.

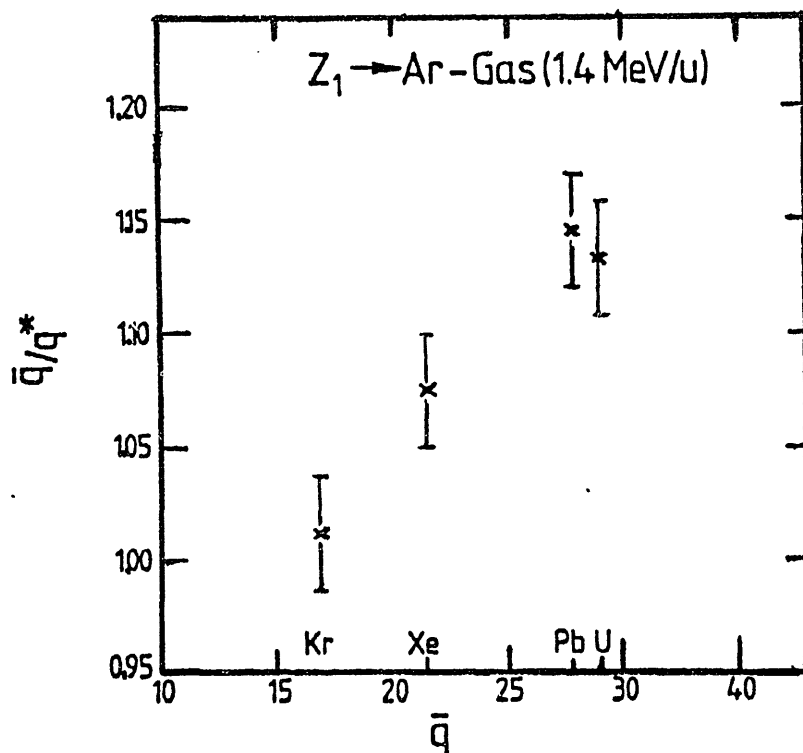


Fig.36 Comparison between \bar{q} (average equilibrium charge) and q^* (effective charge) values for different projectiles in Ar ($\bar{q} = (\sum \phi_i q_i^2)^{1/2}$ equals $\sum \phi_i q_i$ within less than 1 %).

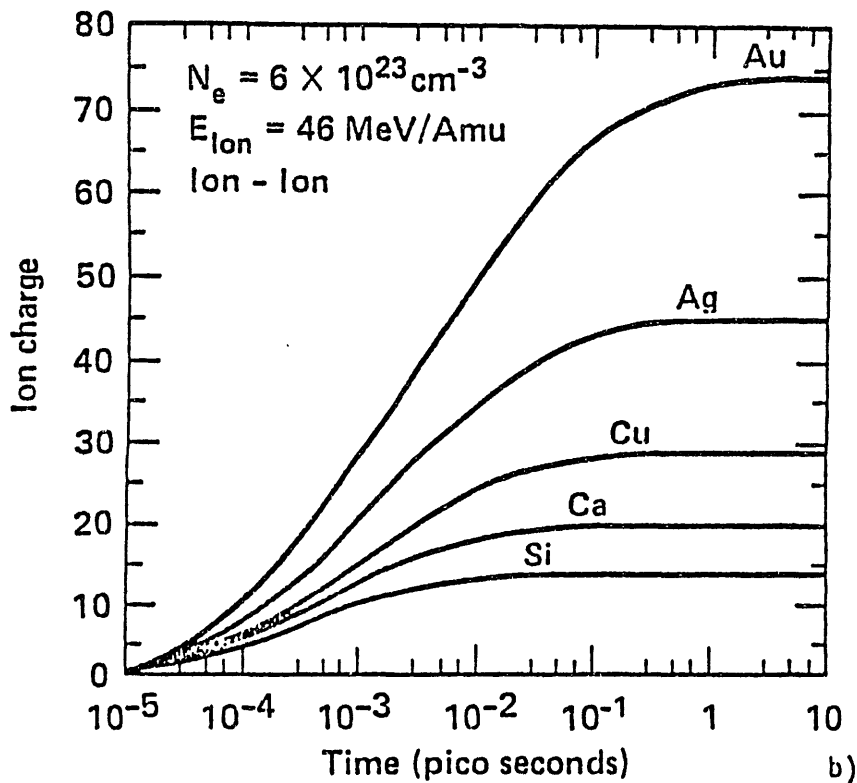
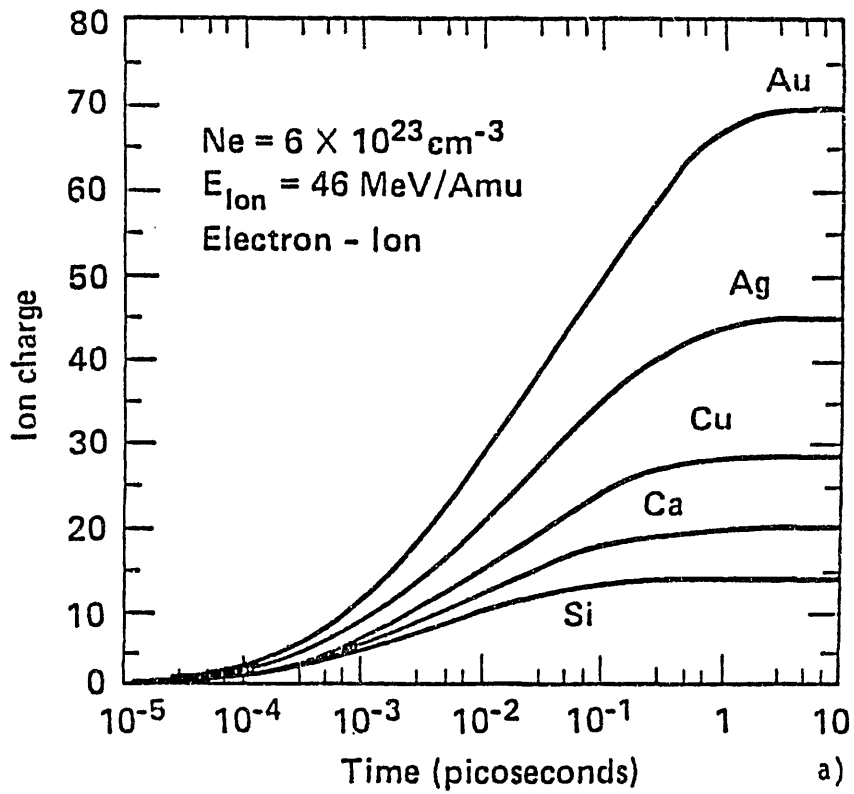


Fig.37 Time dependent charge state for several ions for electron collisions (a) and ion collisions (b) for the fully stripped Al target with solid density.

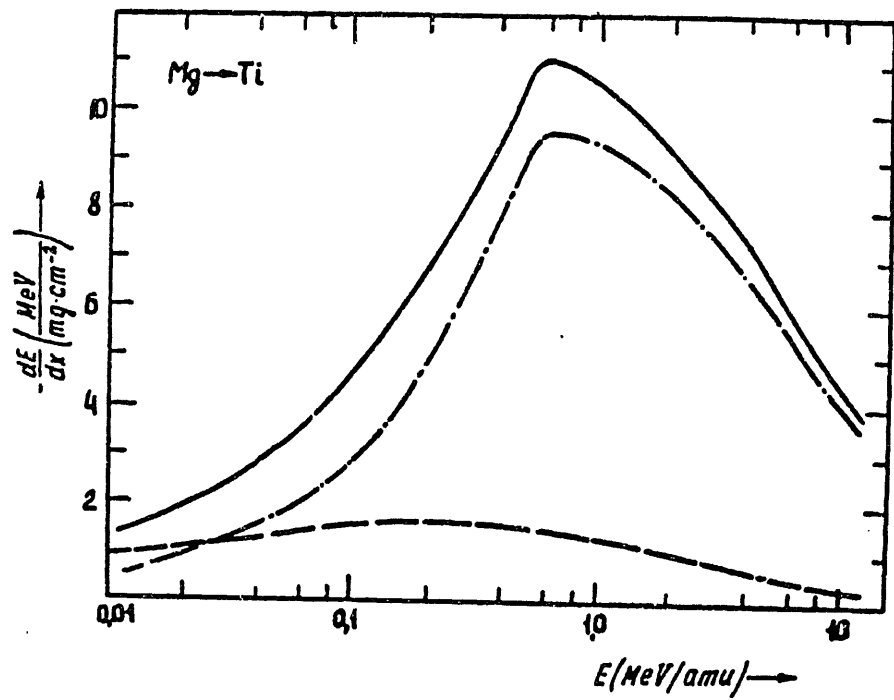


Fig.38 Calculated energy loss of Mg-ions in Ti. The broken curve: the energy loss due to electron exchange; the chain curve: the energy loss due to excitation or ionization of the medium electrons by projectile nucleus field; the solid curve: total energy loss.

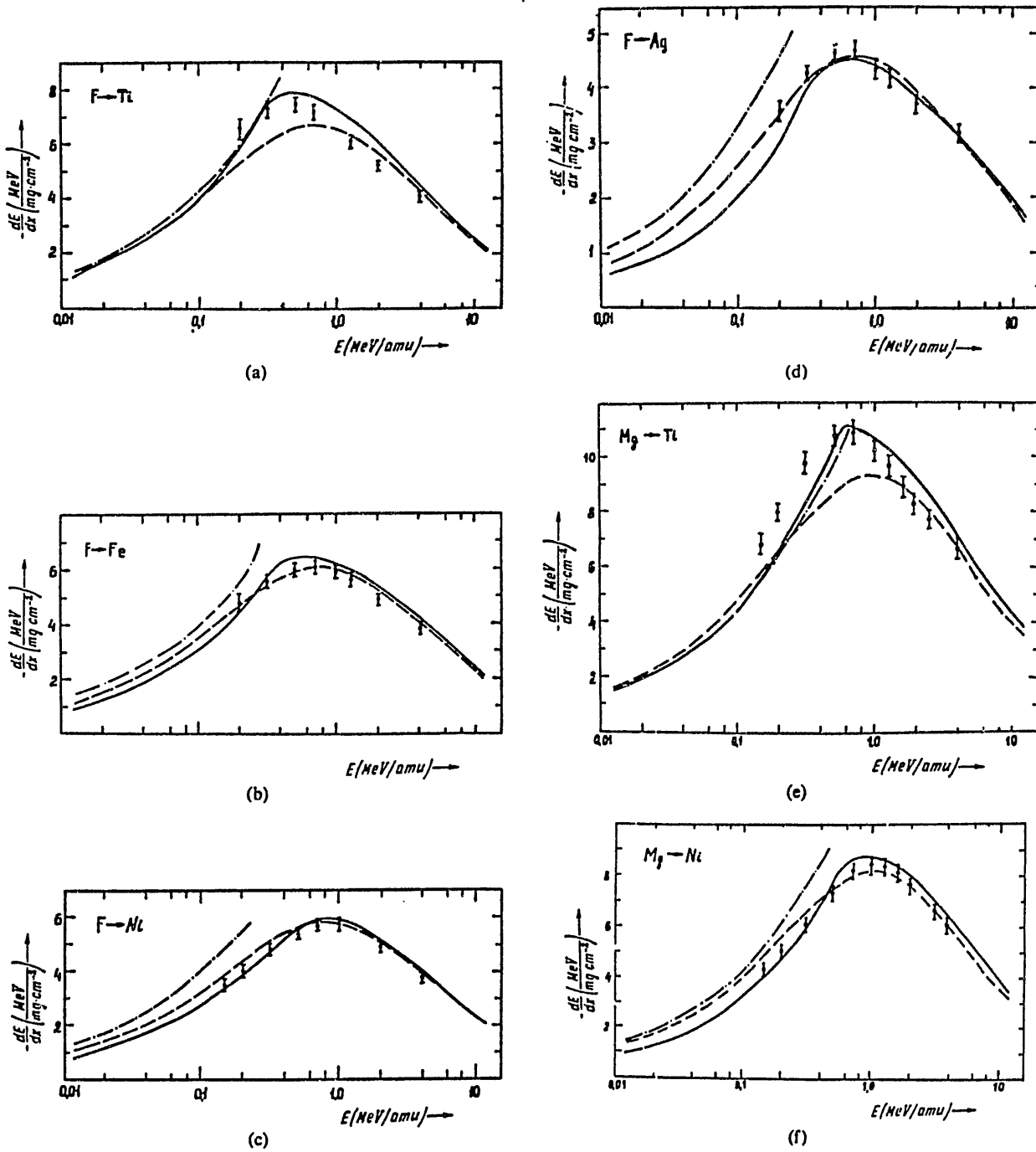


Fig.39 The heavy ions energy losses in various materials. The broken curve: NS data; the chain curve: calculations according to Firsov theory; the solid curve: calculations by Burenkov et al. Experimental points are from Foster et al. (Nucl. Inst. Meth. 136 (1976) 349) for solid targets and from Pierce and Blann (Phys. Rev. 173 (1968) 390) for gaseous targets.

LIST OF IPPJ-AM REPORTS

- IPPJ-AM-1* "Cross Sections for Charge Transfer of Hydrogen Beams in Gases and Vapors in the Energy Range 10 eV–10 keV"
H. Tawara (1977) [Published in Atomic Data and Nuclear Data Tables 22, 491 (1978)]
- IPPJ-AM-2* "Ionization and Excitation of Ions by Electron Impact –Review of Empirical Formulae–"
T. Kato (1977)
- IPPJ-AM-3 "Grotrian Diagrams of Highly Ionized Iron FeVIII-FeXXVI"
K. Mori, M. Otsuka and T. Kato (1977) [Published in Atomic Data and Nuclear Data Tables 23, 196 (1979)]
- IPPJ-AM-4 "Atomic Processes in Hot Plasmas and X-Ray Emission"
T. Kato (1978)
- IPPJ-AM-5* "Charge Transfer between a Proton and a Heavy Metal Atom"
S. Hiraide, Y. Kigoshi and M. Matsuzawa (1978)
- IPPJ-AM-6* "Free-Free Transition in a Plasma –Review of Cross Sections and Spectra–"
T. Kato and H. Narumi (1978)
- IPPJ-AM-7* "Bibliography on Electron Collisions with Atomic Positive Ions: 1940 Through 1977"
K. Takayanagi and T. Iwai (1978)
- IPPJ-AM-8 "Semi-Empirical Cross Sections and Rate Coefficients for Excitation and Ionization by Electron Collision and Photoionization of Helium"
T. Fujimoto (1978)
- IPPJ-AM-9 "Charge Changing Cross Sections for Heavy-Particle Collisions in the Energy Range from 0.1 eV to 10 MeV I. Incidence of He, Li, Be, B and Their Ions"
Kazuhiko Okuno (1978)
- IPPJ-AM-10 "Charge Changing Cross Sections for Heavy-Particle Collisions in the Energy Range from 0.1 eV to 10 MeV II. Incidence of C, N, O and Their Ions"
Kazuhiko Okuno (1978)
- IPPJ-AM-11 "Charge Changing Cross Sections for Heavy-Particle Collisions in the Energy Range from 0.1 eV to 10 MeV III. Incidence of F, Ne, Na and Their Ions"
Kazuhiko Okuno (1978)
- IPPJ-AM-12* "Electron Impact Excitation of Positive Ions Calculated in the Coulomb-Born Approximation –A Data List and Comparative Survey–"
S. Nakazaki and T. Hashino (1979)
- IPPJ-AM-13 "Atomic Processes in Fusion Plasmas – Proceedings of the Nagoya Seminar on Atomic Processes in Fusion Plasmas Sept. 5-7, 1979"
Ed. by Y. Itikawa and T. Kato (1979)
- IPPJ-AM-14 "Energy Dependence of Sputtering Yields of Monatomic Solids"
N. Matsunami, Y. Yamamura, Y. Itikawa, N. Itoh, Y. Kazumata, S. Miyagawa, K. Morita and R. Shimizu (1980)

- IPPJ-AM-15 "Cross Sections for Charge Transfer Collisions Involving Hydrogen Atoms"
Y. Kaneko, T. Arikawa, Y. Itikawa, T. Iwai, T. Kato, M. Matsuzawa,
Y. Nakai, K. Okuno, H. Ryufuku, H. Tawara and T. Watanabe (1980)
- IPPJ-AM-16 "Two-Centre Coulomb Phaseshifts and Radial Functions"
H. Nakamura and H. Takagi (1980)
- IPPJ-AM-17 "Empirical Formulas for Ionization Cross Section of Atomic Ions for
Electron Collisions –Critical Review with Compilation of Experimental
Data–"
Y. Itikawa and T. Kato (1981)
- IPPJ-AM-18 "Data on the Backscattering Coefficients of Light Ions from Solids"
T. Tabata, R. Ito, Y. Itikawa, N. Itoh and K. Morita (1981)
- IPPJ-AM-19 "Recommended Values of Transport Cross Sections for Elastic Collision and
Total Collision Cross Section for Electrons in Atomic and Molecular Gases"
M. Hayashi (1981)
- IPPJ-AM-20 "Electron Capture and Loss Cross Sections for Collisions between Heavy
Ions and Hydrogen Molecules"
Y. Kaneko, Y. Itikawa, T. Iwai, T. Kato, Y. Nakai, K. Okuno and H. Tawara
(1981)
- IPPJ-AM-21 "Surface Data for Fusion Devices – Proceedings of the U.S–Japan Work-
shop on Surface Data Review Dec. 14-18, 1981"
Ed. by N. Itoh and E.W. Thomas (1982)
- IPPJ-AM-22 "Desorption and Related Phenomena Relevant to Fusion Devices"
Ed. by A. Koma (1982)
- IPPJ-AM-23 "Dielectronic Recombination of Hydrogenic Ions"
T. Fujimoto, T. Kato and Y. Nakamura (1982)
- IPPJ-AM-24 "Bibliography on Electron Collisions with Atomic Positive Ions: 1978
Through 1982 (Supplement to IPPJ-AM-7)"
Y. Itikawa (1982)
- IPPJ-AM-25 "Bibliography on Ionization and Charge Transfer Processes in Ion-Ion
Collision"
H. Tawara (1983)
- IPPJ-AM-26 "Angular Dependence of Sputtering Yields of Monatomic Solids"
Y. Yamamura, Y. Itikawa and N. Itoh (1983)
- IPPJ-AM-27 "Recommended Data on Excitation of Carbon and Oxygen Ions by Electron
Collisions"
Y. Itikawa, S. Hara, T. Kato, S. Nakazaki, M.S. Pindzola and D.H. Crandall
(1983)
- IPPJ-AM-28 "Electron Capture and Loss Cross Sections for Collisions Between Heavy
Ions and Hydrogen Molecules (Up-dated version of IPPJ-AM-20)
H. Tawara, T. Kato and Y. Nakai (1983)

- IPPJ-AM-29 "Bibliography on Atomic Processes in Hot Dense Plasmas"
T. Kato, J. Hama, T. Kagawa, S. Karashima, N. Miyanaga, H. Tawara, N. Yamaguchi, K. Yamamoto and K. Yonei (1983)
- IPPJ-AM-30 "Cross Sections for Charge Transfers of Highly Ionized Ions in Hydrogen Atoms (Up-dated version of IPPJ-AM-15)"
H. Tawara, T. Kato and Y. Nakai (1983)
- IPPJ-AM-31. "Atomic Processes in Hot Dense Plasmas"
T. Kagawa, T. Kato, T. Watanabe and S. Karashima (1983)
- IPPJ-AM-32 "Energy Dependence of the Yields of Ion-Induced Sputtering of Monatomic Solids"
N. Matsunami, Y. Yamamura, Y. Itikawa, N. Itoh, Y. Kazumata, S. Miyagawa, K. Morita, R. Shimizu and H. Tawara (1983)
- IPPJ-AM-33 "Proceedings on Symposium on Atomic Collision Data for Diagnostics and Modelling of Fusion Plasmas, Aug. 29 – 30, 1983"
Ed. by H. Tawara (1983)
- IPPJ-AM-34 "Dependence of the Backscattering Coefficients of Light Ions upon Angle of Incidence"
T. Tabata, R. Ito, Y. Itikawa, N. Itoh, K. Morita and H. Tawara (1984)
- IPPJ-AM-35 "Proceedings of Workshop on Synergistic Effects in Surface Phenomena Related to Plasma-Wall Interactions, May 21 – 23, 1984"
Ed. by N. Itoh, K. Kamada and H. Tawara (1984)
- IPPJ-AM-36 "Equilibrium Charge State Distributions of Ions ($Z_1 \geq 4$) after Passage through Foils – Compilation of Data after 1972"
K. Shima, T. Mikumo and H. Tawara (1985)
- IPPJ-AM-37 "Ionization Cross Sections of Atoms and Ions by Electron Impact"
H. Tawara, T. Kato and M. Ohnishi (1985)
- IPPJ-AM-38 "Rate Coefficients for the Electron-Impact Excitations of C-like Ions"
Y. Itikawa (1985)
- IPPJ-AM-39 "Proceedings of the Japan-U.S. Workshop on Impurity and Particle Control, Theory and Modeling, Mar. 12 – 16, 1984"
Ed. by T. Kawamura (1985)
- IPPJ-AM-40 "Low-Energy Sputterings with the Monte Carlo Program ACAT"
Y. Yamamura and Y. Mizuno (1985)

- IPPJ-AM-41 "Data on the Backscattering Coefficients of Light Ions from Solids (a Revision)"
R. Ito, T. Tabata, N. Itoh, K. Morita, T. Kato and H. Tawara (1985)
- IPPJ-AM-42 "Stopping Power Theories for Charged Particles in Inertial Confinement Fusion Plasmas (Emphasis on Hot and Dense Matters)"
S. Karashima, T. Watanabe, T. Kato and H. Tawara (1985)